Elucidation of Circulatory miRNA Levels Regulating NFATC3/ANP/BNP Signaling Nexus for the Early Diagnosis of Myocardial Infarction

By

Aqsa Naeem

Department of Biochemistry
Faculty of Biological Sciences
Quaid-i-Azam University
Islamabad, Pakistan
2022

Elucidation of Circulatory miRNA Levels Regulating NFATC3/ANP/BNP Signaling Nexus for the Early Diagnosis of Myocardial Infarction

A dissertation submitted in the fulfillment of requirements for the

Degree of Master of Philosophy In

Biochemistry/ Molecular Biology

By

Aqsa Naeem

Department of Biochemistry
Faculty of Biological Sciences
Quaid-i-Azam University
Islamabad, Pakistan
2022

DECLARATION

By submitting this thesis, I hereby declare that the entirety of the work contained therein is my own effort and hard work, that I am the authorship owner thereof and that I have not previously submitted it for obtaining any qualification.

Aqsa Naeem

This thesis is dedicated to my parents.

For their endless love, support and encouragement

ACKNOWLEDGEMENT

All praises and thanks to Allah ﷻ, The Lord of the universe, The Most Beneficent and The Merciful, who showered His countless blessings upon us and helped me to contribute in the field of knowledge and enabled me to compile my humble endeavours in the shape of this thesis. Countless salutations upon The Holy Prophet, Hazrat Muhammmad ﷺ, who is the source of knowledge and guidance for the entire humanity.

I would like to pay my sincere gratitude to my research supervisor and chairperson, Department of Biochemistry, **Dr. Iram Murtaza**, for giving me the opportunity to do my research under her supervision. Her keen interest, encouragement, dedication, guidance and scholarly advice throughout this research helped me to achieve my goal.

It is a genuine pleasure to express my deep sense of thanks and gratitude to my guide, **Ayesha Ishtiaq**. Her scientific approach, timely advice and overwhelming attitude to guide me had been mainly responsible for completing my work. I would also like to appreciate my seniors, **Iram Mushtaq, Mehmand Khan** and **Khadam Hussain** for Ssupporting and helping me to become a researcher with their cooperative attitude.

A special and kind regards to my friends **Amna Saeed** and **Syeda Laiba Tayyab** for their unshakable help and encouragement which incented me to strive towards my goal. I also want to pay the heartiest gratitude to my dearest friends, **Mahnoor Zakir** and **Kainat Riaz** for being there to provide moral help in every kind of trouble and stress.

A special thanks to my lab fellows, **Ayesha Jabeen** and **Muhammad Yousaf** for their cooperation and help. Sincere regards to my seniors **Iqra Azhar, Sana Karim, Rafia Gul** for their support and help.

I am most indebted to my **Parents** and siblings **Hajra Naeem, Aiman Naeem, Furqan Naeem and Suleman Naeem** for their endless prayers, matchless love, and care. Words become meaningless when I have to say thanks to them; their prayers gave me strength and hope to accomplish this task and to pursue my goals. Lastly, I offer my kind regards and blessings to all who supported me in any respect during the completion of this thesis.

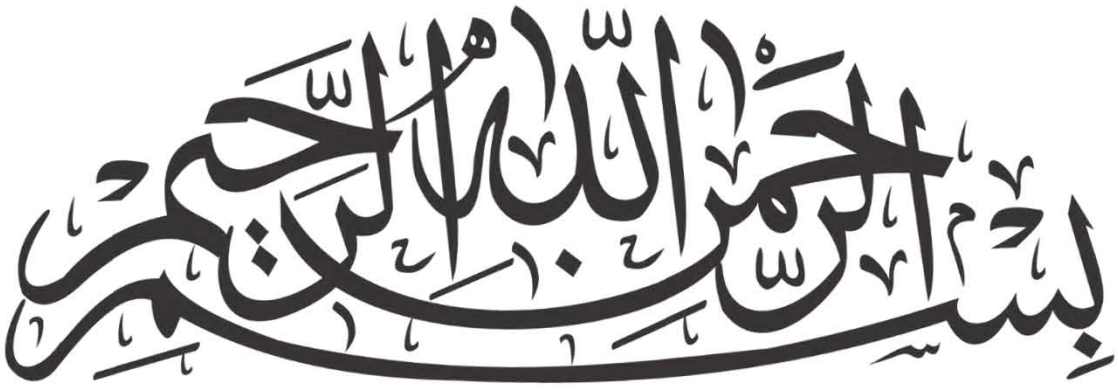
بسم الله الرحمن الرحيم

TABLE OF CONENTS

LIST OF ABBREVIATIONS

AC	Adenylyl Cyclase
AGO	Argonaute
ALT	Alanine Aminotransferase
AMI	Acute Myocardial Infarction
ANP	Atrial Natriuretic Peptide
AP1	Activating Protein
APAF-1	Apoptotic Protease Activating Factor-1
APS	Ammonium Persulphate
APX	Ascorbate Peroxidase
AST	Aspartate Aminotransferase
ATF2	Activating Transcription Factor 2
ATP	Adenosine Triphosphate
BCIP	5-Bromo-4-Chloro-3-Indolylphosphate
BNP	Brain Natriuretic Peptide
BSA	Bovine Serum Albumin
Ca^{+2}	Calcium
CAD	Coronary Artery Disease
cAMP	Cyclic Adenosine Monophosphate
CAT	Catalase
CK-MB	Creatine Kinase Myocardial Band
CRP	C-Reactive Protein
cTn	Cardiac Troponin
CVDs	Cardiovascular Diseases
cyt c	Cytochrome Complex
DAG	Diacylglycerol
DEPPD	N, N-Diethyl Para-Phenylenediamine
DGCR8	DiGeorge Syndrome Critical Region 8
DNA	Deoxyribonucleic Acid

dNTPs	Deoxynucleotide Triphosphates
DTNB	5,5'-Dithiobis-2-Nitrobenzoic Acid
ECG	Electrocardiogram
EDTA	Ethylene diamine tetraacetic acid
EIK1	Eukaryotic Initiation Factor 1
ER	Endoplasmic Reticulum
ERK	Extracellular Signal Regulated Kinase
ET-1	Endothelin-1
EVs	Extracellular Vesicles
$FeSO_4$	Ferrous Sulphate
GDP	Guanosine Diphosphate
GPCR	G-Protein Coupled Receptor
GSH	Reduced Glutathione
GTP	Guanosine Triphosphate
H&E	Hematoxylin and Eosin
H_2O_2	Hydrogen Peroxide
HDL	High-Density Lipoprotein
I/R	Ischemia/Reperfusion
IP3	Inositol Trisphosphate
ISO	Isoproterenol
JNK	Jun N-terminal Kinases
LDH	Lactate Dehydrogenase
LDL	Low-Density Lipoprotein
MAPK	Mitogen Activated Protein Kinase
MAPKK	Mitogen Activated Protein Kinase Kinase
MAPKKK	Mitogen Activated Protein Kinase Kinase Kinase
MDA	Malondialdehyde
MDH	Malate Dehydrogenase
MDHA	Mono-Dehydroascorbic Acid
MEF-2	Myocyte Enhancer Factor-2

MI	Myocardial Infarction
miRNA	MircoRNA
MOMP	Mitochondrial Outer Membrane Permeability Pore
MPTP	Mitochondrial Permeability Transition Pore
MRI	Magnetic Resonance Imaging
mRNA	Messenger RNA
NaCl	Sodium Chloride
NBT	Nitro-Blue Tetrazolium
NC	Nitrocellulose
NFATC3	Nuclear Factor of Activated T-Cells Cytoplasmic 3
NIH	National Institute of Health
PCR	Polymerase Chain Reaction
PIP2	Phosphatidylinositol 4,5-Bisphophate
PKA	Protein Kinase A
PKC	Protein Kinase C
PLC	Phospholipase
PMSF	Phenyl Methylsulfonyl Fluoride
POD	Peroxidase
pre-miRNA	Precursor miRNAs
pri-miRNA	Primary miRNAs
RIPA	Radio Immune Precipitation Assay
RISC	RNA-Induced Silencing Complex
RNA	Ribonucleic acid
ROS	Reactive Oxygen Species
RT-qPCR	Real Time-quantitative Polymerase Chain Reaction
SDS	Sodium Dodecyl Sulfate
SNS	Sympathetic Nervous System
SOD	Super Oxide Dismutase
STEMI	ST Elevation Myocardial Infarction
TBA	Thiobarbituric Acid

TBARs	Thiobarbituric Acid Reactive Substances
TBST	Tris Buffered Saline With 0.1% Tween-20
TCA	Trichloroacetic Acid
TNB	5'-Thio-2-Nitrobenzoic Acid
TNF	Tumor Necrotic Factor
TRBP	Trans Activation Response RNA Binding Protein
UTR	Untranslated Region
WHO	World Health Organization
XDH	Xanthine Dehydrogenase
XO	Xanthine Oxidase
XOR	Xanthine Oxidoreductase

LIST OF FIGURES

LIST OF TABLES

ABSTRACT

Myocardial infarction (MI), also known as heart attack, is caused by reduced or complete cessation of blood flow to the part of myocardium. MicroRNAs (miRNAs) are key regulators in various cellular mechanisms and have the potential to be used as diagnostic markers in certain diseases such as MI, atherosclerosis, heart failure coronary artery disease, hypertrophy and fibrosis. The present research was conducted to study the early diagnostic potential of circulatory miRNAs which were dysregulated in MI patients and isoproterenol induced MI rat model. The expression of miRNA-1 and miRNA-15a was markedly upregulated in the blood of MI patients while the expression of miRNA-98 was significantly downregulated in MI patients' blood and isoproterenol induced MI rats' blood and tissue. By using bioinformatics tool, TargetScan, it was confirmed that NFATC3, BCL2 and ET-1 were the putative targets of miRNA-1, miRNA-15a and miRNA-98, respectively. The decreased levels of NFATC3 and BCL2 in circulation were confirmed by qRT-PCR. In blood, the increased level of ET-1 and its downstream targets ANP and BNP were confirmed by qRT-PCR. The increased protein expressions of NFATC3 and ET-1 in tissue and serum sample were evaluated by western blotting in isoproterenol induced MI rat model. The toxic potential of isoproterenol for MI induction in rat was confirmed by disrupted heart tissue histology, increased reactive oxygen species (ROS) and decreased antioxidative enzymes such as super oxide dismutase (SOD), catalase (CAT), peroxidase (POD), reduced glutathione (GSH) and ascorbate peroxidase (APX) in rat serum and tissue homogenates samples. In serum samples, the liver function tests and lipid profiling were also done to check the elevated levels of enzymes in isoproterenol induced MI rat model. Concludingly, this study provides future insights for miRNA research that will advance the development of diagnostic markers for the early detection of MI in patients.

1 INTRODUCTION

1.1 Cardiovascular Diseases

Cardiovascular system comprises of heart and blood vessels. Cardiovascular diseases (CVDs) are heart and blood vessel abnormalities that affect the morphology and functionality of the heart. These are the leading cause of mortality globally. Cardiovascular disease comprises various disorders such as atherosclerosis and other subtypes leading to myocardial infarction, cardiac ischemia, arterial thrombosis, heart failure and arrhythmia (Corday, 2018). All these diseases represent specific cellular and molecular feature including apoptosis, DNA damage, mitochondrial damage and oxidative stress (Chiuve *et al.,* 2014).

1.2 Prevalence

Cardiovascular diseases are the major causes of death worldwide. According to World Health Organization (WHO) report, in 2019, it has been evaluated that 17.9 million deaths were reported due to cardiovascular diseases, depicting 32% of all deaths worldwide as shown in Figure 1.1. Out of all these deaths, 85% of cardiovascular patients died due to stroke and heart attack. About 3/4 of deaths take place in middle-income and low-income countries. It has been reported that in 2019, out of 17 million deaths under the age of 70 were due to long-term diseases, 38% of deaths were caused by cardiovascular diseases (Cardiovascular Diseases (CVDs), 2021). Out of 87% of cardiovascular diseases deaths, 47% of deaths were due to ischemic heart disease and 40% of deaths were due to stroke (Dong Zhao, 2021).

Compared with 2010, an increase of 26.6% was estimated in 2019 in which there are more than 523.2 million cases of CVDs ("Heart Disease and Stroke Statistics-2021 Update A Report from the American Heart Association," 2021). In the beginning of the 20th century, CVDs were responsible for lesser than 10% of the mortality globally. Cardiovascular diseases cause 30% of deaths worldwide (T. A. Gaziano, 2005). The Asian people are more vulnerable to myocardial infarction (Joshi *et al.,* 2007; Kearney *et al.,* 2005). It has been estimated that myocardial infarction is 50% greater in South Asian population than in UK (Bellary *et al.,* 2010). In Pakistan there is high prevalence of myocardial infarction risk factors, a study reported that more than 30% of people over 45 years of age are more affected by this disease (T. A. Gaziano *et al.,* 2010).

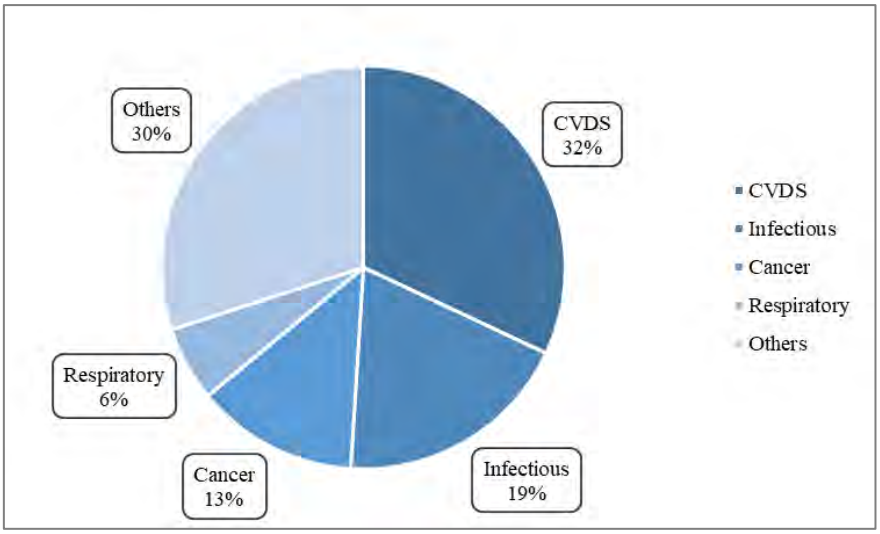

Figure 1.1 Comparison of CVDs with other causes of death (Adapted from Roth et al., 2020)

1.3 Myocardial Infarction

Myocardial infarction (MI) occurs when flow of blood to the portion of heart is reduced or completely stopped. MI may remain silent but it can lead to severe hemodynamic deterioration and sudden death (Thygesen *et al.,* 2012). MI may be the first symptom of coronary artery blockage resulting in the deprivation of oxygen in the myocardium as shown in Figure 1.2. Protracted distress of oxygen supply to the cardiac muscle can eventually result in cardiac cell death and necrosis (Reimer *et al.,* 1983). MI is cell death of cardiac cells caused by reduced supply of oxygen, which occurred due to the imbalance of oxygen supply and demand.

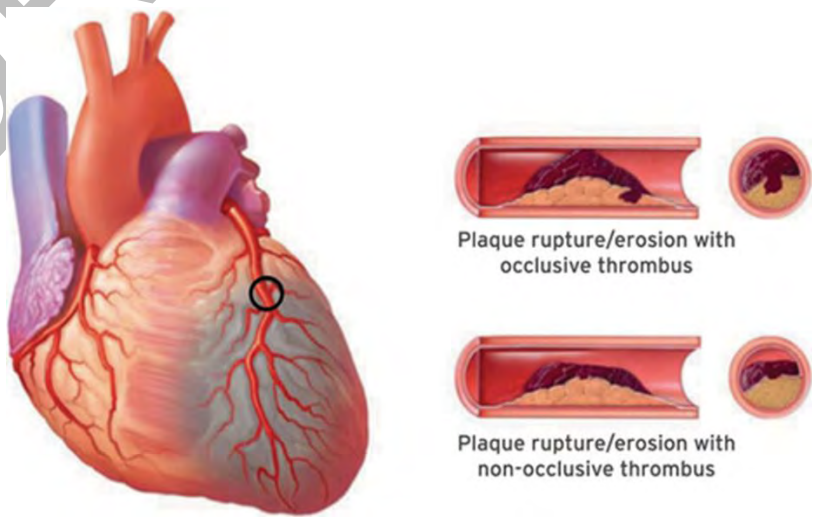

Figure 1.2 Myocardial Infarction (Thygesen et al., 2018)

1.4 Diagnosis of Myocardial Infarction

AMI is myocardium cell death which occurred due to the acute occlusion of coronary artery. Myocardial infarction can be diagnosed by serial electrocardiograms (ECGs), variation in ST segment representing cardiac pathology, serum analysis of cardiac markers and coronary angiography. Blood test serves as an important clinical way for disease diagnosis (Cohen *et al.,* 2018; Nakamura *et al.,* 2018), as they are more accurate and convenient comparative to the conventional methods such as ECG and physical examination (Chaudhury *et al.,* 2017; Wei *et al.,* 2017).

Cardiac markers are the myocardial cell injury serum markers which include myocardial enzymes such as creatine kinase myocardial band (CK-MB) and release of cell contents such as cardiac troponin (cTn) I and T into the blood stream after cardiac cell injury. The markers express at various stages of tissue cell injury and their expression drop at different rates. The increase and decrease of cTn levels are linked with the symptoms of cardiac ischemia (Thygesen et al., 2018; Weil et al., 2018). The severity and time span of MI can be estimated by the serial testing of cTn values at 0 hour, 3hours, 6hours. For the diagnosis of MI, creatine kinase MB can also be used but it is less sensitive and precise than cTn levels (Goodman *et al.,* 2006; Thygesen *et al.,* 2012). To observe the myocardial perfusion, myocardial thickness and myocardial viability, different imaging techniques such as echocardiography, radionuclide imaging and cardiac magnetic resonance imaging (MRI) can be used. Echocardiography can detect ischemia induced regional wall motion abnormalities, whereas cardiac MRI can provide accurate assessment of myocardial structure and function (Thygesen et al., 2018).

1.5 Pathophysiology

The obstruction of epicardial coronary arteries can result in acute myocardial infarction. The breakdown of atherosclerotic plaque formed in coronary arteries results in acute myocardial infarction (AMI) (Ojha & Dhamoon, 2021). The obstruction results in the reduced supply of oxygen in cardiac muscle, as a result disruption of sarcolemma and relaxation of myofibrils take place (Reimer *et al.,* 1983). In the process of myocardial infarction, these events are the first ultrastructural changes which are followed by changings in mitochondria. The reduce supply of oxygen results in death of myocardium which extends from sub-endocardium to sub-epicardium. Due to increased collateral circulation, the sub-epicardium delays death (Reimer *et al.,* 1983). The

cardiac function is disturbed in the specific region of the heart affected by MI. There is no regeneration capacity of the myocardium so the infarcted region restores by scar formation. The remodeled heart is distinguished by hypertrophy and cardiac dysfunctionality (Frangogiannis, 2015).

1.6 Risk Factors

Myocardial infarction is the growing cause of death worldwide. There are various factors which extend the prevalence of acute myocardial infarction (AMI) such as lack of physical activity, obesity and other metabolic diseases. There are numerous risk factors which should be considered when treating the patients of AMI. AMI can be prevented by avoiding the risk factors which include smoking, hypertension, stress, obesity and physical inactivity. The major risk factors of AMI are shown below in Figure 1.3.

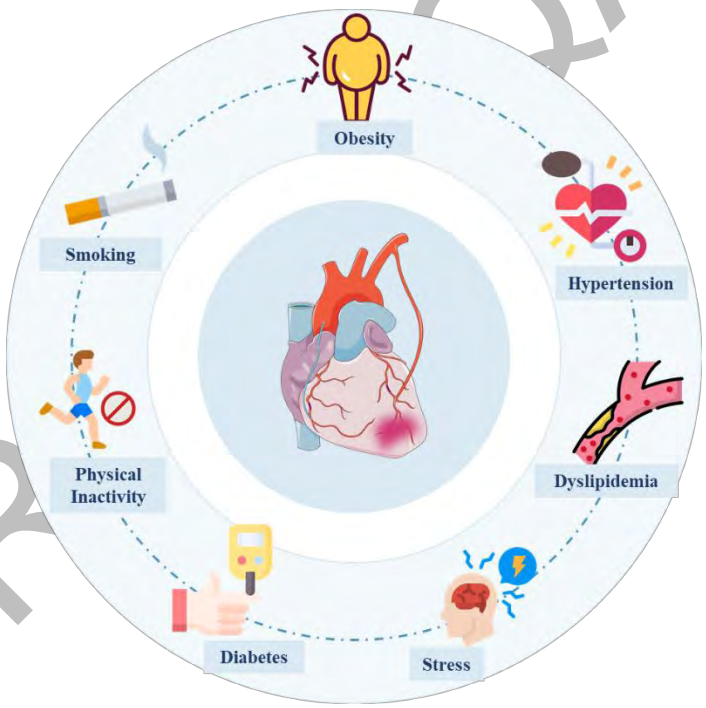

Figure 1.3 Risk Factors of Myocardial Infarction

Created with PowerPoint

1.6.1 Lack of Physical Activity

AMI is more likely to develop in people who are physically inactive with multiple cardiac risk factors (Giri *et al.,* 1999). According to studies, the risk of CVDs may vary depending on the type of physical activity. Some physical activities like running,

walking and climbing may provide protection against cardiac diseases (Rathore *et al.,* 2018). It has been reported that risk of MI was reduced upto 20 % to 30 % due to physical activity (Gong *et al.,* 2013). The relation between physical activity and AMI was observed and it was confirmed that physical inactivity is a measure of subsequent risk of CVDs (Rathore *et al.,* 2018).

1.6.2 Smoking

Smoking the strong contributor of AMI, atherosclerosis and sudden cardiac death. The risk of CVDs increases by different mechanisms (Alemu *et al.,* 2011). In healthier patients, smoking results in early ST elevation myocardial infarction (STEMI). Smoking increases serum low-density lipoprotein (LDL) cholesterol and triglycerides level whereas it reduces serum high-density lipoprotein (HDL) cholesterol. The free radical damage to LDL is enhanced by cigarette smoking, leading to agglomeration of oxidized LDL cholesterol with the walls of arteries (Rathore *et al.,* 2018). In smokers, smoking causes vascular inflammation which causes high levels of C-reactive protein (CRP) (Yusuf *et al.,* 2004). Cigarette nicotine activates the sympathetic nervous system (SNS) increasing heart rate and systolic blood pressure. The increased SNS activity raises heart rate which causes coronary artery vasoconstrictor, alleviating myocardial blood flow and increasing the demand of oxygen to the myocardium (Moliterno *et al.,* 1994).

1.6.3 Hypertension

The hypertension increases the risk of AMI due to fluctuations in systolic and diastolic blood pressure (Kannel, 2000). The atherosclerotic plaque in coronary artery lead to myocardial infarction. There is the close relationship between hyper tension and myocardial infarction. In old age, hypertension is adverse to heart and is responsible for 70% cardiac diseases (Kannel, 2000). High blood pressure increases shear stress on plaque, causes severe functional effects on coronary circulation and leads to the impairment of endothelial function (Hurtubise *et al.,* 2016). Studies reported that the risk of MI was reduced by controlling hypertension with the help of proper medication and adoption of healthy lifestyle (Saleheen *et al.,* 2009).

1.6.4 Obesity

Obesity is the major risk factor of myocardial infarction. Studies reported that obesity results to the greater risk of AMI (Zhu *et al.,* 2014). Increased BMI is directly linked to

the incidence of cardiac diseases. One should take measures to control body mass index (BMI) to prevent myocardial infarction risk. Researchers correlated obesity with AMI and demonstrated that obesity of abdominal region elevates the possibility of AMI in males and females of all ages and regions (Yusuf *et al.,* 2004).

1.6.5 Diabetes

Diabetes mellitus is another risk factor for CVDs. Type 2 diabetes mellitus is a condition when the ability of pancreatic β cells to produce insulin is affected or the cells are unable to uptake insulin. People with diabetes have greater cardiovascular morbidity and mortality rates and are more at risk to develop CVDs compared to non-diabetic subjects. In diabetic patients, coronary heart disease risk is accelerated by 2 to 4 times. There is a higher risk of atherosclerotic plaque in arterial walls and other vascularized areas in diabetic patients. Studies reported that there is greater risk of plaque rupture among patients with diabetes. The risk of myocardial infarction is increased in diabetic patients as it accelerates atherosclerotic plaque formation and severely affects the lipid contents. Due to the high rate of fatality, myocardial infarction is often fatal in diabetic patients than in myocardial infarction patients without diabetes.

1.6.6 Dyslipidemia

The major risk factor for myocardial infarction is the increased levels of triglycerides and LDL cholesterol. The raised levels of LDL, cholesterol, triglycerides and low levels of HDL are major factors for coronary atherosclerosis (Rathore *et al.,* 2018). The metabolic disturbance is the major cause of low HDL levels and increased triglycerides levels, thus leading to severe consequences (J. M. Gaziano, 1999). Studies reported that in young patients with AMI, there is high rate of dyslipidemia with hypertriglyceridemia, hypercholesterolemia, increased LDL and decreased HDL (N. S. Ali *et al.,* 2016). The risk of myocardial infarction can be reduced by the proper treatment of dyslipidemia (Borgia & Medici, 1998).

1.6.7 Stress

The risk factors of heart attack is depression, stress and social isolation (Huma *et al.,* 2012). It has been reported that psychological stress is related to high risk of coronary heart disease and the extreme sorrow after the death of an important person may increase the risk of myocardial infarction (Mostofsky *et al.,* 2012). It has been assumed

that emotional stress is associated with hemodynamic stress in the arteries and the rupture of atherosclerotic plaque (Muller *et al.,* 1994).

1.7 Role of Oxidative Stress in Myocardial Infarction

In cardiomyocytes, oxidative stress is defined as the imbalance between oxidants and antioxidants that promotes the accumulation of reactive oxygen species resulting in cellular damage (Navarro-Yepes *et al.,* 2014). Normally, an adaptive system for the protection of cells is initiated against the oxidative stress but when the levels of oxidants surpasses the adaptive ability of cell, the cell will experience severe oxidative stress (Kurian *et al.,* 2016). The antioxidant defense system provides protection against oxidative stress. The antioxidant machinery includes efficient enzymes like super oxide dismutase (SOD), catalase (CAT), ascorbate peroxidase (APX), glutathione (GSH) (Gill & Tuteja, 2010).

The term oxidative stress means the imbalance between redox species. The term free radical describes the changes in function and structure of biomolecules (Kurian *et al.,* 2016). Free radicals linked oxidative stress contributes in the peroxidation of lipids and protein oxidation leads to DNA double strand breaks eventually leading to apoptotic cell death (Navarro-Yepes *et al.,* 2014). Accumulation of free radicals result in increased oxidative stress in myocardial infarction (Kurian *et al.,* 2016).

At cellular level, oxidative stress is linked with increase in reactive oxygen species (ROS). At suboptimal level, ROS acts as a signal in protecting the cardiac function. While elevated ROS levels can cause physio-pathological effect by causing damage to biomolecules such as lipids, proteins and DNA. Cardiac pathology linked with oxidative stress is observed in ischemia/reperfusion injury, diabetic cardiomyopathy and atherosclerosis (A. Thandavarayan *et al.,* 2011; Keaney & Vita, 1995; Venditti *et al.,* 2001). Studies suggested that cytokines are generated by ROS and are involved to induce ROS production (Meldrum *et al.,* 1998). Hydrogen peroxide (H_2O_2) can accelerate the production of myocardial tumor necrotic factor (TNF) by activating p38 mitogen activated protein kinase (MAPK) pathway and, as a result, promote myocardial dysfunction and apoptosis (Meldrum *et al.,* 1998; Nian *et al.,* 2004).

The metalloproteinases are activated due to ROS and lead to the plaque rupture (Moris *et al.,* 2017). After MI, ROS is produced in myocardial tissue through different mechanisms. Previous studies showed that in re-perfused tissue xanthine

oxidoreductase (XOR) was potential source of ROS. In reduced supply of oxygen, xanthine dehydrogenase (XDH) is changed to xanthine oxidase (XO), resulting in superoxide formation (Berry & Hare, 2004). It has been reported that in ischemia, adenosine triphosphate (ATP) production is in surplus resulting in increased Ca^{+2} levels. As a result, Ca^{+2} dependent proteases become activated converting XDH to XO (Engberding *et al.,* 2004). Experimental data depicted that in cardiomyocytes Nox2 expression is upregulated after MI (Krijnen *et al.,* 2003). Reduction in ROS levels have pragmatic effects on left ventricular remodelling after heart attack (Engberding *et al.,* 2004).

In cardiac signaling, ROS acts as a secondary messenger in cardiomyocyte death where stress stimulated transcription factors are activated by MAPK, guanosine triphosphate (GTP) binding proteins, cytokines and protein tyrosine kinase receptor resulting in cellular hypertrophy and cell death (Khaper & Singal, 2001; Sia *et al.,* 2002). The agglomeration of oxidized cellular lipids and proteins due to oxidative stress result in myocardial cell death (Borchi *et al.,* 2009). The mitochondrial ROS formation closely linked with mitochondrial calcium (Ca^{+2}) channels dysfunction and activation of extracellular signal-regulated kinase (ERK) and Jun N-terminal kinase (JNK) signaling pathways leading to cardiomyocyte death (Sucher *et al.,* 2009). However, it has been reported that the activation of antioxidant Nrf2 pathway provides cardio-protection against cardiac pathologies by reducing oxidative stress (J. Li *et al.,* 2009).

1.8 Isoproterenol induced Myocardial Infarction in Animal Model

Isoproterenol (ISO) binds to β-adrenergic receptor to induce myocardial infarction. Other procedures can also be used to induce myocardial infarction including banding of the ascending aorta (Hsu *et al.,* 2019), coronary artery ligation (Gao *et al.,* 2010), all these are time consuming and complicated procedures with a high risk of mortality and morbidity. Whereas isoproterenol is non-invasive method and at specific dose it has low mortality rate and high reproductivity rate to induce myocardial infarction.

ISO generates cytotoxic free radicals that elevates the phospholipid membrane peroxidation leading to ROS production and ultimately cause damage to the myocardium. The acute myocardial infarction is linked with inflammatory response that causes change in extracellular matrix due to the release of free radicals and proteolytic enzymes which results in the remodelling of myocardium (Sakuma &

Yamaguchi, 2010). ISO binds to β-1 and β-2 adrenergic receptor and induces myocardial infarction by the stimulation of secondary messengers. Upon binding of ISO to the extracellular domain of β-1 receptor, G-α protein becomes activated and it is dissociated from intracellular domain due to the exchange of guanosine diphosphate (GDP) molecule into GTP molecule. The activated G-α stimulatory protein activates adenylyl cyclase in the membrane which subsequently converts intracellular ATP into cyclic adenosine monophosphate (cAMP) (Xiang, 2011). cAMP acts as a secondary messenger to activate protein kinase A (PKA). In cardiac monocytes, the activated PKA phosphorylates the calcium channels and leads to the increase in intracellular calcium levels. PKA also stimulates the ryanodine receptors on the sarcoplasmic reticulum for the excessive release of calcium in cytosol (Abel & Rorabaugh, 2021). Increased intracellular calcium levels stimulate the ROS producing enzymes and upregulate the free radical generation (Görlach *et al.,* 2015). PKA also leads to the phosphorylation of transcription factors via the activation of MAPK signaling to promote cell growth and survival. Signaling through extracellular signal regulated kinase (ERK) is stimulated at the cell membrane by Ras activation, Ras directly interacts with MAPK kinase kinase (MAPKKK) Raf, which then interacts with MAPK kinase (MAPKK) MEK1, MEK2. MEK1/2 directly phosphorylate ERK1 and ERK2 kinases (Molkentin, 2004).

In eukaryotes, when calcium binds to calmodulin, then the structural and conformational change take place and the protein interaction sites are exposed (Strynadka & James, 2003). Calcineurin is a serine/threonine phosphatase and it is activated by the binding of Ca^{+2}/calmodulin with very high affinity (Stansfield *et al.,* 2014). The calcineurin dependent pathway plays critical role in cardiac development and cardiac hypertrophy response in adults (Deshpande *et al.,* 2022). This complex further dephosphorylates the phosphorylated nuclear factor of activated T-cells (NFAT) in the cytosol and translocate it into the nucleus. In nucleus, NFATC3 acts along with other transcription factors i.e., GATA4. GATA4 along with the NFATC3 and myocyte enhancer factor-2 (MEF-2) synergistically activate the promoter of endothelin-1 (ET-1) gene and regulate the expression of atrial natriuretic peptide (ANP) and brain natriuretic peptide (BNP) gene (Molkentin, 2004).

1.9 Detection Strategies under Investigation

Despite advancements in cardiovascular studies and medical therapies, heart diseases are the main cause of death globally. The new and innovative technologies are required

for improving the diagnostic and therapeutic purposes. The pathological process responsible for cardiac dysfunctionality is analogous to the change in gene expression that is critical for heart functions. There are different techniques to improve morphological and electromechanical properties of various heart disorders i.e., stem cell derived exosomes, cell-based therapies and gene-based therapies secreting growth factors, cytokines and miRNAs to enhance cardiac regeneration (Duelen & Sampaolesi, 2017).

1.9.1 Diagnostic Potential of MicroRNAs

In CVDs, miRNAs are used as diagnostic markers and circulating miRNAs are altered in certain disease conditions such as MI, heart failure, coronary artery disease and hypertrophy (Fichtlscherer *et al.,* 2010; Gomes Da Silva & Silbiger, 2014). Under pathological conditions, intracellular miRNAs are associated with the expression and regulation of genes. Various studies have recognized the importance of circulatory miRNAs, which have been stably detected as extracellular messengers in blood circulation i-e., plasma and serum (Mitchell *et al.,* 2008) that are involved in cell to cell communication and their potential role as circulating biomarker for cardiac pathologies (Reid *et al.,* 2011; Simons & Raposo, 2009). Circulatory miRNAs are found to be stable in exosomes, micro-vesicles and apoptotic bodies as well as in combination with RNA binding proteins (Arroyo *et al.,* 2011) or in HDL lipoprotein conjugated complexes (Vickers *et al.,* 2011). The miRNAs are released in the extracellular compartments and then finally into blood stream which have presented the probability to non-invasively detect the circulatory miRNAs and to use them as diagnostic biomarkers (Mitchell *et al.,* 2008; Schulte & Zeller, 2015).

1.9.1.1 Biogenesis of miRNAs

miRNAs are key regulatory molecules that are associated with the expression and regulation of genes by targeting various genes and inhibiting their action. Alteration in gene expression patterns related to pathological cardiac state can lead to heart failure (Bui *et al.,* 2011; Clerk *et al.,* 2007). miRNAs are small non-coding RNAs which are ~22 nucleotides in length (Ha & Kim, 2014). Mostly miRNAs bind with 3' untranslated region (UTR) of messenger RNA (mRNA) target to suppress its expression (O'Brien *et al.,* 2018). The biogenesis of miRNA begins with the processing of transcripts by RNA polymerase II/III post- transcriptionally or co-transcriptionally (Ha & Kim,

2014). miRNAs are mostly processed from introns and relatively few from exons of protein coding genes, while the remaining are intergenic. The non-canonical miRNA biogenesis is Drosha/DGCR8 independent pathway. The miRNA formed by Drosha/DGCR8 independent pathway relate with Dicer substrates such as pre-miRNA mirtrons, which are formed during splicing from the introns of mRNA (Babiarz *et al.,* 2008; Ruby *et al.,* 2007). In case of canonical biogenesis of miRNA, RNA polymerase II transcribes the genes of miRNAs into pri-miRNA which are then processed into pre-miRNA by the microprocessor complex consisting of RNA binding protein DiGeorge Syndrome Critical Region 8 (DGCR8) and a ribonuclease III enzyme, Drosha (Denli *et al.,* 2004). N6- methyl adenylated GGAC and other motifs are recognized by DGCR8 while Drosha cleaves the pri-miRNA (Alarcón *et al.,* 2015). This results in the formation of precursor miRNA as shown in Figure 1.4.

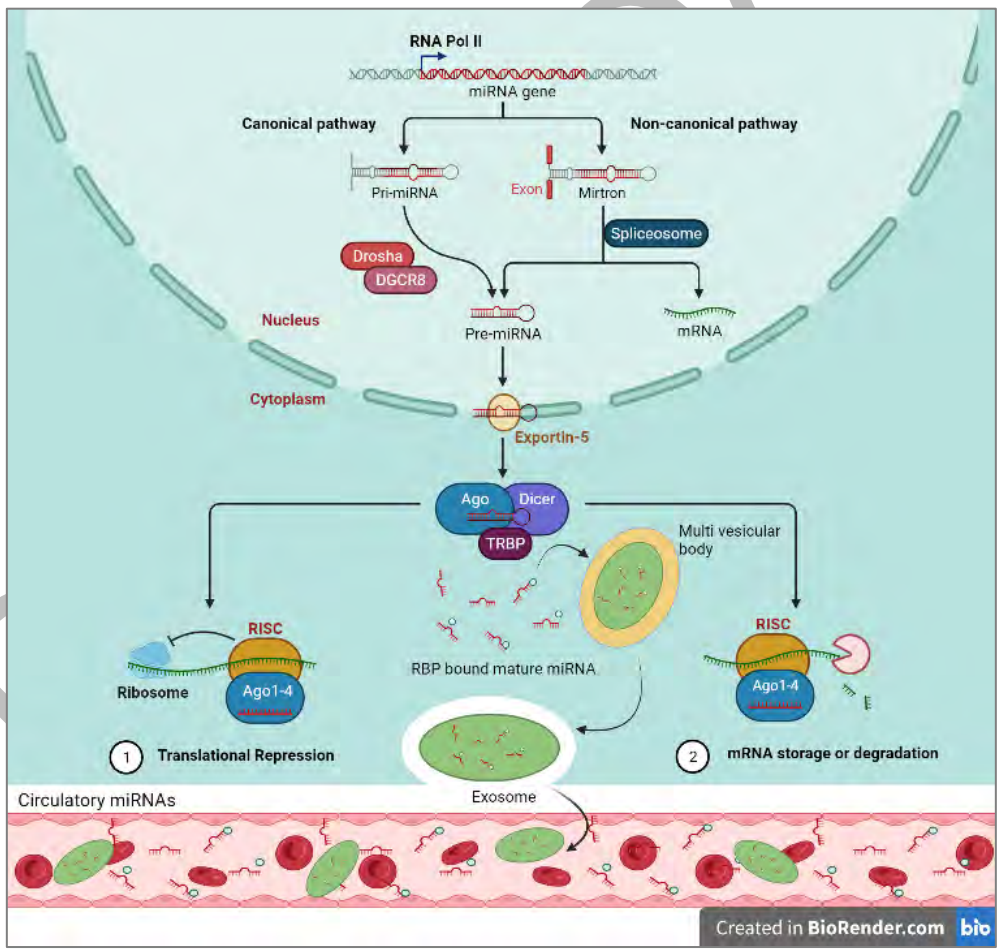

Figure 1.4 Biogenesis of miRNA

The precursor miRNAs are exported to the cytoplasm by an exportin 5/ Ran GTP complex which is further processed by RNase III endonuclease, Dicer (Denli *et al.,*

2004; Okada *et al.,* 2009). Finally, the terminal loop of pre-miRNA was removed and as a result the mature miRNA was formed (Zhang et al., 2004). The name of the mature miRNA form was determined by the directionality of the miRNA strand. The 5p strand originates from the 5' end of the pre-miRNA hairpin loop while the 3p strand arises from the 3'end of the pre-miRNA loop. Both strands of the mature miRNA duplex can be loaded into the Argonaute (AGO) family of proteins i.e., AGO1-4 in humans, in ATP dependent manner (Yoda *et al.,* 2010). The Argonaute protein and dicer with trans activation response RNA binding protein (TRBP) form RNA-induced silencing complex (RISC). Several proteins are then recruited to form RNA induced silencing complex (RISC)in which passenger strand was removed and the other strand served as a guide strand. The resultant miRNA-RISC complex complementarily binds to the 3' UTR of target mRNA. The miRNA-RISC complex induces the translational inhibition or mRNA degradation leading to post-transcriptional repression of gene (Yao, 2016).

1.9.1.2 miRNA-1 targeted pathway in ISO induced Myocardial Infarction

Many studies addressed that the circulatory miRNAs can be used as potential markers in the diagnosis of MI (Sala *et al.,* 2014). In AMI, there is abundance of specific cardiac miRNAs that act as a measure of cardiac injury in circulating cardiac extracellular vesicles (EVs). miRNA-1 is a muscle specific miRNA reported to be highly linked with CVDs. miRNA-1 is widely reported miRNA that is found to be highly upregulated in serum/plasma of myocardial infarction patients and has potential to be used as diagnostic biomarker (Ai *et al.,* 2010; Cheng *et al.,* 2010; Kuwabara *et al.,* 2011; Long *et al.,* 2012). Studies have reported that the levels of miRNA-1 are reduced in heart tissue while on the other hands the levels of circulatory miRNA-1 are found to be elevated in AMI patients. In heart tissues of rats, miRNA-1 was found to be down-regulated in response to myocardial Ischemia/Reperfusion (I/R) injury. Inhibition of miRNA-1 was found to have cardio-protective role against I/R injury in rats via accelerating MAPK3/PIK3/Akt signaling.

Isoproterenol binds to β-adrenergic receptor that induces MI by causing oxidative stress, thrombosis, inflammation, Ca^{+2} overload and alter downstream signaling pathways. The activation of β-adrenergic receptor elevates the concentration of cAMP by activating adenylyl cyclase that further activates protein kinase A (PKA) which phosphorylates calcium channels. As a result, intracellular calcium levels are elevated followed by aberrant gene transcription due to necrosis and apoptosis (Garg & Khanna,

2014; Mann, 1996). The Ca^{+2}/calmodulin/calcineurin complex further dephosphorylates the phosphorylated NFATC3 in the cytosol and translocate it into the nucleus.

NFATC3 is the putative target of miRNA-1-3p as shown in Figure 1.5. In nucleus, NFATC3 acts along with other transcription factors and cofactors i.e., GATA4 and activating protein (AP1), respectively. GATA4 along with the NFATC3 and AP1 synergistically activate the promoter of ET-1 gene and regulate the expression of atrial natriuretic peptide (ANP) and brain natriuretic peptide (BNP) gene (Molkentin, 2004).

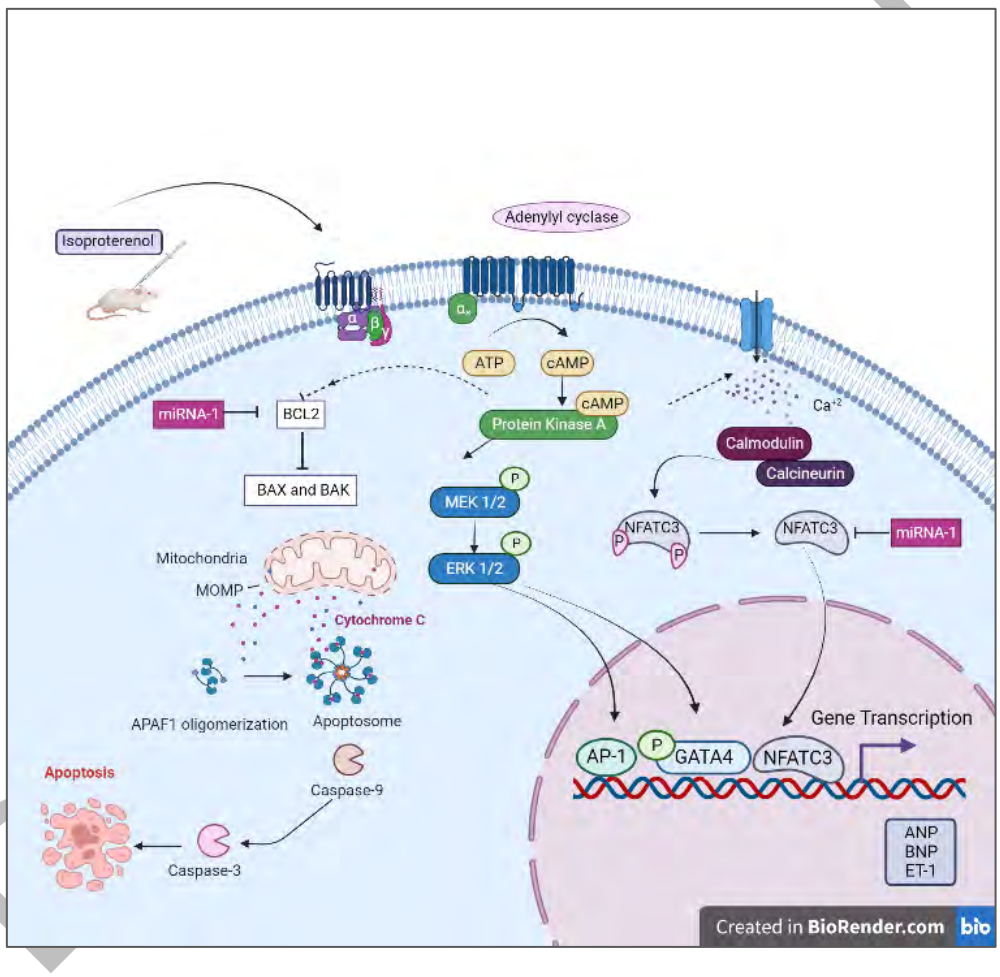

Figure 1.5 miR-1-3p targeted signaling pathway in myocardial infarction

miRNA-1-3p directly targets BCL2 in myocardial infarction (Korshunova *et al.,* 2021) as shown in Figure 1.4. BCL2 causes conformational change of BAK and BAX, which causes the permeability of mitochondrial outer membrane as a result cytochrome C is released from the mitochondria (Jung *et al.,* 2001). Cytochrome complex (cyt c) assembles with apoptotic protease activating factor-1 (APAF-1) leading to the apoptosome formation which results in the activation of caspases (cas-9 and cas-3)

ultimately causing the apoptosis of cardiomyocytes (H. Sun *et al.,* 2006; Youle & Strasser, 2008).

1.9.1.3 miRNA-15a targeted pathway in ISO induced Myocardial Infarction

Isoproterenol directly binds to G-protein coupled receptor (GPCR) which has three subunits i.e., α, β, γ. The α subunit of G-protein is further divided into $G\alpha_s$, $G\alpha_q$ and $G\alpha_i$. The $G\alpha_s$ activates adenylyl cyclase (AC) which converts ATP into cAMP. Increased levels of cAMP further stimulate cAMP dependent PKA which is involved in the phosphorylation of multiple targets.

The $G\alpha_q$ activates phospholipase (PLC) which further cleaves phosphatidylinositol 4,5-bisphophate (PIP2) and results in the formation of inositol trisphosphate (IP3) and diacylglycerol (DAG). IP3 triggers calcium release from endoplasmic reticulum in the intracellular environment. Synthesis of DAG activates Protein Kinase C (PKC). Prolonged ischemia leads to the activation of PKC resulting in the translocation of PKC into the mitochondria where cytochrome C is released from the mitochondria resulting in the suppression of mitochondrial functions. Mitochondrial dysfunction and elevated levels of ROS leads to apoptosis and cardiac dysfunction (Singh *et al.,* 2017). Ischemia expends cellular ATP, decreases calcium efflux, reduces the uptake of intracellular calcium by the endoplasmic reticulum (ER), thereby increasing calcium overload. These changes go along with the opening of mitochondrial permeability transition pore (MPTP) as a result mitochondrial membrane potential is dissipated and impairment of ATP production occurs (Kalogeris *et al.,* 2012).

The activation strength β-adrenergic receptor decides the fate of cardiomyocytes from cell survival to cell death due to the changes in BCL2 expression (Shin *et al.,* 2014). The high concentration range of isoproterenol activates PKA-CREB-ICER pathway that negatively regulates BCL2 expression and promotes cell death (Shin *et al.,* 2014). BCL2 inhibits cell death by preventing the oligomerization of BAK/BAX, which would otherwise cause the release of cytochrome C from the mitochondria as shown in Figure 1.6. The binding of BCL2 will inactivate pro apoptotic genes, thereby inhibiting apoptosis (Tzifi *et al.,* 2012).

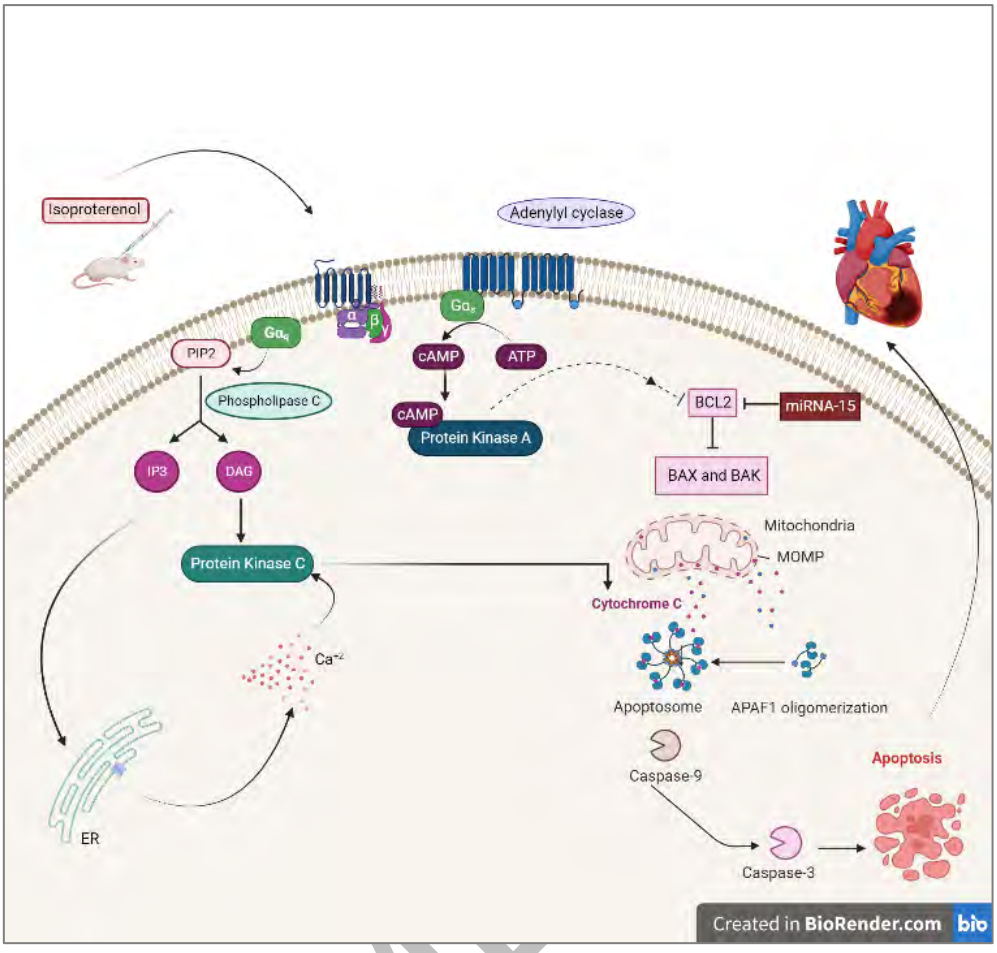

Figure 1.6 miRNA-15a-5p targeted signaling pathway in myocardial infarctions

Studies reported using real time quantitative PCR (RT-qPCR) that the expression of miRNA-15 family is upregulated in myocardial ischemia and heart failure (Liu *et al.,* 2012). miRNA-15a is capable of targeting multiple genes such as BCL2, CCND1, MCL1 and WNT3a. The silencing of antiapoptotic gene i.e., BCL2, by miRNA-15a can inhibits cell growth, induce apoptotic cell death and downregulates the gene expression of miRNA-15a (Ghaffari *et al.,* 2021). Overexpression of miRNA-15a downregulates BCL2 expression and promote apoptosis (Jensen *et al.,* 2014). miRNA-15a regulate apoptosis by down-regulating the expression of BCL2 post-transcriptionally (Cimmino *et al.,* 2005; Guo *et al.,* 2009; Xia *et al.,* 2008). BCL2 is the direct target of miRNA-15a as shown in Figure 1.5 that causes conformational change in the expression of pro apoptotic genes, BAK and BAX, resulting in the release of cytochrome C from the mitochondria (Jung *et al.,* 2001). Cytochrome C assembles with APAF1 leading to the apoptosome formation which results in the activation of caspases (cas-9 and cas-3) ultimately causing the death of cardiomyocytes (H. Sun *et al.,* 2006; Youle & Strasser, 2008).

1.9.1.4 miRNA-98 targeted pathway in ISO induced Myocardial Infarction

The activation of GPCR by isoproterenol stimulates $G\alpha_s$ which results in the activation of adenylyl cyclase and is involved in the conversion of ATP into cAMP. The increased intracellular cAMP activates cAMP dependent PKA results in the phosphorylation of multiple targets. This causes increased intracellular calcium level by opening the calcium channel present on the membrane and also leads to the activation of p38 MAPK pathway. The high levels of calcium in the cytosol causes mitochondrial impairment resulting in ROS production and decreasing the antioxidative enzymes ultimately leading to the death of cardiomyocytes (Eltobshy *et al.,* 2019). Along with these changes, the opening of MPTP results in mitochondrial membrane potential dissipation and leads to impairment of ATP production (Kalogeris *et al.,* 2012). The p38 MAPK is phosphorylated in response to oxidative stress. There is an increase generation of ROS during hypoxic conditions.

Studies reported that to the activation of p38 MAPK depends on small GTPase RhoA. The activated p38 MAPK activates GATA4 which belongs to a family of transcription factors that contains zinc finger motifs. It is demonstrated that ERK1/2 phosphorylates GATA4 at serine 105 as a response to stress induced activation or agonist stimulation, but the same phosphorylation occurs weakly through other branches of MAPK such as JNK. The MAPK/ERK1/2 dependent phosphorylation of GATA4 is associated with the stress induced upregulation of ET-1 promoter (Mutlak & Kehat, 2015). A study reported ROCK-1 to be involved in transcription of ET-1 by GATA4 while inhibition of the Rho/ROCK pathway leads to ERK1/2 phosphorylation and increases transcriptional activity of GATA4 in cardiomyocytes (Yanazume *et al.,* 2002). It has been reported that ET-1 gene contains specific binding site for GATA4. Studies conducted on rat models have also shown that the ET-1 gene promoter has particular binding site for GATA4 (Kalogeris *et al.,* 2012). In myocytes, GATA4 has a key role in the regulation of various genes like BNP, ANP, α-myosin and β-myosin heavy chain, muscarinic receptor, cardiac troponin C and A1 adenosine receptors (Cargnello & Roux, 2011).

In MAPK signaling cascade, various protein kinases are involved such as ERK, JNK and p38 MAPK. Upon activation of these protein kinases, phosphorylation of transcription factors such as MEF2, activating transcription factor 2 (ATF2), eukaryotic initiation factor 1 (EIK1), p53, NFATC3, Max, c-Jun and c-Myc take place (Xu *et al.,*

2012). On the other side, the stimulation of β-adrenergic receptor also leads to the increased intracellular calcium level due to the influx of calcium via calcium channel. The calcium will bind to calmodulin which is a calcium binding protein and changes its conformation as a result calmodulin regulated phosphatase, calcineurin, is activated (Creamer, 2020; Schulman & Anderson, 2010). The calmodulin-calcineurin complex dephosphorylates NFATC3 and then dephosphorylated NFATC3 moves towards the nucleus as shown in Figure 1.7. Studies revealed that NFATC3 shows specific interaction with GATA4 and is involved in the expression of cardiac ischemia and hypertrophy linked genes i.e., ANP, BNP and ET-1 (Molkentin, 2004).

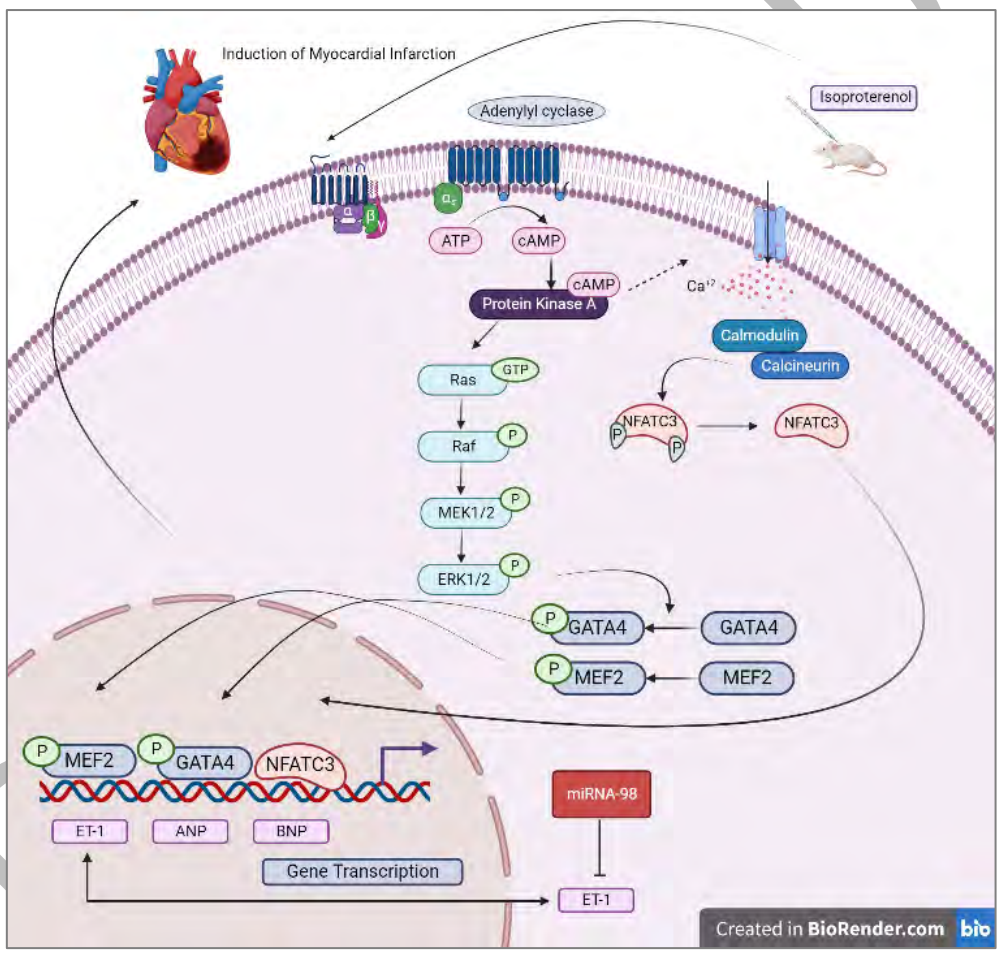

Figure 1.7 miRNA-98-5p targeted signaling pathway in myocardial infarction

miRNA-98 directly targets at 3'UTR of ET-1 mRNA as shown in Figure 1.6. Studies revealed that miRNA-98 acts as a potent marker for renal injury caused by cardiac ischemia (Wang *et al.,* 2014) and involved in the protection of endothelial cells against cardiac ischemia induced cell death (H. W. Li *et al.,* 2015). It is also known that miRNA-98 plays cardioprotective role against cardiac infarction (C. Sun *et al.,* 2017).

Moreover, it is also involved in regulating cardiac ischemia as ET-1 is the direct target of miRNA-98 so as a result ANP and BNP genes will be downregulated.

1.10 Aims and Objectives

- ✓ To evaluate the expression of miRNA-1, miRNA-15a, miRNA-98 to understand the underlying molecular mechanism in circulation of myocardial infarction patients and *in vivo* rat model.
- ✓ To investigate the expression of target genes of miRNAs i.e., NFATC3, ANP, BNP, BCL2 and ET-1 in myocardial infarction patients and *in vivo* rat model.
- ✓ To design an early diagnostic system to assess the dysregulated levels of different circulatory miRNAs in myocardial infarction patients.

2 MATERIALS AND METHODS

2.1 Ethical Consideration

For the current study, myocardial infarction patients' blood samples were taken from Lady Reading Hospital, Peshawar and Sprague Dawley male rats were taken from the primate facility of Faculty of Biological Sciences at Quaid-i-Azam University, Islamabad. All the experiments were conducted by following the guidelines of National Institute of Health (NIH) Islamabad, Pakistan under the instructions provided by the ethical committee of Quaid-i-Azam University Islamabad, Pakistan.

2.2 Study Design

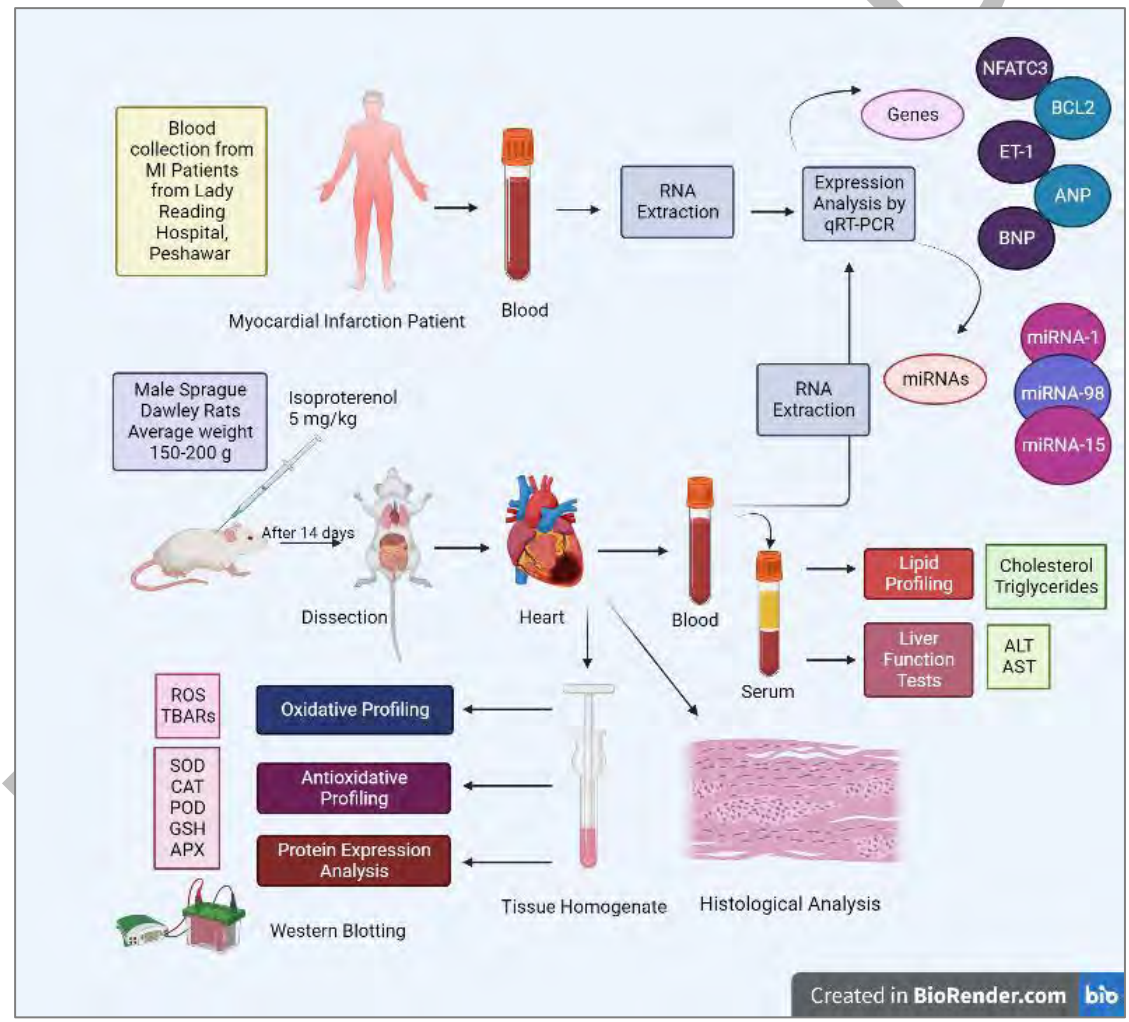

Figure 2.1 Study Design

2.3 Selection of Patients

The blood was collected from eleven patients who were diagnosed with myocardial infarction and were under treatment at Lady Reading Hospital, Khyber Pakhtunkhwa,

Pakistan. The questionnaires were filled by taking interviews from patients and their guardians, individually. It comprised of various parameters such as weight, blood pressure, family history, time since diagnosis of myocardial infarction and smoking status of patients. The demographic data sheet consisted of gender, age, ethnicity and marital status of patients. Other diseases like lung disease, liver disease and diabetes were also included. Eleven healthy control subjects with the same age and social conditions as that of patients were selected.

2.4 Blood Collection from Human

The blood was collected from the cephalic vein of patient's forearm with the help of sterile syringe using vein puncture method. 1 mL of blood was collected in EDTA tube containing 2 mL TRIzol and stored in ice. Then the blood was shifted into eppendorf and centrifuged at 13,500 rpm for 10 minutes. Upper layer of plasma was isolated and 300 µL of TRIzol was added in whole blood samples and stored at -80 °C.

2.5 Dose Regimen

Male Sprague Dawley rats of the average weight 150 g were selected. To induce cardiac ischemia, isoproterenol of 5 mg/kg was dissolved in 500 µL of injection water. Seven alternative doses of isoproterenol were administered subcutaneously for 14 days (T. Ali *et al.,* 2019). Control group was administered with 500 µL normal saline water for 14 days, alternatively.

2.6 Tissue Collection

Once the dosage period was completed, the experimental rats were observed, weighed and dissected. Blood was collected from the hearts of the dissected rats into clot tubes and centrifuged at 6000 rpm for 15 minutes. The upper layer of serum was separated into eppendorf. Then for RNA extraction and protein analysis, heart tissues were weighed and collected which were then divided into different fractions, some parts were treated with TRIzol followed by RNA extraction and some were stored for tissue homogenization. For histological analysis, remaining parts were fixed in 10% formalin.

2.7 Tissue Homogenization

Organs were homogenized and lysates were prepared by using Radio immune precipitation assay (RIPA) extraction buffer.

Following reagents were required to make RIPA extraction buffer:

Reagents	Concentration
Tris Cl (pH 8.0)	10 mM
EDTA	1 mM
Triton X-100	1%
Phenyl methylsulfonyl fluoride (PMSF)	1 mM
Sodium deoxycholate	0.1%
Sodium Chloride (NaCl)	140 mM
Sodium Dodecyl Sulfate (SDS)	0.1%

Procedure

The tissues collected from the rats were weighed 100 mg approximately and homogenized in 350 µL of RIPA extraction buffer containing phenylmethylsulphonyl fluoride (PMSF) by using electric homogenizer (Bio-Gen PRO200, PRO Scientific). Then the homogenized samples were centrifuged at 13000 rpm for 10 minutes at 4 °C. After centrifugation, supernatant was collected in separate tubes and stored at -20 °C for further analysis.

2.8 Oxidative Profiling

To check the oxidative stress in the serum and tissue lysates samples of experimental rats, ROS and TBARs assays were performed.

2.8.1 Reactive Oxygen Species (ROS) Assay

ROS assay was carried out according to the protocol described in (Hayashi *et al.,* 2007). This assay was performed on both serum and tissue homogenates samples.

Principle

Free radicals present in the samples interact with N, N-Diethyl para-phenylenediamine (DEPPD) in the presence of ferrous ion leading to the formation of stable colored cation. Greater the number of free radicals present in the sample, greater will be the production of colored cation which is directly proportional to the absorbance measured.

Reagents required for this assay are mentioned below along with their concentrations:

Reagents	Concentration	Volume
Sample		6.6 µL

Sodium Acetate Buffer pH 4.8	0.1 M	133.3 µL
R1: DEPPD	1 mg/mL	1/25
R2: $FeSO_4$	0.5%	24/25

Procedure

Firstly, reagent 1 and reagent 2 were prepared by dissolving DEPPD and ferrous sulphate in sodium acetate buffer, respectively. Then reagent mixture was prepared by dissolving 1 volume of reagent 1 and 24 volumes of reagent 2 followed by 2 minutes of incubation in dark. Hydrogen peroxide dilutions of 1 M to 10 M were prepared in order to generate standard curve. 5 µL of distilled water, 5 µL of H_2O_2 dilution (1 M to 10 M) and 5 µL of samples were added in separate wells of microtiter plate. Then in each well, 140 µL of sodium acetate buffer (pH 4.8) and 100 µL of reagent mixture were added. Then the mixture was incubated for 60 seconds and absorbance was determined at 505 nm. Three number of readings were taken after every 15 seconds by Multiskan GO (Thermo Fisher Scientific, USA) spectrophotometer.

2.8.2 Thiobarbituric Acid Reactive substances (TBARs) Assay

TBARs activity was measured in the samples as per the protocol mentioned in (Tsai *et al.,* 2014).

Principle

Malondialdehyde (MDA) is formed as result of peroxidation of lipids. MDA interacts with Thiobarbituric acid (TBA) and results in the formation of colored product. Production of colored product is directly proportional to the levels of MDA in the samples which is an indication of thiobarbituric acid reactive substances.

Following reagents were required for TBARs assay:

Reagents	Concentration	Volume
Sample		20 µL
Tris HCl	150 mM	8.33 µL
Ferrous Sulphate ($FeSO_4$)	1 mM	8.33 µL
Ascorbic acid	1.5 mM	8.33 µL
Trichloroacetic acid (TCA)	10%	83.3 µL
Thiobarbituric acid (TBA)	0.375%	83.3 µL

Distilled water		50 µL

Procedure

8.33 µL of sample was added in eppendorf tube followed by the addition of 8.33 µL of Tris HCL, 8.33 µL of ferrous sulphate and 8.33 µL of ascorbic acid, respectively. 50 µL of distilled H_2O was added in the mixture and plate incubated at room temperature for 15 minutes. After the completion of incubation period, 83.3 µL of TCA and 83.3 µL of TBA was added in the mixture. Then the eppendorfs containing mixture were placed in water bath at 95 °C for 10 minutes and centrifuged at 3000 rpm for 10 minutes. After that, 250 µL of supernatant was collected and added in the well of microtiter plate. Absorbance was determined at 532 nm by Multiskan GO (Thermo Fisher Scientific, USA) spectrophotometer. Three readings were taken after every 15 seconds and the level of lipid peroxidation was calculated by the formula given below:

TBARS (nM/mg of protein) = O.D * Sample volume * 1.56 * 105 * Total volume * protein (mg/mL)

2.9 Anti-Oxidative Profile

In the serum and heart homogenate samples of experimental rats, the anti-oxidant levels were checked by performing SOD, CAT, POD, APX and GSH assays

2.9.1 Super Oxide Dismutase (SOD) Assay

Anti-oxidative profiling was performed to measure SOD activity in the homogenates and serum samples according to the protocol described in (Ishtiaq *et al.,* 2020).

Principle

SOD converts free radicals into H_2O_2 and molecular oxygen. The activity of SOD can be measured by the ability of free radicals to interact with nitro-blue tetrazolium (NBT) and the conversion of yellow colored tetrazolium into blue colored product, formazan. Absorbance of the end product is measured at 560 nm. Greater the intensity of absorbance, lesser will be the activity of SOD. Riboflavin acts as a reaction initiator whereby L-methionine acts as an electron donor.

Following reagents were required for SOD assay:

Reagents	Concentration	Volume
Sample		5 µL
Potassium Phosphate Buffer; pH 7.8	50 mM	26.75 mL
L-Methionine	9.9 µM	1.5 mL
NBT	57 µM	1 mL
Triton X-100	0.025%	750 µL
Riboflavin	0.9 µM	3 µL

Procedure

1.5 mL L-methionine, 750 µL Triton X-100 and 1 mL NBT were mixed together to prepare 3.25 µL of reagent mixture followed by the addition of 26.75 mL of potassium phosphate buffer resulting in 30 mL reagent mixture. In each well of the 96 well microtiter plate, 5 µL of sample and 250 µL of the reagent mixture were added. Reagent mixture except sample was taken as blank in one of the wells of the plate. Fluorescent light was given to illuminate the microtiter plate at room temperature for 7 minutes followed by 5 minutes of incubation at 37 °C. Then 3 µL of riboflavin was added to each well followed by 8 minutes of incubation at 40 °C. After incubation, three readings were recorded with a gap of 1 minute at a wavelength of 560 nm by Multiskan GO (Thermo Fisher Scientific, USA) spectrophotometer. NBT inhibition value was calculated by the formula given below:

$(Abs._{Blank} - Abs._{Sample}) / (Abs._{Blank}) * 100$

2.9.2 Catalase Activity (CAT) Assay

CAT assay was performed to measure free H_2O_2 present in the sample as per the protocol described in (T. Ali *et al.,* 2019).

Principle

Catalase enzyme functions to convert H_2O_2 into water and oxygen. Activity of the enzyme can be measured by measuring the levels of unconverted H_2O_2 in the sample. Reagents and unconverted H_2O_2 interact to form a product whose absorbance can be measured at 240 nm. Greater the intensity of absorbance, lesser will be the activity of enzyme.

Following reagents were required for CAT assay:

Reagents	Concentration	Volume
Sample		8.09 µL
Potassium Phosphate Buffer; pH 7.0	50 mM	161 µL
H_2O_2	5.9 mM	80.90 µL

Procedure

161 µL of potassium phosphate buffer, 80.90 µL of H_2O_2 and 8.90 µL of sample were added in each well of the 96-well microtiter plate. Mixture of all reagents except sample was taken as blank in one of the wells of the microtiter plate. Absorbance was measured at 240 nm by Multiskan GO (Thermo Fisher Scientific, USA) spectrophotometer. Three readings were recorded with a gap of 30 seconds.

2.9.3 Peroxidase (POD) Assay

Principle

Peroxidase enzyme converts H_2O_2 into water and oxygen. Activity of the enzyme can be measured by measuring the levels of H_2O_2 in the sample. Interaction of reagents with H_2O_2 results in the formation of a product whose absorbance was measured at 420 nm.

Following reagents were required for POD assay (T. Ali *et al.,* 2019):

Reagents	Concentration	Volume
Sample		8.33 µL
Potassium Phosphate Buffer; pH 5.0	50 mM	208.3 µL
Guaiacol	20 mM	8.33 µL
H_2O_2	40 mM	25 µL

Procedure

208.3 µL of potassium phosphate buffer, 8.33 µL of guaiacol and 8.33 µL of sample were added in each well of the 96-well microtiter plate. 25 µL of H_2O_2 was added at the end. Mixture of all reagents except sample was added as blank in one of the wells of the plate. Absorbance was determined at 470 nm. Three number of readings were recorded with an interval of 1 minute by Multiskan GO (Thermo Fisher Scientific, USA) spectrophotometer.

2.9.4 Ascorbate Peroxidase (APX) Assay

APX assay was performed as per the protocol described in (T. Ali *et al.,* 2019)

Principle

Ascorbate peroxidase reduces hydrogen peroxide into water and oxygen. H_2O_2 uses ascorbic acid as its substrate. Another end product of this reaction is mono-dehydroascorbic acid (MDHA). MDHA is reduced to ascorbate by a reductase enzyme which leads to the reduction in absorbance measured at 290 nm.

Following reagents were required for APX assay:

Reagents	Concentration	Volume
Sample		15 µL
Potassium Phosphate Buffer; pH 7.0	50 mM	150 µL
EDTA	1 mM	15 µL
Ascorbate	5 mM	15 µL
H_2O_2	1 mM	15 µL

Procedure

105 µL of potassium phosphate buffer, 15 µL of ascorbate, 15 µL of EDTA and 15 µL of H_2O_2 was added in one of the wells of 96-well microtiter plate which was considered as blank. In other wells, 15 µL of sample, 90 µL of potassium phosphate buffer, 15 µL of ascorbate, 15 µL of EDTA and 15 µL of H_2O_2. Absorbance was determined at 290 nm by Multiskan GO (Thermo Fisher Scientific, USA) spectrophotometer. Three readings were recorded and the enzyme activity was measured by using following formula:

Ascorbate Activity = Absorbance * Extinction co-efficient of ascorbate

2.9.5 Reduced Glutathione (GSH) Assay

Principle

5,5'-dithiobis-2-nitrobenzoic acid (DTNB) oxidizes GSH, as a result a yellow colored product, 5'-thio-2-nitrobenzoic acid (TNB), whose absorbance can be measured at 412 nm.

Following reagents were required for GSH assay:

Reagents	Concentration	Volume
Sample		15.62 µL
DTNB	0.4%	78.12 µL
Sodium Phosphate Buffer	0.4 M	156.25 µL

Procedure

15.62 µL sample was added in each well of the of 96-well microtiter plate followed by the addition of 156.25 µL of buffer and 78.12 µL of DTNB. Appearance of yellow color was an indication that GSH was present in the sample. Absorbance was measured at 412 nm by Multiskan GO (Thermo Fisher Scientific, USA) spectrophotometer.

2.10 Liver Function Tests

The important markers to check the functionality of liver are alanine aminotransferase (ALT) and aspartate aminotransferase (AST) enzymes. ALT and AST assays were performed to check the levels of these enzymes.

2.10.1 Alanine Aminotransferase (ALT) Assay

AMP Diagnostics Kit protocol was used to measure the level of ALT enzyme in the serum samples.

Following reagents of kit were used for ALT assay:

Reagents	Concentration	Volume
Sample		10 µL
Reagent 1 (Tris-buffer, L- Alanine, Lactate Dehydrogenase) pH 7.3	150mM, 750mM/L, >1.350 U/L	4/5
Reagent 2 (NADH, 2- Oxoglutarate, Biocides)	1.3 mM, 75mM	1/5

Procedure

Reagents from the kit were mixed to prepare the reaction mixture. Four volumes of R1 and one volume of R2 were mixed depending upon the number of samples. 10 µL of serum sample was added in each well of the 96-well microtiter plate followed by the addition of 200 µL of reagent mixture. Mixture was incubated for 1 minute at room temperature. Absorbance was recorded at 340 nm by Multiskan GO (Thermo Fisher

Scientific, USA) spectrophotometer. Three readings were taken with a gap of 60 seconds. ALT levels were calculated by using the kit formula mentioned below:

ALT Activity (unit/L) at 37 °C = ΔA / min * 3333

2.10.2 Aspartate Aminotransferase (AST) Assay

AMP Diagnostics Kit protocol was used to check the levels of AST enzyme in serum samples.

Following reagents of kit were used for AST assay:

Reagents	Concentration	Volume
Sample		10 µL
Reagent 1 (Tris-buffer, L-aspartate, MDH, LDH) pH 7.8	121 mM, 362 mM/L, >460 U/L, >600 U/L	4/5
Reagent 2 (NADH, 2- Oxoglutarate, Biocides)	1.3 mM/L	1/5

Procedure

Reagents from the kit were mixed to prepare the reagent mixture. Depending upon the number of samples, reagent 1 and reagent 2 were mixed at the ratio of 4:1. In each well of 96-well microtiter plate, 10 µL of serum sample and 200 µL of reagent mixture were added. Plate was incubated at room temperature for 1 minute. Three readings were taken with a gap of 60 seconds at a wavelength of 340 nm by Multiskan GO (Thermo Fisher Scientific, USA) spectrophotometer. The level of AST in serum samples was calculated by using the kit formula mentioned below:

AST Activity (unit/L) at 37 °C = ΔA / min * 3333

2.11 Lipid Profile

Lipid profiling was done by performing cholesterol and triglycerides assays.

2.11.1 Cholesterol Assay

AMP Diagnostics Kit protocol was used to perform cholesterol assay

Principle

Enzymes such as peroxidase, cholesterol oxidase and esterase contain H_2O_2, which when interact with 4-aminoantipyrine and phenol present in the reaction mixture, result

in the formation of quinonimine dye which is directly proportional to cholesterol present in the samples.

Following reagents of kit were used for cholesterol assay:

Reagents	Volume
Sample	2 µL
Standard	2 µL
Cholesterol reagent	200 µL

Procedure

2 µL of standard was added in one of the wells of 96-well microtiter plate. 2 µL of serum samples were added in the remaining wells of microtiter plate. 200 µL of reagent was added in all the wells of the plate. The mixture was incubated for 5 minutes at room temperature. Then the absorbance was recorded at 500 nm. Three readings were taken by using Multiskan GO (Thermo Fisher Scientific, USA) spectrophotometer. The amount of total cholesterol was calculated by using the formula given below:

Cholesterol (mg/dL) = Sample $_{abs}$ / Standard $_{abs}$ * Concentration of Standard

2.11.2 Triglycerides Assay

Levels of triglycerides were measured in the serum samples by following the protocol mentioned in AMP Diagnostics Kit.

Following reagents of the kit were required for triglycerides assay:

Reagents	Volume
Sample	2 µL
Standard	2 µL
Triglyceride reagent	200 µL

Principle

Triglycerides are converted into fatty acids and glycerol. The phosphorylated glycerol, is oxidized into dihydroxyacetone phosphate and H_2O_2 by oxidase enzyme. When H_2O_2 interacts with 4-aminoantipyrine and phenol present in the reaction reagent mixture, red colored product is formed which shows the triglycerides present in the sample.

Procedure

2 µL of standard was added in one of the wells of 96-well microtiter plate. 2 µL of serum samples were added in the remaining wells of the microtiter plate. 200 µL of reagent was added in all the wells of the plate. The mixture was incubated for 5 minutes at room temperature. Then the absorbance was determined at 500 nm. Three readings were taken by Mutiskan GO (Thermo Fisher Scientific, USA) spectrophotometer. The number of total triglycerides were calculated by using the formula given below:

Total Triglycerides (mg/dL) = Sample $_{abs}$ / Standard $_{abs}$ * Concentration of Standard

2.12 Bradford Assay for Quantification of Protein

Bradford assay was used to quantify proteins in tissue homogenates and serum samples. 10 M stock solution of bovine serum albumin (BSA) was prepared and diluted with distilled water. For the generation of standard curve, 1 M to 10 M dilutions were prepared. Absorbance of proteins and BSA dilutions were measured at the wavelength of 595 nm by Multiskan GO (Thermo Fisher Scientific, USA) microplate spectrophotometer.

Reagents

Following reagents were used for Bradford assay:

Reagents	Concentration	Volume
BSA dilutions	1 M – 10 M	5 µL
Distilled water		5 µL
Bradford Reagent		200 µL

Procedure

Bradford reagent mixture was prepared by mixing 1 volume of reagent with 4 volumes of distilled water. After the preparation of reagent mixture, 5 µL of BSA dilutions (1 M to 10 M) and 5 µL sample were added in each well of the 96-well microtiter plate. 200 µL of Bradford reagent mixture was added in each well followed by 30 minutes incubation in dark at room temperature. After 30 minutes, absorbance was measured at a wavelength of 595 nm by Multiskan GO (Thermo Fisher Scientific, USA) spectrophotometer. Three readings were recorded and a standard curve of BSA serial dilutions was plotted by using linear line equation as shown in Figure 2.2.

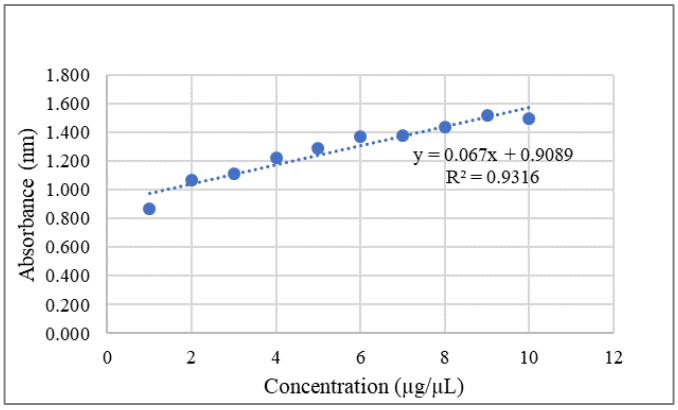

Figure 2.2 Standard Curve of BSA

2.13 Western Blotting

To identify the expression of proteins in different samples, western blotting was performed. For this technique, (Ma *et al.,* 2005) protocol was followed.

Following steps are involved in western blotting:

- Gel preparation
- Gel electrophoresis
- Transfer of protein from gel onto nitrocellulose (NC) membrane
- Blocking
- Treatment with primary and secondary antibodies
- Detection

2.13.1 Gel Preparation and Gel Electrophoresis

SDS gel was prepared from the reagents mentioned below:

Separating Gel (12%)

Reagents	Volume
Distilled water	4125 µL
Tris HCl (1.5 M; pH 8.8)	3125 µL
SDS (10%)	125 µL
Bis-acrylamide (30%)	5000 µL
APS (10%)	125 µL
TEMED	7.5 µL

Stacking Gel (4%)

Reagents	Volume
Distilled water	4187.5 µL
Tris HCl (0.5 M; pH 6.8)	625 µL
SDS (!0%)	62.5 µL
Bis-acrylamide (30%)	875 µL
APS (10 %)	75 µL
TEMED	9.3 µL

Procedure

First of all, spacer plate and cover glass were placed on top of each other and secured in gel cassette to set the gel casting apparatus. Distilled water was added to check the leakage, then the plates were dried with filter paper. Separating gel (12%) was prepared by mixing all the reagents and poured in between the gel plates. After that isopropanol was added on the surface of separating gel to remove the bubbles. The separating gel was solidified at room temperature for about 40 to 45 minutes. After gel solidification, isopropanol was discarded and the polymerized gel was washed with distilled H_2O for three times and then dried with the help of filter paper. In the next step, stacking gel (4%) was prepared by mixing all the reagents and was poured on the top of separating gel followed by the insertion of comb to create wells in the gel. Then the stacking gel was solidified at room temperature for about 30 minutes. After solidification, the cassettes were separated from the gel casting apparatus and were placed onto clamping apparatus in running buffer.

2.13.2 Sample Preparation

Reagents

For the preparation of sample following reagents were required:

2X SDS Gel Loading Buffer

Reagents	Concentration
Dithiothreitol	200 mM
Glycerol	0.2%
Tris HCl; pH 6.8	62.5 mM

SDS	2%
Bromophenol blue	0.01%

Procedure

For loading of samples in the wells, samples (30 µg protein) were mixed with 5 µL of SDS loading dye and running buffer was added in a way to make total volume of 15 µL. Samples were incubated in water bath at 95 °C for 10 minutes followed by 1 minute of centrifugation at 2000 rpm.

2.13.3 Sample Loading and Gel Running

Reagents

SDS Running Buffer 5X, pH 8.3

Reagents	Concentration
Tris base	125 mM
Glycine	1.25%
SDS	0.50%

Procedure

Firstly, SDS running buffer 1X was prepared by adding 200 mL of SDS running buffer 5X in 800 mL of distilled water. Gel plates were placed inside the clamping apparatus and 1X running buffer was poured into the tank. Ladder was loaded in the first well and other samples were loaded in the separate wells. Initially, the gel was run at 90 volts for 45 minutes till the dye reached the separating gel, then the voltage was changed to 120 volts till the loading dye reached the end of the plates. Finally, the voltage was changed to 150 volts for 5 minutes.

2.13.4 Gel Staining

Reagents

For gel staining solutions, following reagents were required:

Solutions	Reagents
Fixing Solution	50% Methanol
	10% Glacial acetic acid
	Distilled water

Staining Solution	0.1% Coomassie R-250
	50% Methanol
	10% Glacial acetic acid
	Distilled water
Destaining Solution	40% Methanol
	10% Glacial acetic acid
	Distilled water
Storage Solution	5% Glacial acetic acid

Procedure

Gel was carefully taken out from the cassette and soaked in the fixing solution followed by overnight incubation at room temperature with continuous shaking. After fixing the gel, the fixing solution was replaced by staining solution and gel was stained for 20 minutes with continuous shaking. Then staining solution was discarded and the gel was shifted in destaining solution for half an hour which was restored several times until the background became clear. Gel was stored in storage solution and the bands were seen. Staining of gel was not required for the gel which was processed for the transfer of proteins onto nitrocellulose membrane.

2.13.5 Transferring Proteins onto Nitrocellulose Membrane

For the transfer of protein from gel onto nitrocellulose membrane, transfer buffer, ponceau stain and Tris buffered saline with 0.1% Tween-20 (TBST) were required.

Transfer Buffer

6.05 g of Tris base was dissolved in 50 mL of distilled H_2O to prepare 1 M solution. From 50 mL of Tris base solution, 25 mL of solution was taken followed by the addition of 14.4 g of glycine and 200 mL of absolute methanol. Finally, the volume was raised to 1000 mL by the addition of distilled H_2O.

Reagents	Concentration	Volume
Tris base	1 M	25 mL
Glycine	192 mM	14.4 g
Methanol	Absolute	200 mL
Distilled water		Raise volume upto 1 L

Ponceau Stain

0.5 g of ponceau stain was dissolved in 5 mL of glacial acetic acid and volume was raised to 500 mL by the addition of distilled H_2O.

Reagents	Volume
Ponceau stain	0.5 g
Glacial acetic acid	5 mL
Distilled water	

Tris buffered saline with Tween (TBST)

6.057 g of Tris base was dissolved in 50 mL of distilled H_2O and its pH was maintained at 8.0. 3 M NaCl was prepared by adding 8.775 g of salt in 50 mL of distilled H_2O. Then 25 mL of Tris base solution was taken and added in 50 mL of NaCl solution followed by the addition of 1 mL Tween-20. Finally, the volume of the solution was raised to 1000 mL by the addition of distilled H_2O.

Reagents	Concentration	Volume
Tris base; pH 8	1 M	25 mL
NaCl	3 M	50 mL
Tween-20		1 mL
Distilled water		Raise volume upto 1 L

Procedure

For transfer of gel onto nitrocellulose membrane, 12 filter papers were cut into equal sizes. Six filter papers were soaked in transfer buffer and were placed on blotting apparatus. In the next step, nitrocellulose membrane was soaked in transfer buffer and was placed on previously arranged filter papers followed by the placement of gel on top of nitrocellulose membrane. Then six more filter papers were soaked in transfer buffer and were placed on top of the gel creating a sandwich like arrangement in which nitrocellulose membrane is embedded in between filter papers and gel. 10 volts of voltage was applied for about 40 minutes. To confirm protein transfer onto nitrocellulose membrane, ponceau staining was performed followed by membrane washing by TBST.

2.13.6 Blocking

Preparation of Blocking Solution

5% of blocking solution was prepared by adding 0.5 g of skimmed milk or BSA in 10 mL of TBST.

Procedure

Nitrocellulose membrane was soaked in 5% of blocking solution to block all those sites on membrane where non-specific binding could occur. After soaking the membrane for 45 minutes, nitrocellulose membrane was washed with TBST for three times.

2.13.7 Antibody Treatment

Primary Antibody

Target Proteins	Primary Antibodies
GAPDH	SC-332233 Santa Cruz Biotechnology
NFATC3	SC-8405 Santa Cruz Biotechnology
Et-1	MA3-005 ThermoFisher Scientific

Secondary Antibody

Secondary Antibody
Goat Antimouse (IgG) ThermoFisher

Dilution of Antibody

Primary and secondary antibodies were diluted in 5% of BSA solution at the ratio of 1:2000 and 1:7000, respectively.

Procedure

Nitrocellulose membrane was incubated overnight at 4 °C. After 24 hours, membrane was washed with TBST for three times. The membrane was then incubated continuously on shaker with secondary antibody for two hours at room temperature. After incubation of secondary antibody, membrane was washed with TBST.

2.13.8 Detection

Chromogenic detection method was used in this protocol. For the detection of the signal, 5-bromo-4-chloro-3-indolylphosphate (BCIP) / Nitro Blue Tetrazolium (NBT) was used as a substrate.

Procedure

Nitrocellulose membrane was treated with 1 mL of NBT substrate followed by 30 minutes of incubation in dark. After that, bands were observed and photographs were taken. Densitometric analysis was done by using ImageJ software.

2.14 Expression Analysis of miRNAs and Genes

To analyze the expression of miRNAs and the targeted genes, qRT-PCR was performed. Firstly, RNA was extracted from the blood and tissue samples which was used as a template for cDNA synthesis followed by Quantitative Real Time PCR (qRT-PCR) (Ishtiaq *et al.,* 2020).

2.14.1 RNA Extraction from Human Blood

Following reagents were required for this protocol:

Reagents	Volume
TRIzol	500 µL
Chloroform	50 µL
Isopropanol	150 µL
Glycogen	1 µL
Ethanol (70%)	500 µL
DEPC treated water	10 µL

Procedure

500 µL of TRIzol were added to 1 mL of blood sample and was properly minced with syringe. Then the samples were vortexed for 20 seconds. Then 50 µL of chloroform was added. The samples were vigorously shaken then incubated for 3 minutes at room temperature. For phase separation, samples were placed in centrifuge at 13,500 rpm for 15 minutes keeping the temperature at 4 °C. After this, two layers were formed. Upper aqueous layer was separated and the pellet was discarded. Then 150 µL of isopropanol and 1 µL of glycogen were added to the aqueous layer. Samples were incubated for 5 minutes at room temperature and then transferred onto ice for another 5 minutes. Again, samples were placed in centrifuge at 13,500 rpm for 15 minutes at 4 °C. Then supernatant was discarded and the pellet was washed with 500 µL of 70% ethanol. Samples were vortexed to dissolve the pellet in ethanol and again placed in centrifuge at13,500 rpm for 15 minutes at 4 °C. Supernatant was discarded and to completely

remove ethanol droplets, the pellet was air dried for 10 minutes. Then10 µL of DEPC water was added and vortexed. Quantification of RNA was done by using UV/VIS NanoDrop-1000^{TM} (Nanodrop, V3.7, Thermo Fisher Scientific, USA).

2.14.2 RNA Extraction from Rat Tissue

Following reagents were required for this protocol:

Reagents	Volume
TRIzol	500 µL
Chloroform	50 µL
Isopropanol	150 µL
Ethanol (70%)	500 µL
DEPC treated water	25 µL

Procedure

After the dissection of rats, different organs such as heart, kidneys and liver were collected. The organs were divided into four equal parts. Two parts of heart were finely minced in 300 µL of TRIzol. Then the minced samples were vortexed and 200 µL of TRIzol was added and then sample was minced with the syringe. Then the samples were vortexed for 20 seconds. Then 50 µL of chloroform was added. The samples were vigorously shaken then incubated for 3 minutes at room temperature. For phase separation, samples were placed in centrifuge at 13,500 rpm for 15 minutes keeping the temperature at 4 °C. After this, two layers were formed. Upper aqueous layer was separated and the pellet was discarded. Then 150 µL of isopropanol and 1 µL of glycogen were added to the aqueous layer. Samples were incubated for 5 minutes at room temperature and then transferred onto ice for another 5 minutes. Again, samples were placed in centrifuge at 13,500 rpm for 15 minutes at 4 °C. Then supernatant was discarded and the pellet was washed with 500 µL of 70% ethanol. Samples were vortexed to dissolve the pellet in ethanol and again placed in centrifuge at13,500 rpm for 15 minutes at 4 °C. Supernatant was discarded and to completely remove ethanol droplets, the pellet was air dried for 10 minutes. Then10 µL of DEPC water was added and vortexed. Quantification of RNA was done by using UV/VIS NanoDrop-1000^{TM} (Nanodrop, V3.7, Thermo Fisher Scientific, USA).

2.14.3 cDNA Synthesis

"Revert Aid First Strand cDNA Synthesis Kit" (Thermo Fisher Scientific, USA) was used for the synthesis of cDNA. Following reagents were used in cDNA synthesis kit:

Reagents	Volume
Template RNA	1 µg/5 µg
Random Hexamer Primer	1 µL
Reaction Buffer (5X)	4.5 µL
Ribolock RNase Inhibitor	0.5 µL
dNTP mix (10 mM)	2 µL
RevertAid M-MuLV RT	1 µL
Nuclease Free Water	

Procedure

Components of the kit were thawed properly and a mixture of 12 µL was prepared by mixing template RNA, nuclease free water and random hexamer primer in polymerase chain reaction (PCR) tubes. Then PCR tubes were incubated for 5 minutes at 65 ˚C. After incubation, the PCR tubes were placed on ice and the remaining components of the kit were added in each tube. 4.5 µL of Reaction Buffer, 2 µL of deoxynucleotide triphosphates (dNTPs) mix, 0.5 µL of Ribolock RNase Inhibitor and 1 µL of RevertAid M-MuLV Reverse Transcriptase was added to the previously prepared 12 µL mixture to make total volume of 20 µL. Then the mixture was mixed by tapping the tubes and incubated in thermocycler at 42 °C for 1 hour followed by the termination of reaction at 70 °C for 5 minutes. The cDNA formed was stored at -80 °C.

2.14.4 Quantitative Real Time Polymerase Chain Reaction (qRT-PCR)

For qRT-PCR, firstly cDNA dilutions were prepared. 5 µL of cDNA was added in 20 µL of nuclease free water to make cDNA dilution. For each reaction, 8 µL of reaction mixture was prepared and 2 µL of cDNA dilution was added in each PCR vial making total volume of 10 µL. Following components were required to make reaction mixture for qRT-PCR:

Reagents	Volume
cDNA	2 µL
Forward Primer (gene specific)	0.37 µL
Reverse Primer (gene specific)	0.37 µL
Eva Green	2 µL
Nuclease Free Water	5.26 µL

Procedure

Firstly, reaction mixture was prepared by mixing 5.26 µL of nuclease free water, 0.37 µL of gene or miRNA specific forward primer, 0.37 µL of gene or miRNA specific reverse primer and 2 µL of Eva green dye. 2 µL of cDNA dilution was added in PCR vials and then 8 µL of reaction mixture was added resulting in total volume of 10 µL. PCR vials were placed in the wells of RT machine and expression analysis of particular gene or miRNA was done by running the program designed and saved in MyGoPro. After the reaction was completed, Ct values were recorded. miRNA U6 was taken as an endogenous control and change in fold activity of miRNAs was calculated. Expression of GAPDH in each group was taken as an internal control and fold activity of genes was calculated.

2.15 Histological analysis

After dissection, tissues were fixed in fixatives *i.e.,* 10% formalin, 60% absolute alcohol and 10% acetic acid, to analyze the cellular architecture of tissues under light microscope (DIALUX 20 EB).

2.16 Statistical Analysis

For statistical analysis, all experimental data were evaluated by applying t-test using GraphPad Prism 9.0.0 software which showed that statistics were significant at p value < 0.01 or < 0.05. GraphPad Prism 9.0.0 software was used to plot the graphs.

3 RESULTS

3.1 Demographic Data Analysis of Myocardial Infarction Patients

3.1.1 Gender-wise Distribution

The myocardial infarction patients were divided into two groups on the basis of gender as shown in Figure 3.1. The first group comprised of 8 MI male patients (72.72%). The second group comprised of 3 MI female patients (27%) as shown in Table 3.1.

Table 3.1 Gender-wise Distribution of MI Patients

Gender	No of Patients	Percentage
Male	8	72.72%
Female	3	27.27%

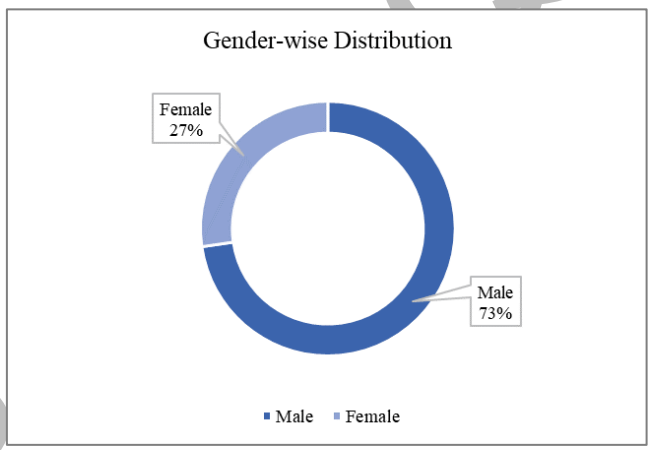

Figure 3.1 Graphical Representation of Gender-wise Distribution of MI Patients

3.1.2 Age-wise Distribution

The myocardial infarction patients were distributed into four groups on the basis of age as shown in Figure 3.2. The first group comprised of MI patients in below 20 age group with 1 patient (9%). The second group comprised of MI patients between 21-40 age group with 2 patients (18%). The third group comprised of MI patients between 41-60 age group with 3 patients (27%). The forth group comprised of MI patients in above 60 age group with 5 patients (45%) as shown in Table 3.2.

Table 3.2 Age-wise Distribution of MI Patients

Age Group	No of Patients	Percentage
< 20	1	9.09%
21-40	2	18.18%
41-60	3	27.27%
> 60	5	45.45%
Grand Total	11	100%

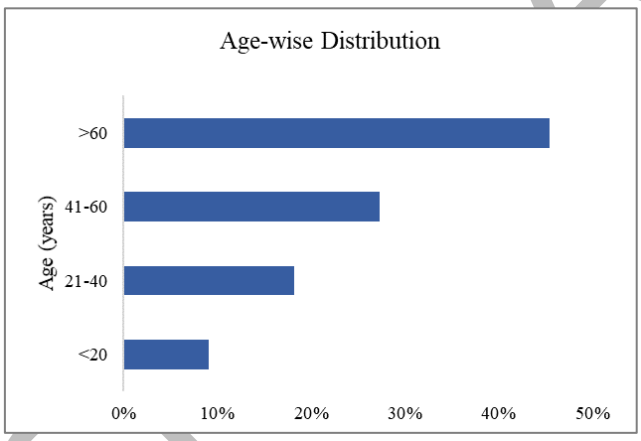

Figure 3.2 Graphical Representation of Age-wise Distribution of MI Patients

3.1.3 Other Diseases in Myocardial Infarction Patients

It was recorded that no patient suffered from asthma and lung disease. All the patients of myocardial infarction were not diagnosed with liver disease. About 27.27% of MI patients were suffering from diabetes as shown in Table 3.3. It was also recorded that 45.45% of myocardial infarction patients were suffering from hypertension. 45.45% of myocardial infarction patients showed high blood pressure as shown in Figure 3.3.

Table 3.3 Other Diseases in MI Patients

Other Diseases	No of Patients	Percentage
Diabetes	3	27.27%
Hypertension	5	45.45%

Blood Pressure	5	45.45%

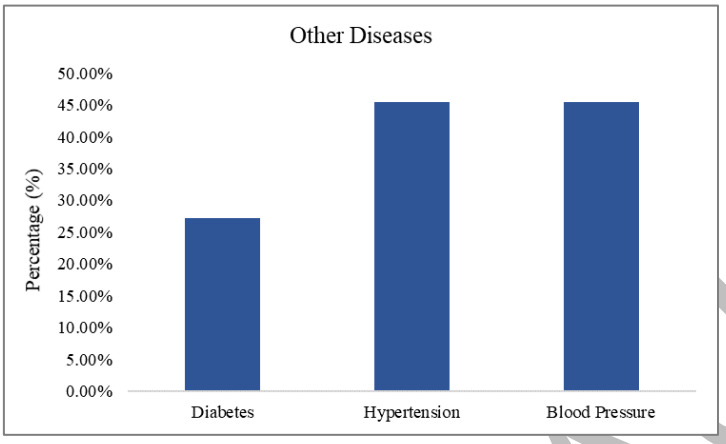

Figure 3.3 Graphical Representation of other diseases in MI patients

3.1.4 Smoking status of Myocardial Infarction Patients

27.27% of myocardial infarction patients were smokers as shown in Figure 3.4 while others were non-smokers as shown in Table 3.4.

Table 3.4 Smoking status of MI Patients

	No of Patients	**Percentage**
Smokers	3	27.27%
Non-Smokers	8	72.72%

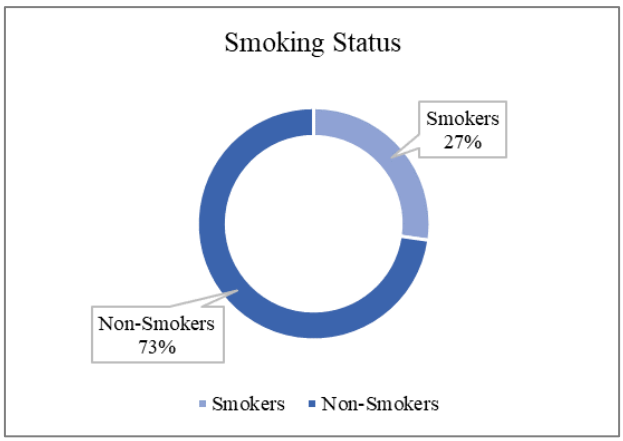

Figure 3.4 Graphical Representation of Smoking Status of MI Patients

3.1.5 Time since diagnosis of Myocardial Infarction in Patients

Out of total 11 patients of myocardial infarction, 3 patients (27.27%) were diagnosed between 3-15 days ago, 2 patients (18.18%) were diagnosed between 2-6 months ago, 1 patient (9.09%) was diagnosed 8 months ago and other patients (45.45%) were diagnosed 2-6 years ago as shown in Figure 3.5.

Table 3.5 Time since diagnosis of MI in Patients

Time since Diagnosis	No of Patients	Percentage
< 15 Days	3	27.27%
< 6 Months	2	18.18%
> 6 Months	1	9.09%
> 2 Years	5	45.45%

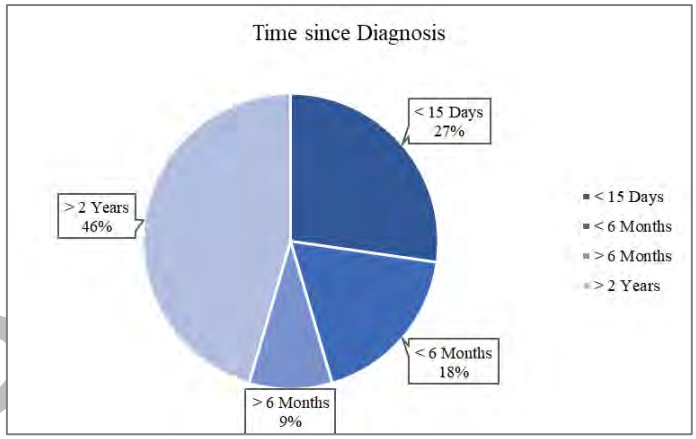

Figure 3.5 Graphical Representation of Time since Diagnosis

3.1.6 Family History of Myocardial Infarction Patients

Out of 11 patients, 5 myocardial infarction patients (45.45%) were recorded with a family history of cardiac diseases.

3.2 Expression of miR-1-3p in Myocardial Infarction Patients' Blood

To validate the expression of miRNA-1-3p in the blood samples of control and MI patients, qRT-PCR was used. U6 was taken as endogenous control and relative fold activity was calculated for miRNA-1-3p. The expression of miRNA-1-3p was

significantly upregulated (relative fold change of 58.97) in the blood samples of MI patients as compared to that of control blood samples as shown in Figure 3.6.

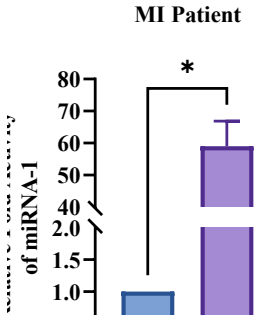

Figure 3.6 Graphical Representation of miRNA-1 Expression in Patients' Blood

(*) Significant in comparison to Control at p value < 0.05

3.3 Expression of miR-15a-5p in Myocardial Infarction Patients' Blood

To validate the expression of miRNA-15a-5p in the blood samples of control and MI patients, qRT-PCR was used. U6 was taken as internal control and relative fold activity was calculated for miRNA-15a-5p. The expression of miRNA-15a-5p was significantly upregulated (relative fold change of 11.48) in the blood samples of MI patients as compared to that of control blood samples as shown in Figure 3.7. For statistical analysis, t-test was applied by using GraphPad Prism software 9.0.0.

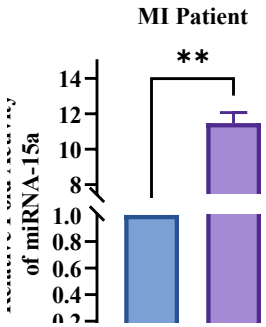

Figure 3.7 Graphical Representation of miRNA-15a Expression in Patients' Blood

(**) Significant in comparison to Control at *p* value < 0.01

3.4 Expression of miR-98-5p in Myocardial Infarction Patients' Blood

miRNA-98-5p plays important role in the regulation of cardiovascular diseases. To validate the expression of miRNA-98-5p in the blood samples of control and MI patients, qRT-PCR was used. U6 was taken as internal control and relative fold activity was calculated for miRNA-98-5p. The expression of miRNA-98-5p was significantly downregulated (relative fold change of 0.03797) in the blood samples of MI patients as compared to that of control blood samples as shown in Figure 3.8. For statistical analysis, t-test was applied by using GraphPad Prism software 9.0.0.

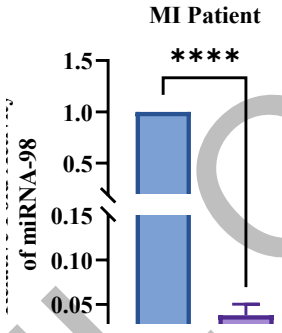

Figure 3.8 Graphical Representation of miRNA-98 Expression in Patients' Blood

(****) Significant in comparison to Control at *p* value < 0.0001

3.5 Expression of NFATC3 in Myocardial Infarction Patients' Blood

By using TargetScan it was confirmed that NFATC3 is the target of miRNA1-3p as shown in Figure 3.9. The expression analysis of NFATC3 was done by qRT-PCR. GAPDH was used as a control and relative fold activity of NFATC3 was calculated. The expression of NFATC3 was significantly downregulated (relative fold change of 0.00549) in the blood samples of MI patients as compared to that of control blood samples as shown in Figure 3.10. For statistical analysis, t-test was applied using GraphPad Prism software 9.0.0.

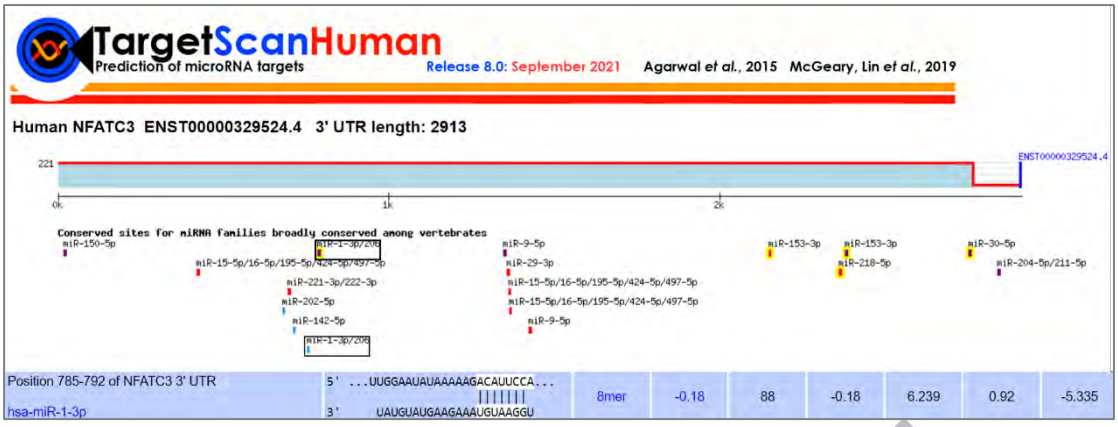

Figure 3.9 Putative miRNA-1-3p Target Binding Sites Predicted by TargetScan

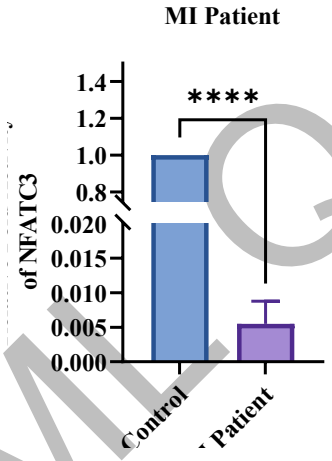

Figure 3.10 Graphical Representation of NFATC3 Expression in MI Patients' Blood

(****) Significant in comparison to Control at *p* value < 0.0001

3.6 Expression of BCL2 in Myocardial Infarction Patients' Blood

By using TargetScan it was confirmed that BCL2 is the target of miRNA15a-5p as shown in Figure 3.11. The expression analysis of BCL2 was done by qRT-PCR. GAPDH was used as control and relative fold activity of BCL2 was calculated. The expression of BCL2 was significantly downregulated (relative fold change of 0.005239) in the blood samples of MI patients as compared to that of control blood samples as shown in Figure 3.12. For statistical analysis, all the data was analyzed by t-test using GraphPad Prism software 9.0.0.

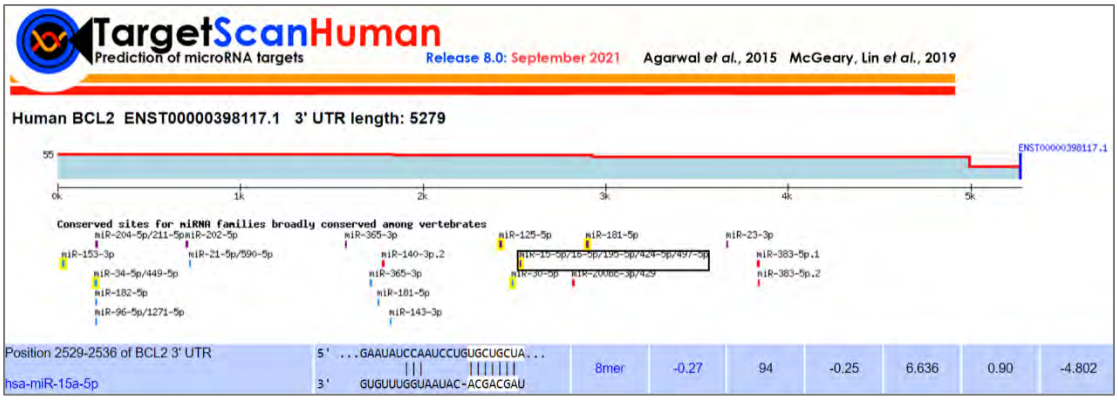

Figure 3.11 Putative miRNA-15a-5p Target Binding Sites Predicted by TargetScan

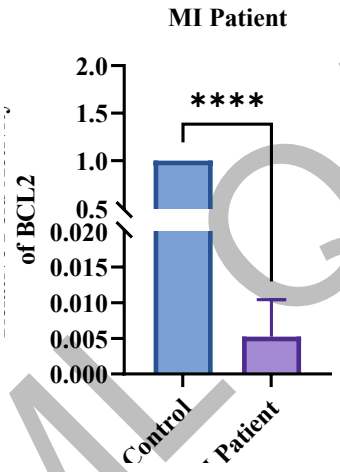

Figure 3.12 Graphical Representation of BCL2 Expression in MI Patients' Blood

(****) Significant in comparison to Control at *p* value < 0.0001

3.7 Expression of ET-1 in Myocardial Infarction Patients' Blood

Endothelin-1 (ET-1) is a vasoconstrictor, involved in the regulation of different signaling pathways in cardiovascular diseases. In cardiomyocytes, ET-1 is the target of MAPK signaling pathway. In cardiovascular diseases, particularly myocardial infarction, the expression of ET-1 is dysregulated. By using TargetScan it was confirmed that ET-1 is the putative target of miRNA98-5p as shown in Figure 3.13. The expression of ET-1 is significantly increased by the ERK dependent activation of GATA4 in myocardial infarction. The expression analysis of ET-1 was done by qRT-PCR. GAPDH was used as a control and relative fold activity of ET-1 was calculated. The expression of ET-1 was significantly upregulated (relative fold change of 15.72378) in the blood samples of MI patients as compared to that of control blood

samples as shown in Figure 3.14. For statistical analysis, t-test was performed by using GraphPad Prism software 9.0.0.

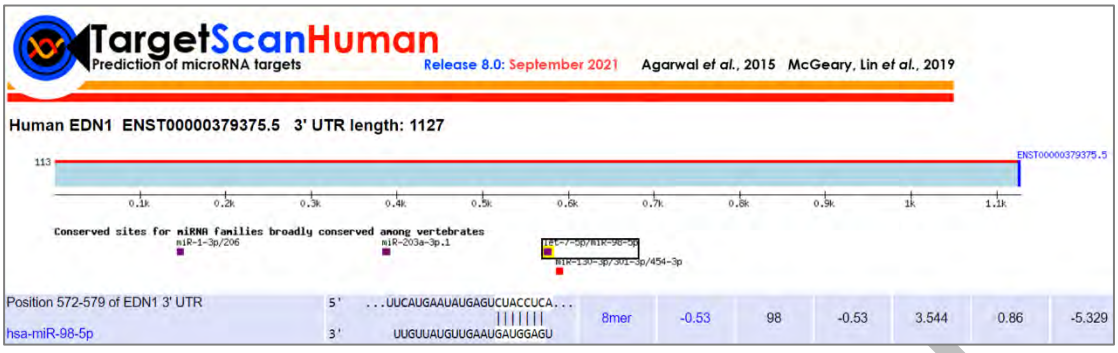

Figure 3.13 Putative miRNA-98-5p Target Binding Sites Predicted by TargetScan

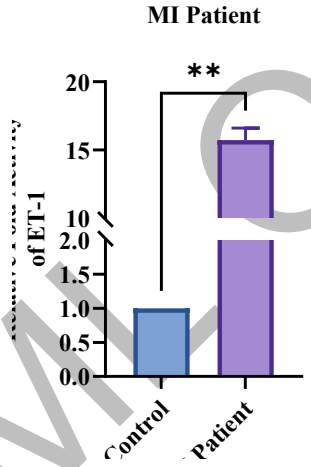

Figure 3.14 Graphical Representation of ET-1 Expression in MI Patients' Blood

(**) Significant in comparison to Control at p value < 0.01

3.8 Expression of ANP in Myocardial Infarction Patients' Blood

ANP controls the blood volume and blood pressure in normal and pathological conditions. The expression analysis of ANP was done by qRT-PCR. GAPDH was used as control and relative fold activity of ANP was calculated. The expression of ANP was significantly upregulated (relative fold change of 94.48367) in the blood samples of MI patients as compared to that of control blood samples as shown in Figure 3.15. All the data was statistically analyzed by applying t-test using GraphPad Prism software 9.0.0.

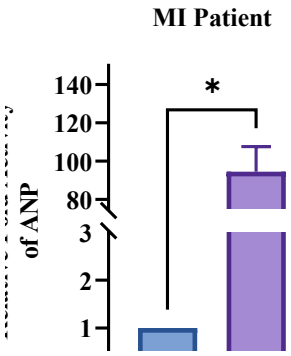

Figure 3.15 Graphical Representation of ANP Expression in MI Patients' Blood

(*) Significant in comparison to Control at p value < 0.05

3.9 Expression of BNP in Myocardial Infarction Patients' Blood

The increased levels of BNP reflect the extent of myocardial infarction. The expression analysis of BNP was done by qRT-PCR. GAPDH was used as control and relative fold activity of BNP was calculated. The expression of BNP was significantly upregulated (relative fold change of 3.708269) in the blood samples of MI patients as compared to that of control blood samples as shown in Figure 3.16. All the data was statistically analyzed by t-test using GraphPad Prism software 9.0.0.

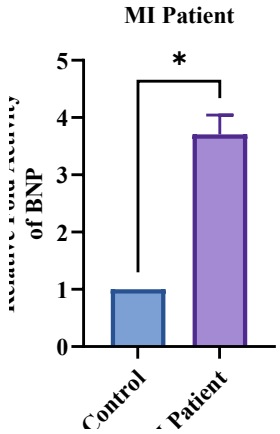

Figure 3.16 Graphical Representation of BNP Expression in MI Patients' Blood

(*) Significant in comparison to Control at p value < 0.05

3.10 Expression of miR-15a-5p in Rats' Blood and Tissue

The expression analysis of miRNA-15a-5p was done by qRT-PCR in rat tissue sample and blood sample of ISO induced MI group and control group. U6 was used as internal control and relative fold activity of miRNA-15a-5p was calculated. The circulatory levels of miRNA-98-5p were significantly upregulated (relative fold change of 3.456) in the rat blood of ISO induced MI group as compared to that of control group as shown in Figure 3.17. Likewise, in rat tissue of ISO induced MI group, the expression of miRNA-15a-5p was significantly upregulated (relative fold change of 3.16) as compared to that of control group as shown in Figure 3.17. For statistical analysis, t-test was applied using GraphPad Prism software 9.0.0.

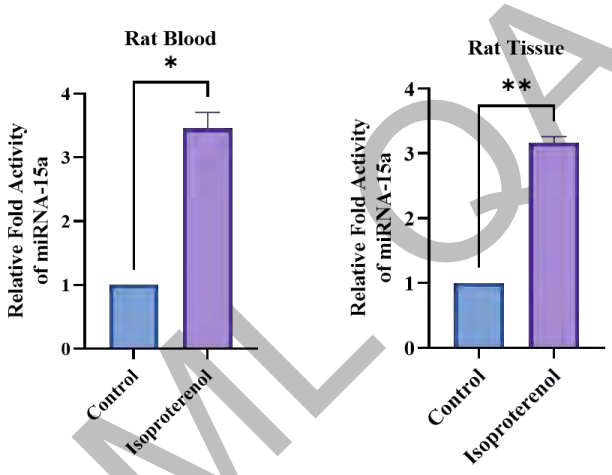

Figure 3.17 Graphical Representation of miRNA-15a Expression in Rat Blood and Tissue

(*) Significant in comparison to Control at p value < 0.05

(**) Significant in comparison to Control at p value < 0.01

3.11 Expression of miR-98-5p in Rats' Blood and Tissue

The expression analysis of miRNA-98-5p was done by qRT-PCR in rat tissue sample and blood sample of ISO induced MI group and control group. U6 was used as internal control and relative fold activity of miRNA-98-5p was calculated. The circulatory levels of miRNA-98-5p were significantly downregulated in the rat blood (relative fold change of 0.04184) and rat tissue (relative fold change of 0.01647) of ISO induced MI group as compared to that of control group as shown in Figure 3.18. For statistical analysis, t-test was applied by using GraphPad Prism software 9.0.0.

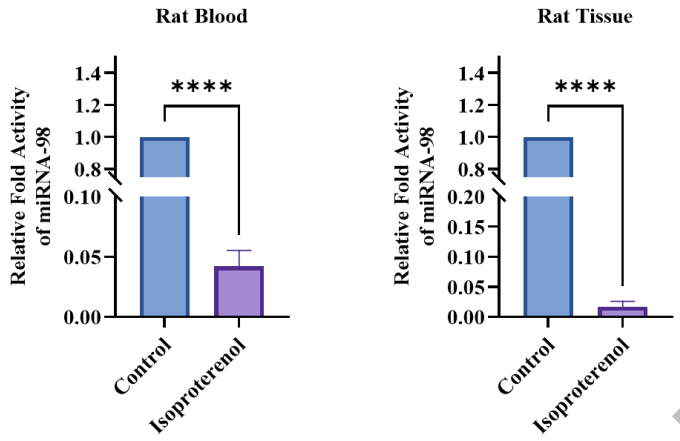

Figure 3.18 Graphical Representation of miRNA-98 Expression in Rat Blood and Tissue

(****) Significant in comparison to Control at p value < 0.0001

3.12 Expression of NFATC3 in Rats' Blood and Tissue

The expression analysis of NFATC3 was done by qRT-PCR in rat tissue sample and blood sample of ISO induced MI group as well as control group. GAPDH was used as control and relative fold activity of NFATC3 was calculated. Compared to that of control group, the circulatory levels of NFATC3 were significantly downregulated (relative fold change of 0.26983) in the rat blood of ISO induced MI group as shown in Figure 3.19. Contrarily, the expression of NFATC3 was significantly upregulated (relative fold change of 7.408) in the tissue samples of ISO induced MI group as compared to that of control group as shown in Figure 3.19. For statistical analysis, t-test was applied by using GraphPad Prism software 9.0.0.

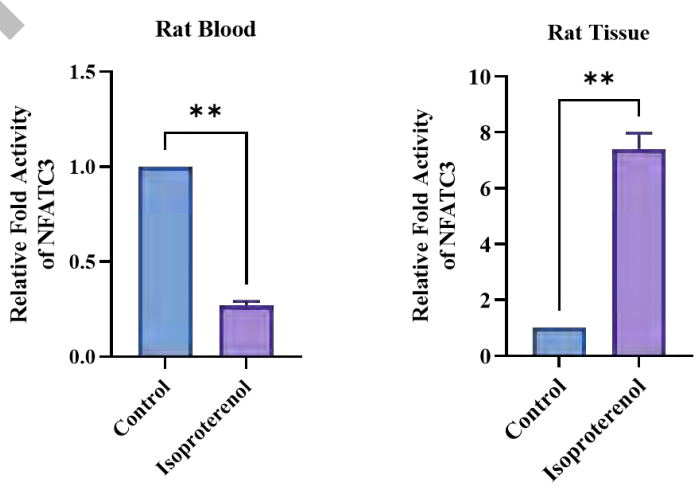

Figure 3.19 Graphical Representation of NFATC3 Expression in Rat Blood and Tissue

(**) Significant in comparison to Control at *p* value < 0.01

3.13 Expression of BCL2 in Rats' Blood and Tissue

The expression analysis of BCL2 was done by qRT-PCR in rat tissue sample and blood sample of ISO induced MI group as well as control group. GAPDH was taken as control and relative fold activity of BCL2 was calculated. Compared to that of control group, the circulatory levels of BCL2 were significantly downregulated (relative fold change of 0.279087) in the rat blood of ISO induced MI group as shown in Figure 3.20. Uniformly, the expression of BCL2 was significantly downregulated (relative fold change of 0.068872) in the tissue samples of ISO induced MI group as compared to that of control group as shown in Figure 3.20. For statistical analysis, t-test was applied by using GraphPad Prism software 9.0.0.

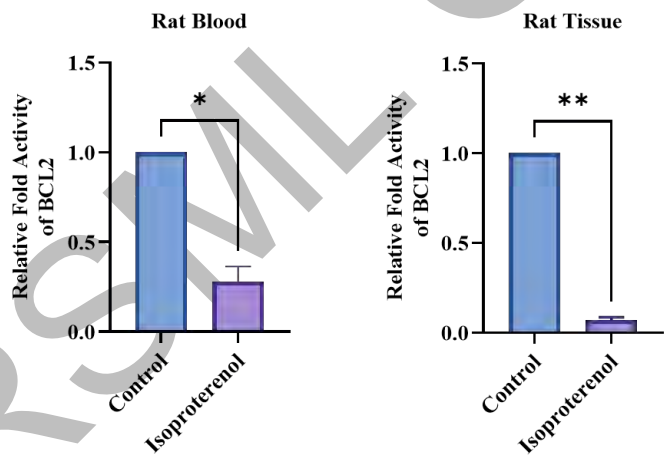

Figure 3.20 Graphical Representation of BCL2 Expression in Rat Blood and Tissue

(*) Significant in comparison to Control at *p* value < 0.05

(**) Significant in comparison to Control at *p* value < 0.01

3.14 Expression of ET-1 in Rats' Blood and Tissue

The expression analysis of ET-1 was done by qRT-PCR in rat tissue sample and blood sample of ISO induced MI group as well as control group. GAPDH was used as control and relative fold activity of ET-1 was calculated. Compared to that of control group, the circulatory levels of ET-1 were significantly upregulated in the rat blood (relative

fold change of 2.039359) and rat tissue (relative fold change of 2.65543) of ISO induced MI group as shown in Figure 3.21.

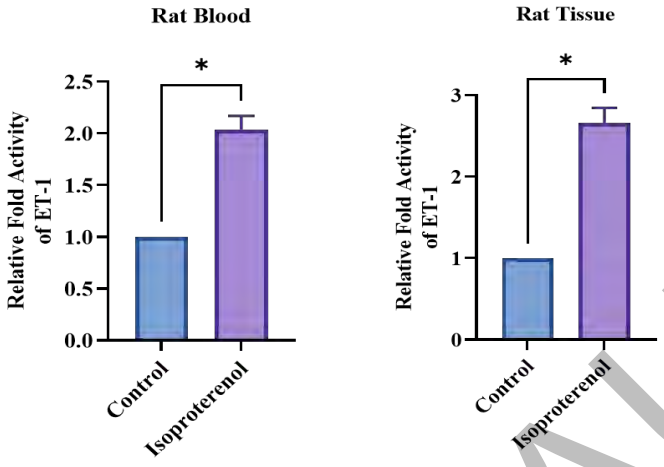

Figure 3.21 Graphical Representation of ET-1 Expression in Rat Blood and Tissue

(*) Significant in comparison to Control at p value < 0.05

3.15 Expression of ANP in Rats' Blood and Tissue

The expression analysis of ANP was done by qRT-PCR in rat tissue sample and blood sample of ISO induced MI group as well as control group. For normalization, GAPDH was used as control and relative fold activity of ANP was calculated. Compared to that of control group, the circulatory levels of ANP were significantly upregulated in the rat blood (relative fold change of 5.009637) and rat tissue samples (relative fold change of 10.65654) of ISO induced MI group as shown in Figure 3.22. For statistical analysis, t-test was performed by using GraphPad Prism software 9.0.0.

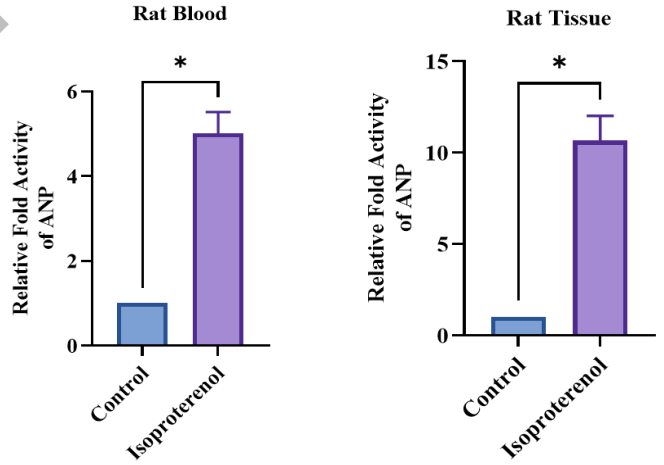

Figure 3.22 Graphical Representation of ANP Expression in Rat Blood and Tissue

(*) Significant in comparison to Control at p value < 0.05

3.16 Expression of BNP in Rats' Blood and Tissue

The expression analysis of BNP was done by qRT-PCR in rat tissue sample and blood sample of ISO induced MI group as well as control group. GAPDH was used as control for normalization and relative fold activity of BNP was calculated. Compared to that of control group, the circulatory levels of BNP were significantly upregulated (relative fold change of 8.681822) in the rat blood of ISO induced MI group as shown in Figure 3.23. Uniformly, the expression of BNP was significantly upregulated (relative fold change of 7.832541) in the tissue samples of ISO induced MI group as compared to that of control group as shown in Figure 3.23. For statistical analysis, t-test was performed by using GraphPad Prism software 9.0.0.

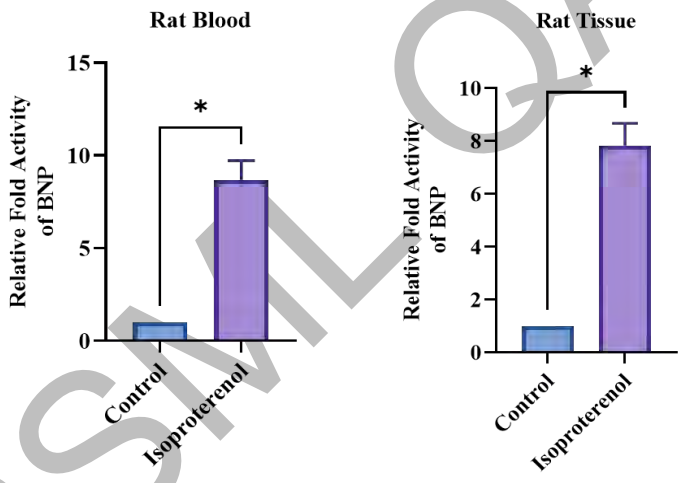

Figure 3.23 Graphical Representation of BNP Expression in Rat Blood and Tissue

(*) Significant in comparison to Control at p value < 0.05

3.17 Protein Expression Analysis of NFATC3

To check the protein expression level of NFATC3, western blotting was performed on serum samples and tissue homogenate samples of ISO induced MI group as well as control group. GAPDH was used as a control for normalization. Compared to that of control group, the expression of NFATC3 was significantly downregulated in the serum samples of ISO induced MI group as shown in Figure 3.24. The densitometric analysis was performed to quantify the protein expression level of NFATC3 in serum samples as shown in Figure 3.25 respectively. The results were statistically analyzed by t-test using GraphPad Prism software 9.0.0.

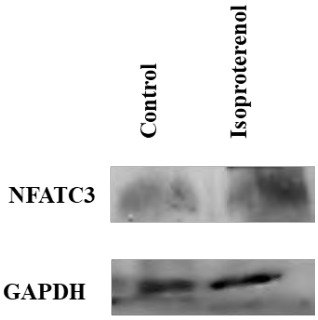

Figure 3.24 Expression Analysis of NFATC3 in Serum Samples

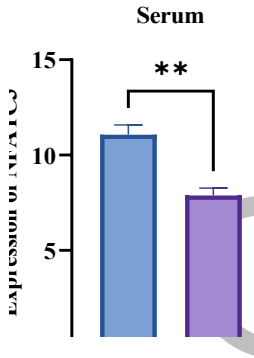

Figure 3.25 Graphical Representation of Expression of NFATC3 in Serum Samples

(**) Significant in comparison to Control at *p* value < 0.01

3.18 Protein Expression Analysis of ET-1

To check the protein expression level of ET-1, western blotting was performed on serum samples and tissue homogenate samples of ISO induced MI group as well as control group. GAPDH was used as a control for normalization. The protein expression of ET-1 was significantly upregulated in the serum samples of ISO induced MI group as compared to that of control group as shown in Figure 3.26. Similarly, significant increase in the protein expression of ET-1 was observed in tissue homogenate samples of ISO induced MI group in comparison to that of control group as shown in Figure3.28. The densitometric analysis was performed to quantify the protein expression level of ET-1 in both serum and tissue homogenate samples as shown in Figure 3.27 and Figure 3.29, respectively. For statistical analysis, t-test was performed by using GraphPad Prism software 9.0.0.

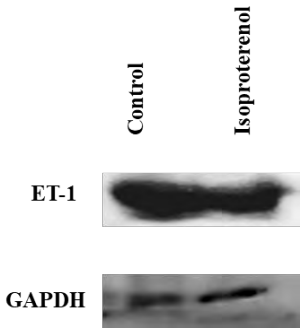

Figure 3.26 Expression Analysis of ET-1 in Serum Samples

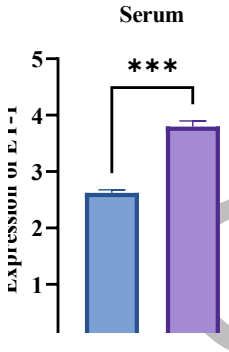

Figure 3.27 Graphical Representation of Expression of ET-1 in Serum Samples

(***) Significant in comparison to Control at *p* value < 0.001

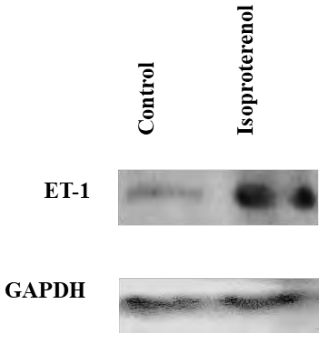

Figure 3.28 Expression Analysis of ET-1 in Tissue Homogenate Samples

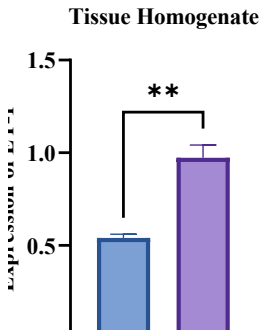

Figure 3.29 Graphical Representation of Expression of ET-1 in Tissue Homogenate Samples

(**) Significant in comparison to Control at *p* value < 0.01

3.19 Effects of Isoproterenol on Baseline Characteristics

Isoproterenol was used to induce myocardial infarction in rats in the experimental group, as a result different signaling pathways are activated which lead to the apoptosis of cardiomyocytes. The tibia length, body weight, heart weight and the weight of other organs were measured. The analysis of these characteristics revealed increased heart size of isoproterenol treated rats as shown in Figure 3.30. The comparative analysis was performed in which a significant increase in heart weight to body weight ratio was observed in ISO induced myocardial infarction experimental group than that of control group as shown in Figure 3.31. Similarly, an increase in heart weight to tibia length ratio was observed in ISO induced myocardial infarction experimental group as compared to the control group, shown in Figure 3.32. These observations suggested that isoproterenol induced myocardial infarction in experimental groups. For statistical analysis, t-test was performed by using GraphPad Prism software 9.0.0.

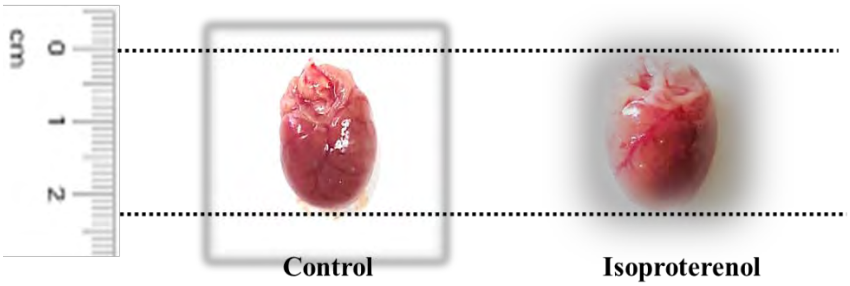

Figure 3.30 Comparative analysis of Heart size in Experimental Groups

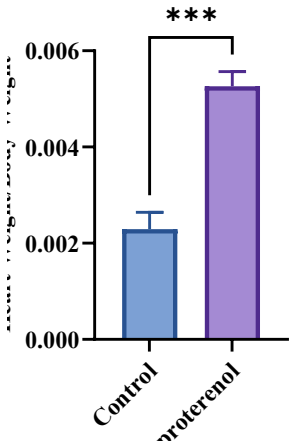

Figure 3.31 Graphical Representation of Heart Weight/Body Weight

(***) Significant in comparison to Control at *p* value < 0.001

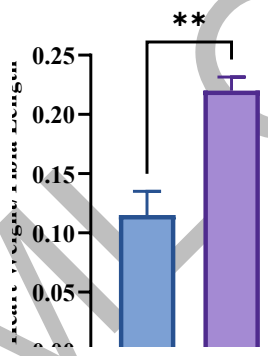

Figure 3.32 Graphical Representation of Heart Weight/Tibia Length

(**) Significant in comparison to Control at *p* value < 0.01

3.20 Effects of Isoproterenol on Cellular Organization

To check the induction of myocardial infarction in experimental groups, histological analysis was performed. Hematoxylin and Eosin staining (H&E) revealed the disturbed cellular organization, increase nuclei number, disruption of cell membrane, increase nucleus to cytoplasm ratio, enlarged size of cardiomyocytes, increase cell surface area and asymmetrical arrangement of cardiac myofibrils in isoproterenol induced MI rat model which confirms the cardiac cell injury and damage as shown in Figure 3.33. The arrow head shows the abnormal cells. However, in comparison to the control group, the

cellular architecture was intact, nuclei number and nucleus to cytoplasm ratio were normal as shown in Figure 3.33.

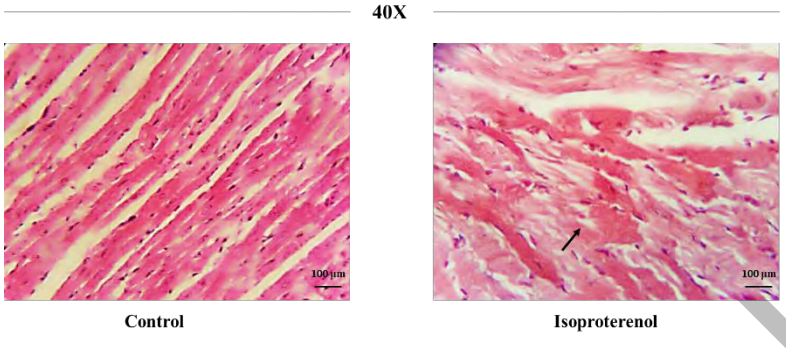

Figure 3.33 Histological Analysis of Heart in Isoproterenol induced MI Rat Group

3.21 Assessment of Oxidativess Stress Profile in Experimental Groups

3.21.1 Analysis of ROS in Serum and Tissue Homogenate samples

Compared to that of normal control group (0.07672±0.01240), the serum level of ROS was increased significantly in isoproterenol group (0.1307±0.01351) as shown in Figure 3.34, which showed the toxic effects of isoproterenol. The ROS assay was also performed on tissue homogenates of the experimental groups. Compared to that of normal control group (0.1123±0.04330). the tissue homogenate level of ROS was increased significantly in isoproterenol group (0.1495±0.02656) as shown in Figure 3.34. For statistical analysis, t-test was performed by using GraphPad Prism software 9.0.0. The values are provided as Mean ± SEM, (***) at *p* value < 0.001 and (**) at *p* value < 0.01.

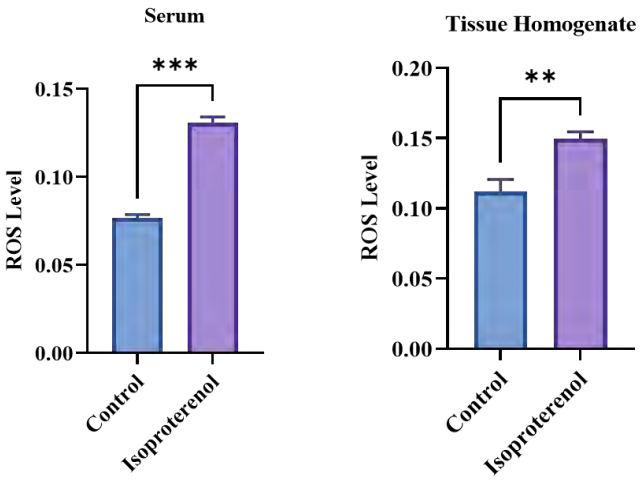

Figure 3.34 Graphical Representation of ROS Level in Serum and Tissue Homogenate Samples

(***) Significant in comparison to Control at *p* value < 0.001

(**) Significant in comparison to Control at *p* value < 0.01

3.21.2 Analysis of TBARs in Serum and Tissue Homogenate samples

The isoproterenol induced lipid peroxidation in the experimental groups which was determined by TBARs assay. TBARs are the by-product which are produced during lipid peroxidation and lead to oxidative stress. The administration of isoproterenol results in the significant increase in the levels of TBARs compared to that of control. Compared to that of control group (10471±22.061783), the serum level of TBARs was significantly increased in isoproterenol group (38517±8.52319) as shown in Figure 3.35, which showed the lipid damage due to isoproterenol. The TBARs assay was also performed on tissue homogenates of the experimental groups. Compared to that of control group (5517±16.162973), the tissue homogenate level of TBARs was significantly increased in isoproterenol group (19817±4.62155) as shown in Figure 3.35. By using GraphPad Prism software 9.0.0, t-test was applied for statistical analysis. The values are provided as Mean ± SEM, (**) at *p* value < 0.01 and (****) at *p* value < 0.0001.

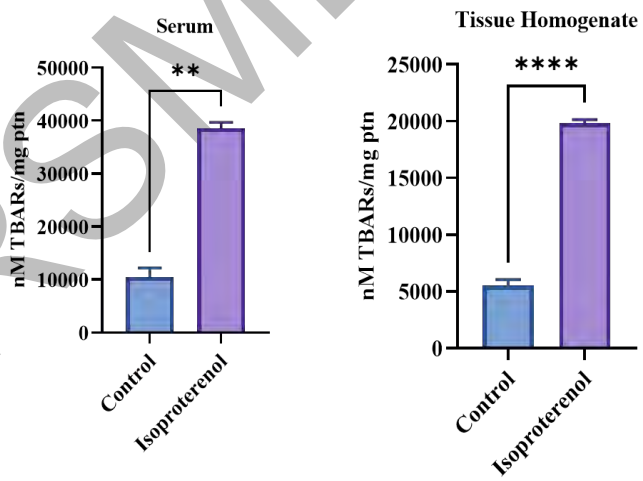

Figure 3.35 Graphical Representation of TBARs Level in Serum and Tissue Homogenate Samples

(**) Significant in comparison to Control at *p* value < 0.01

(****) Significant in comparison to Control at *p* value < 0.0001

3.22 Assessment of Antioxidant levels in Experimental Groups

3.22.1 Analysis of SOD Activity in Serum and Tissue Homogenate samples

Superoxide dismutase (SOD) detoxifies the oxidative stress and provides protection against ROS damage. The increased production of free radical species results in the reduced level of antioxidant enzyme, SOD, resulting in myocardial damage in isoproterenol induced rats. Compared to that of normal control group (18.48±0.01656), the serum level of SOD was decreased significantly in isoproterenol group (16.47±0.06467) as shown in Figure 3.36. The SOD assay was also performed on tissue homogenates of the experimental groups. The tissue homogenate level of SOD was decreased significantly in isoproterenol group (17.33±0.0151) compared to that of normal control group (22.71±0.04053) as shown in Figure 3.36. T-test was applied by using GraphPad Prism software 9.0.0. The values are provided as Mean ± SEM, (***) at p value < 0.001 and (****) at p value < 0.0001.

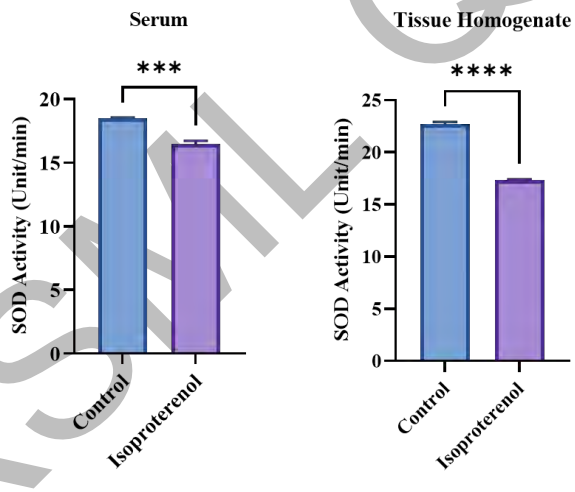

Figure 3.36 Graphical Representation of SOD Activity in Serum and Tissue Homogenate Samples

(***) Significant in comparison to Control at p value < 0.001

(****) Significant in comparison to Control at p value < 0.0001

3.22.2 Analysis of CAT Activity in Serum and Tissue Homogenate samples

Catalase (CAT) enzyme act as a scavenger for reactive oxygen species and provides protection from oxidative stress. In ISO-induced MI models there is a reduction in the activity of antioxidant enzyme, CAT, due to increase in oxidative stress. The serum level of CAT was downregulated significantly in isoproterenol group (0.1129±0.03021)

compared to that of normal control group (0.1455±0.0137) as shown in Figure 3.37. The CAT assay was also performed on tissue homogenates of the experimental groups. The tissue homogenate level of CAT was reduced significantly in isoproterenol group (0.05368±0.04101) compared to that of normal control group (0.1552±0.03939) as shown in Figure 3.37. For statistical analysis, t-test was applied by using GraphPad Prism software 9.0.0. The values are provided as Mean ± SEM, (***) at *p* value < 0.001.

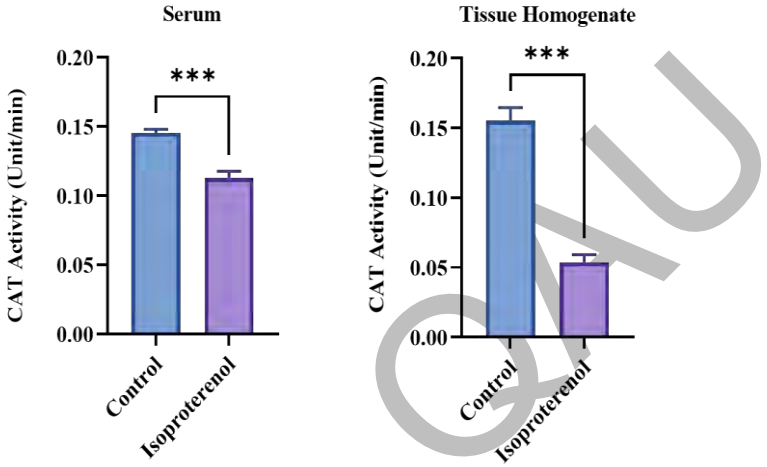

Figure 3.37 Graphical Representation of CAT Activity in Serum and Tissue Homogenate Samples

(***) Significant in comparison to Control at *p* value < 0.001

3.22.3 Analysis of POD Activity in Serum and Tissue Homogenate samples

Peroxidase (POD) enzyme is an antioxidant enzyme which helps the body to scavenge from hydrogen peroxide during oxidative stress. In ISO-induced MI models there is a reduction in the activity of antioxidant enzyme, POD, due to increase in oxidative stress. Compared to that of normal control group (9.364±0.0873), the serum level of POD was decreased significantly in isoproterenol group (6.633±0.08986) as shown in Figure 3.38. The POD assay was also performed on tissue homogenates of the experimental groups. Compared to that of normal control group (13.08±0.16205), the tissue homogenate level of POD was decreased significantly in isoproterenol group (9.552±0.55339) as shown in Figure 3.38. For statistical analysis, t-test was applied by using GraphPad Prism software 9.0.0. The values are provided as Mean ± SEM, (**) at *p* value < 0.01.

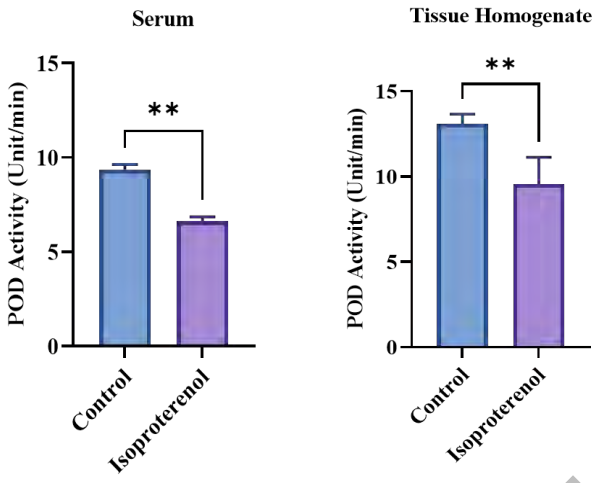

Figure 3.38 Graphical Representation of POD Activity in Serum and Tissue Homogenate Samples

(**) Significant in comparison to Control at *p* value < 0.01

3.22.4 Analysis of GSH Level in Serum and Tissue Homogenate samples

Compared to that of normal control group (0.5257±0.13336), the serum level of GSH was decreased significantly in isoproterenol diseased group (0.1970±0.02215) as shown in Figure 3.39. In case of tissue homogenates, compared to that of normal control group (0.6135±0.04529), the level of GSH was decreased significantly in isoproterenol diseased group (0.5264±0.01501) as shown in Figure 3.39. For statistical analysis, t-test was applied by using GraphPad Prism software 9.0.0. The values are provided as Mean ± SEM, (***) at *p* value < 0.001 and (**) at *p* value < 0.01.

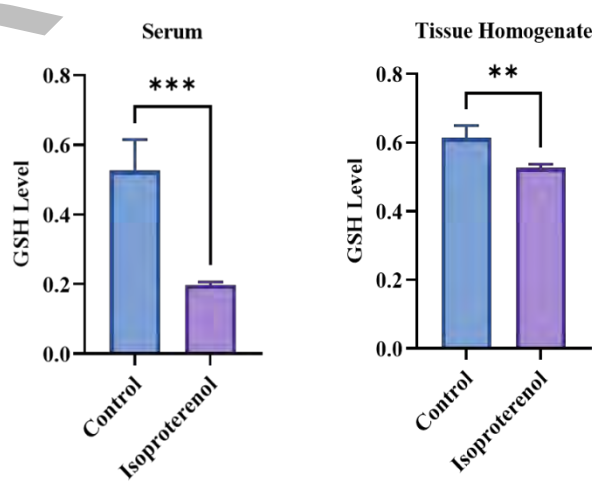

Figure 3.39 Graphical Representation of GSH Level in Serum and Tissue Homogenate Samples

(***) Significant in comparison to Control at *p* value < 0.001

(**) Significant in comparison to Control at *p* value < 0.01

3.22.5 Analysis of APX Level in Serum and Tissue Homogenate samples

Ascorbate peroxidase (APX) is a key antioxidant that helps in scavenging the free radicals like hydrogen peroxide (H_2O_2) in the cell. In ISO-induced MI models there is a reduction in the activity of antioxidant enzyme, APX, due to increase in oxidative stress and free radical production. Compared to that of normal control group (0.4292±0.04588), the serum level of APX was decreased significantly in isoproterenol diseased group (0.2618±0.0428) as shown in Figure 3.40. The APX assay was also performed on tissue homogenates of the experimental groups. Compared to that of normal control group (1.413±0.08293), the tissue homogenate level of APX was decreased significantly in isoproterenol diseased group (1.083±0.01744) as shown in Figure 3.40. The statistical analysis of all the data was performed by t-test using GraphPad Prism software 9.0.0. The values are provided as Mean ± SEM, (***) at *p* value < 0.001.

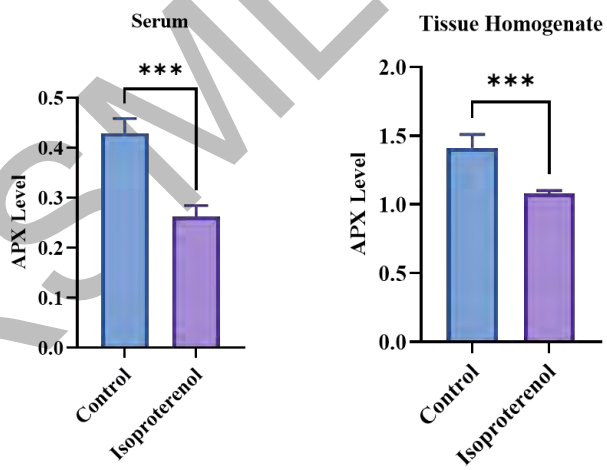

Figure 3.40 Graphical Representation of APX Level in Serum and Tissue Homogenate Samples

(***) Significant in comparison to Control at *p* value < 0.001

3.23 Assessment of Liver Function Test in Experimental Groups

3.23.1 Analysis of ALT levels in Serum samples

Compared to that of control group (158.3±1.3726), the serum levels of APX were increased significantly in isoproterenol diseased group (776.0±3.53948) as shown in Figure 3.41. The values are provided as Mean ± SEM, (**) at *p* value < 0.01.

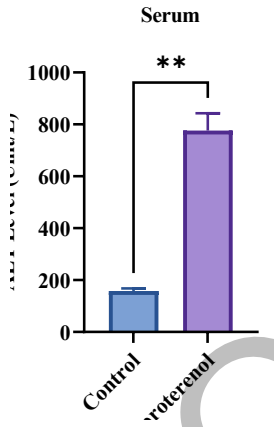

Figure 3.41 Graphical Representation of ALT Level in Serum

(**) Significant in comparison to Control at *p* value < 0.01

3.23.2 Analysis of AST levels in Serum samples

Compared to that of control group (130.9±3.40999), the serum levels of APX were increased significantly in isoproterenol diseased group (381.6±0.47841) as shown in Figure 3.42. By using GraphPad Prism software 9.0.0, the statistical analysis was performed by t-test. The values are provided as Mean ± SEM, (**) at *p* value < 0.01.

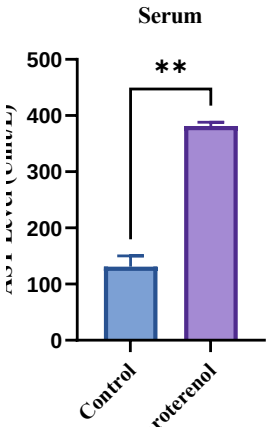

Figure 3.42 Graphical Representation of AST Level in Serum

(**) Significant in comparison to Control at *p* value < 0.01

3.24 Assessment of Lipid Profiling in Experimental Groups

3.24.1 Analysis of Cholesterol levels in Serum samples

Lipid profile analysis was performed by measuring the cholesterol level in the serum samples of the experimental groups. The increased levels of cholesterol in serum is closely related to cardiac injury. Compared to that of control group (0.1709±0.0944), the serum levels of cholesterol were significantly increased in isoproterenol diseased group (0.9146±0.00692) as shown in Figure 3.43. By using GraphPad Prism software 9.0.0, t-test was applied for statistical analysis. The values are provided as Mean ± SEM, (***) at *p* value < 0.001.

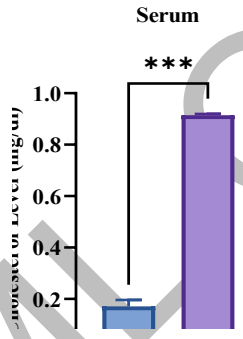

Figure 3.43 Graphical Representation of Cholesterol Level in Serum

(***) Significant in comparison to Control at *p* value < 0.001

3.24.2 Analysis of Triglycerides levels in Serum samples

To assess the levels of triglyceride in circulation, the triglyceride assay in the serum samples of the experimental groups was performed. Compared to that of control group (0.09691±0.08265), the serum levels of triglyceride were increased significantly in isoproterenol diseased group (0.7344±0.0801) as shown in Figure 3.44. By using GraphPad Prism software 9.0.0, t-test was applied. The values are provided as Mean ± SEM, (**)at *p* value < 0.01.

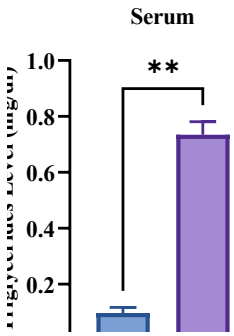

Figure 3.44 Graphical Representation of Triglycerides Level in Serum

(**) Significant in comparison to Control at *p* value < 0.01

4 DISCUSSION

Cardiovascular disease is a broad term used for different cardiomyopathies. Among cardiac diseases, acute myocardial infarction is the growing cause of death with the prevalence leading to three million people worldwide (Mechanic *et al.,* 2022). AMI is the important cause of increased morbidity and mortality (Severino *et al.,* 2020). MI occurs in patients with coronary artery obstruction causing irreversible damage to heart leading to cardiac injury (Mechanic *et al.,* 2022). MicroRNAs are evolving as significant players in gene expression and regulation under various physiological and pathological conditions (Bhaskaran & Mohan, 2014). Under various pathophysiological conditions, the levels of miRNAs are highly dysregulated therefore various studies are under investigation about their potential to act as biomarkers for cardiac diseases. The current study was performed to assess the diagnostic potential of dysregulated expression of miRNAs including miRNA-1, miRNA-15a and miRNA-98 in circulation of myocardial infarction patients and isoproterenol induced myocardial infarction rats and molecular mechanisms of underlying miRNAs targeted signaling pathways. Moreover, the expression of transcription factor NFATC3, anti-apoptotic gene BCL2, vasoconstrictor ET-1 and stress responsive genes ANP and BNP were checked in myocardial infarction patients' blood and isoproterenol induced myocardial infarction rats' blood and tissue. Studies reported that miRNAs bear the required criteria of an ideal biomarker as they are highly distinct, highly sensitive and can be easily found in circulation (Condrat *et al.,* 2020). In order to investigate the potential of miRNAs as biomarker in myocardial infarction, the expression levels of different miRNAs were assessed including miRNA-1-3p, miRNA15a-5p and miRNA-98-5p in circulation. The levels of oxidative and antioxidative enzymes were observed in isoproterenol induced myocardial infarction rat tissue and serum.

Previous studies reported that miRNA-1 and miRNA-133 were shown to be upregulated in the peripheral blood of type 2 diabetes patients, and this overexpression was linked to an increased risk of CVDs (Al-Kafaji *et al.,* 2021; Al-Muhtaresh *et al.,* 2019). As no previous study reported the diagnostic potential of miRNA-1-3p in circulation of MI patients, therefore, in our study we investigated the levels of miRNA-1-3p in MI patient's blood which were found to be significantly upregulated as compared to that of control group. The TargetScan analysis suggested that 3' UTR of NFATC3 has 8-mer binding site of miRNA-1. No previous study reported the

expression of NFATC3 in MI patients. In our study, we found that the expression of NFATC3 was significantly downregulated as compared to that of control group in the blood of MI patients and *in vivo* rat model. In contrast the expression of NFATC3 was upregulated in heart tissue of isoproterenol induced MI rat model in comparison to that of normal control group. The decreased protein expression of NFATC3 was also evaluated in serum samples of isoproterenol induced MI rat model. Our findings suggested that miRNA-1-3p may serve as diagnostic marker for the early detection of MI by regulating NFATC3 signaling nexus.

miRNA-15 targets BCL2 and inhibition of miRNA-15 in ischemic condition promotes cell survival as well as provides protection against ischemic injury (Hullinger *et al.,* 2012). Studies reported that miRNA-15a-5p is upregulated in myocardial fibrosis patients (He *et al.,* 2021). Keeping in view the role of miRNA-15a-5p in myocardial fibrosis patients, we investigated the level of miRNA-15a-5p in MI patients' blood and isoproterenol induced MI rats' blood and tissue which was found to be significantly upregulated in comparison to control groups, respectively. TargetScan analysis suggested that 3'UTR of BCL2 has 8-mer binding sites of miRNA-15a-5p. In current study, we also checked the expression of BCL2 which was found to be downregulated in MI patients' blood and isoproterenol induced MI rats' blood and tissue as compared to that of control. Our findings suggested the early diagnostic potential of miRNA-15a-5p in myocardial infarction patients.

miRNA-98 negatively regulates myocardial infarction induced cardiac cells apoptosis (C. Sun *et al.,* 2017). In our study, we investigated that the expression of miRNA-98-5p was downregulated in both MI patients' blood and *in vivo* rat model. TargetScan analysis suggested that 3'UTR of ET-1 has 8-mer binding sites of miRNA-98-5p. In our study, we examined that the expression of ET-1 was increased in MI patients' blood and isoproterenol induced MI rat's blood and tissue as compared to that of control. At protein level, we also evaluated that the expression of ET-1 was upregulated in both serum and tissue homogenates of isoproterenol induced MI rat model. We also checked the downstream targets of ET-1 such as ANP and BNP in MI patients' blood and isoproterenol induced MI rats' blood and tissue and it was revealed that in comparison to control groups, the expression of ANP and BNP were upregulated in MI patients' blood and isoproterenol induced MI rats' blood and tissue revealing to ANP/BNP signaling nexus in MI.

In current study, the histological analysis of heart tissues depicted the increased number of abnormal and inflammatory cells along with separated muscle fibers. The increased number of abnormal cells are the key indications of isoproterenol induced cardiac apoptosis (Khalil *et al.,* 2015; Patel *et al.,* 2010). In our study, a significant increase in the heart weight of isoproterenol diseased group was observed which resulted in increased heart weight to body weight ratio in isoproterenol induced MI group as compared to that of control group which confirms the induction of MI. In our study, increased heart weight to tibia length ratio was observed in ISO induced MI group as compared to that of normal control group.

ROS is the major contributor of oxidative stress and lead to the pathogenesis of cardiovascular diseases. Activation of β-adrenergic receptors by isoproterenol (Peoples *et al.,* 2019), causes toxicological alterations and is a primary contributor to heart diseases (Burgoyne *et al.,* 2012). Previously our research group has reported the increased ROS levels in cardiac hypertrophy animal model (T. Ali et al., 2019). In our study, increased ROS production in serum and homogenate samples of heart tissue was observed in isoproterenol induced MI group as compared to that of normal control group. Isoproterenol generates free radicals that causes lipid peroxidation and results in irreversible damage to myocardial membrane (Lobo *et al.,* 2017). In our study, increased level of TBARs in serum and homogenate samples of heart tissue was observed in isoproterenol induced MI group as compared to that of normal control group, which confirms the oxidative stress induction by isoproterenol.

The imbalance between ROS production and antioxidant enzymes level leads to various cardiac pathologies. The elevated levels of free radicals are neutralized by various antioxidant enzymes such as superoxide dismutase (SOD), catalase (CAT), peroxidase (POD), ascorbate peroxidase (APX) and reduced glutathione (GSH) (Rajput *et al.,* 2021). SOD and CAT scavenge ROS and provide defence against superoxide anion (Hasanuzzaman *et al.,* 2020). SOD catalysis the dismutation of superoxide radical into molecular oxygen and hydrogen peroxide. CAT further catalysis the degradation of hydrogen peroxide into molecular oxygen and water, consequently, completing the process initiated by SOD (Meng *et al.,* 2014). In our study, decreased levels of SOD and CAT enzymes in serum and homogenate samples of heart tissue were observed in isoproterenol induced MI group as compared to that of normal control group.

Reduced glutathione (GSH), peroxidase (POD) and ascorbate peroxidase (APX) were also assessed to check the oxidative stress induced by isoproterenol. Previously our research group has reported that oxidative stress leads to the alteration of GSH/GSSH ratio and increased lipid peroxidation (Ishtiaq *et al.,* 2020). In our study, decreased levels of GSH, POD and APX enzymes in serum and homogenate samples of heart tissue were observed in isoproterenol induced MI as compared to that of normal control group.

Under hypoxic conditions, the supply of oxygen to the cells is restricted which causes cell damage and increases membrane permeability, thus, resulting in the leakage of cytosolic enzymes in the circulation (Priscilla & Prince, 2009). In the present study, increased levels of cytosolic ALT and AST enzymes in serum samples were observed in ISO induced MI group as compared to that of normal control group. Lipids are the regulators of cardiac functions as they are involved in cell membrane structure and cellular signaling (Horn & Jaiswal, 2019). In the current study, increased levels of cholesterol and triglycerides in serum samples were observed in isoproterenol induced MI group as compared to that of normal control group.

Conclusion and Future Perspective

AMI is the major cause of death worldwide and its mortality and morbidity rates are increasing day by day. The current study well defines the diagnostic potential of cardiac specific miRNAs as an early detection marker of AMI in patients. MicroRNAs such as miRNA-1, miRNA-15a and miRNA-98 were found to be dysregulated in myocardial infarction patient's blood and *in vivo* rat model. The current study highlighted the molecular mechanism of cardiac specific miRNAs targeted NFATC3/ANP/BNP signaling nexus which may provide better understanding for different diagnostic and therapeutic strategies. The potential to use miRNAs as diagnostic marker is still under investigation. Our study provides suggestions for future miRNA research that will advance the development of diagnostic markers and therapeutic tools for AMI.

REFERENCES

A. Thandavarayan, R., V. Giridharan, V., Watanabe, K., & Konishi, T. (2011). Diabetic Cardiomyopathy and Oxidative Stress: Role of Antioxidants. *Cardiovascular & Hematological Agents in Medicinal Chemistry*, *9*(4), 225–230. https://doi.org/10.2174/187152511798120877

Abel, P., & Rorabaugh, B. (2021). Isoproterenol. *XPharm: The Comprehensive Pharmacology Reference*, 1–7. https://doi.org/10.1016/B978-008055232-3.63729-8

Ai, J., Zhang, R., Li, Y., Pu, J., Lu, Y., Jiao, J., Li, K., Yu, B., Li, Z., Wang, R., Wang, L., Li, Q., Wang, N., Shan, H., Li, Z., & Yang, B. (2010). Circulating microRNA-1 as a potential novel biomarker for acute myocardial infarction. *Biochemical and Biophysical Research Communications*, *391*(1), 73–77. https://doi.org/10.1016/J.BBRC.2009.11.005

Al-Kafaji, G., Al-Muhtaresh, H. A., & Salem, A. H. (2021). Expression and clinical significance of miR-1 and miR-133 in pre-diabetes. *Biomedical Reports*, *14*(3), 1–9. https://doi.org/10.3892/BR.2021.1409

Al-Muhtaresh, H. A., Salem, A. H., & Al-Kafaji, G. (2019). Upregulation of Circulating Cardiomyocyte-Enriched miR-1 and miR-133 Associate with the Risk of Coronary Artery Disease in Type 2 Diabetes Patients and Serve as Potential Biomarkers. *Journal of Cardiovascular Translational Research*, *12*(4), 347–357. https://doi.org/10.1007/S12265-018-9857-2

Alarcón, C. R., Lee, H., Goodarzi, H., Halberg, N., & Tavazoie, S. F. (2015). N6-methyladenosine marks primary microRNAs for processing. *Nature*, *519*(7544), 482–485. https://doi.org/10.1038/NATURE14281

Alemu, R., Fuller, E. E., Harper, J. F., & Feldman, M. (2011). Influence of Smoking on the Location of Acute Myocardial Infarctions. *ISRN Cardiology*, *2011*, 1–3. https://doi.org/10.5402/2011/174358

Ali, N. S., Bashir, M., & Sherwani, M. (2016). PATTERN OF DYSLIPIDEMIA IN YOUNG PATIENTS WITH ACUTE ST ELEVATION MYOCARDIAL INFARCTION 1 1 1. *J Sheikh Zayed Med Coll* , *7*, 998–1001.

Ali, T., Mushtaq, I., Maryam, S., Farhan, A., Saba, K., Jan, M. I., Sultan, A., Anees,

M., Duygu, B., Hamera, S., Tabassum, S., Javed, Q., da Costa Martins, P. A., & Murtaza, I. (2019). Interplay of N acetyl cysteine and melatonin in regulating oxidative stress-induced cardiac hypertrophic factors and microRNAs. *Archives of Biochemistry and Biophysics*, *661*, 56–65. https://doi.org/10.1016/J.ABB.2018.11.007

Arroyo, J. D., Chevillet, J. R., Kroh, E. M., Ruf, I. K., Pritchard, C. C., Gibson, D. F., Mitchell, P. S., Bennett, C. F., Pogosova-Agadjanyan, E. L., Stirewalt, D. L., Tait, J. F., & Tewari, M. (2011). Argonaute2 complexes carry a population of circulating microRNAs independent of vesicles in human plasma. *Proceedings of the National Academy of Sciences of the United States of America*, *108*(12), 5003–5008. https://doi.org/10.1073/PNAS.1019055108

Babiarz, J. E., Ruby, J. G., Wang, Y., Bartel, D. P., & Blelloch, R. (2008). Mouse ES cells express endogenous shRNAs, siRNAs, and other Microprocessor-independent, Dicer-dependent small RNAs. *Genes & Development*, *22*(20), 2773–2785. https://doi.org/10.1101/GAD.1705308

Bellary, S., Paul O'Hare, J., Raymond, N. T., Mughal, S., Hanif, W. M., Jones, A., Kumar, S., & Barnett, A. H. (2010). Premature cardiovascular events and mortality in south Asians with type 2 diabetes in the United Kingdom Asian Diabetes Study - effect of ethnicity on risk. *Current Medical Research and Opinion*, *26*(8), 1873–1879. https://doi.org/10.1185/03007995.2010.490468

Berry, C. E., & Hare, J. M. (2004). Xanthine oxidoreductase and cardiovascular disease: molecular mechanisms and pathophysiological implications. *The Journal of Physiology*, *555*(Pt 3), 589–606. https://doi.org/10.1113/JPHYSIOL.2003.055913

Bhaskaran, M., & Mohan, M. (2014). MicroRNAs: History, Biogenesis, and Their Evolving Role in Animal Development and Disease. *Veterinary Pathology*, *51*(4), 759. https://doi.org/10.1177/0300985813502820

Borchi, E., Parri, M., Papucci, L., Becatti, M., Nassi, N., Nassi, P., & Nediani, C. (2009). Role of NADPH oxidase in H9c2 cardiac muscle cells exposed to simulated ischaemia-reperfusion. *Journal of Cellular and Molecular Medicine*, *13*(8B), 2724–2735. https://doi.org/10.1111/J.1582-4934.2008.00485.X

Borgia, M. C., & Medici, F. (1998). Perspectives in the treatment of dyslipidemias in

the prevention of coronary heart disease. *Angiology*, *49*(5), 339–348. https://doi.org/10.1177/000331979804900502

Bui, A. L., Horwich, T. B., & Fonarow, G. C. (2011). Epidemiology and risk profile of heart failure. *Nature Reviews. Cardiology*, *8*(1), 30–41. https://doi.org/10.1038/NRCARDIO.2010.165

Burgoyne, J. R., Mongue-Din, H., Eaton, P., & Shah, A. M. (2012). Redox Signaling in Cardiac Physiology and Pathology. *Circulation Research*, *111*(8), 1091–1106. https://doi.org/10.1161/CIRCRESAHA.111.255216

Cardiovascular diseases (CVDs). (2021). https://www.who.int/news-room/fact-sheets/detail/cardiovascular-diseases-(cvds)

Cargnello, M., & Roux, P. P. (2011). Activation and function of the MAPKs and their substrates, the MAPK-activated protein kinases. *Microbiology and Molecular Biology Reviews : MMBR*, *75*(1), 50–83. https://doi.org/10.1128/MMBR.00031-10

Chaudhury, A., Noiret, L., & Higgins, J. M. (2017). White blood cell population dynamics for risk stratification of acute coronary syndrome. *Proceedings of the National Academy of Sciences of the United States of America*, *114*(46), 12344–12349. https://doi.org/10.1073/PNAS.1709228114

Cheng, Y., Tan, N., Yang, J., Liu, X., Cao, X., He, P., Dong, X., Qin, S., & Zhang, C. (2010). A translational study of circulating cell-free microRNA-1 in acute myocardial infarction. *Clinical Science*, *119*(2), 87–95. https://doi.org/10.1042/CS20090645

Chiuve, S. E., Cook, N. R., Shay, C. M., Rexrode, K. M., Albert, C. M., Manson, J. A. E., Willett, W. C., & Rimm, E. B. (2014). Lifestyle-Based Prediction Model for the Prevention of CVD: The Healthy Heart Score. *Journal of the American Heart Association: Cardiovascular and Cerebrovascular Disease*, *3*(6). https://doi.org/10.1161/JAHA.114.000954

Cimmino, A., Calin, G. A., Fabbri, M., Iorio, M. V., Ferracin, M., Shimizu, M., Wojcik, S. E., Aqeilan, R. I., Zupo, S., Dono, M., Rassenti, L., Alder, H., Volinia, S., Liu, C. G., Kipps, T. J., Negrini, M., & Croce, C. M. (2005). miR-15 and miR-16 induce apoptosis by targeting BCL2. *Proceedings of the National Academy of*

Sciences of the United States of America, *102*(39), 13944. https://doi.org/10.1073/PNAS.0506654102

Clerk, A., Cullingford, T. E., Fuller, S. J., Giraldo, A., Markou, T., Pikkarainen, S., & Sugden, P. H. (2007). Signaling pathways mediating cardiac myocyte gene expression in physiological and stress responses. *Journal of Cellular Physiology*, *212*(2), 311–322. https://doi.org/10.1002/JCP.21094

Cohen, J. D., Li, L., Wang, Y., Thoburn, C., Afsari, B., Danilova, L., Douville, C., Javed, A. A., Wong, F., Mattox, A., Hruban, R. H., Wolfgang, C. L., Goggins, M. G., Molin, M. D., Wang, T. L., Roden, R., Klein, A. P., Ptak, J., Dobbyn, L., … Papadopoulos, N. (2018). Detection and localization of surgically resectable cancers with a multi-analyte blood test. *Science (New York, N.Y.)*, *359*(6378), 926–930. https://doi.org/10.1126/SCIENCE.AAR3247

Condrat, C. E., Thompson, D. C., Barbu, M. G., Bugnar, O. L., Boboc, A., Cretoiu, D., Suciu, N., Cretoiu, S. M., & Voinea, S. C. (2020). miRNAs as Biomarkers in Disease: Latest Findings Regarding Their Role in Diagnosis and Prognosis. *Cells*, *9*(2). https://doi.org/10.3390/CELLS9020276

Creamer, T. P. (2020). Calcineurin. *Cell Communication and Signaling 2020 18:1*, *18*(1), 1–12. https://doi.org/10.1186/S12964-020-00636-4

Denli, A. M., Tops, B. B. J., Plasterk, R. H. A., Ketting, R. F., & Hannon, G. J. (2004). Processing of primary microRNAs by the Microprocessor complex. *Nature*, *432*(7014), 231–235. https://doi.org/10.1038/NATURE03049

Deshpande, A., Shetty, P. M. V., Frey, N., & Rangrez, A. Y. (2022). SRF: a seriously responsible factor in cardiac development and disease. *Journal of Biomedical Science 2022 29:1*, *29*(1), 1–21. https://doi.org/10.1186/S12929-022-00820-3

Dong Zhao, M. P. (2021). Epidemiological Features of Cardiovascular Disease in Asia. *JACC: Asia*, *1*(1), 1–13. https://doi.org/10.1016/J.JACASI.2021.04.007

Duelen, R., & Sampaolesi, M. (2017). Stem Cell Technology in Cardiac Regeneration: A Pluripotent Stem Cell Promise. *EBioMedicine*, *16*, 30–40. https://doi.org/10.1016/J.EBIOM.2017.01.029

Eltobshy, S. A. G., Hussein, A. M., Elmileegy, A. A., Askar, M. H., Khater, Y., Metias, E. F., & Helal, G. M. (2019). Effects of heme oxygenase-1 upregulation on

isoproterenol-induced myocardial infarction. *The Korean Journal of Physiology & Pharmacology : Official Journal of the Korean Physiological Society and the Korean Society of Pharmacology*, *23*(3), 203–217. https://doi.org/10.4196/KJPP.2019.23.3.203

Engberding, N., Spiekermann, S., Schaefer, A., Heineke, A., Wiencke, A., Müller, M., Fuchs, M., Hilfiker-Kleiner, D., Hornig, B., Drexler, H., & Landmesser, U. (2004). Allopurinol attenuates left ventricular remodeling and dysfunction after experimental myocardial infarction: a new action for an old drug? *Circulation*, *110*(15), 2175–2179. https://doi.org/10.1161/01.CIR.0000144303.24894.1C

Fichtlscherer, S., De Rosa, S., Fox, H., Schwietz, T., Fischer, A., Liebetrau, C., Weber, M., Hamm, C. W., Röxe, T., Müller-Ardogan, M., Bonauer, A., Zeiher, A. M., & Dimmeler, S. (2010). Circulating microRNAs in patients with coronary artery disease. *Circulation Research*, *107*(5), 677–684. https://doi.org/10.1161/CIRCRESAHA.109.215566

Frangogiannis, N. G. (2015). Pathophysiology of Myocardial Infarction. *Comprehensive Physiology*, *5*(4), 1841–1875. https://doi.org/10.1002/CPHY.C150006

Gao, E., Lei, Y. H., Shang, X., Huang, Z. M., Zuo, L., Boucher, M., Fan, Q., Chuprun, J. K., Ma, X. L., & Koch, W. J. (2010). A Novel and Efficient Model of Coronary Artery Ligation and Myocardial Infarction in the Mouse. *Circulation Research*, *107*(12), 1445. https://doi.org/10.1161/CIRCRESAHA.110.223925

Garg, M., & Khanna, D. (2014). Exploration of pharmacological interventions to prevent isoproterenol-induced myocardial infarction in experimental models. *Therapeutic Advances in Cardiovascular Disease*, *8*(4), 155–169. https://doi.org/10.1177/1753944714531638

Gaziano, J. M. (1999). Triglycerides and coronary risk. *Current Cardiology Reports*, *1*(2), 125–130. https://doi.org/10.1007/s11886-999-0070-4

Gaziano, T. A. (2005). Cardiovascular disease in the developing world and its cost-effective management. *Circulation*, *112*(23), 3547–3553. https://doi.org/10.1161/CIRCULATIONAHA.105.591792

Gaziano, T. A., Bitton, A., Anand, S., Abrahams-Gessel, S., & Murphy, A. (2010).

Growing epidemic of coronary heart disease in low- and middle-income countries. *Current Problems in Cardiology*, *35*(2), 72–115. https://doi.org/10.1016/J.CPCARDIOL.2009.10.002

Ghaffari, M., Kalantar, S. M., Hemati, M., Dehghani Firoozabadi, A., Asri, A., Shams, A., Jafari Ghalekohneh, S., & Haghiralsadat, F. (2021). Co-delivery of miRNA-15a and miRNA-16–1 using cationic PEGylated niosomes downregulates Bcl-2 and induces apoptosis in prostate cancer cells. *Biotechnology Letters*, *43*(5), 981–994. https://doi.org/10.1007/S10529-021-03085-2/FIGURES/6

Gill, S. S., & Tuteja, N. (2010). Reactive oxygen species and antioxidant machinery in abiotic stress tolerance in crop plants. *Plant Physiology and Biochemistry : PPB*, *48*(12), 909–930. https://doi.org/10.1016/J.PLAPHY.2010.08.016

Giri, S., Thompson, P. D., Kiernan, F. J., Clive, J., Fram, D. B., Mitchel, J. F., Hirst, J. A., McKay, R. G., & Waters, D. D. (1999). Clinical and angiographic characteristics of exertion-related acute myocardial infarction. *JAMA*, *282*(18), 1731–1736. https://doi.org/10.1001/JAMA.282.18.1731

Gomes Da Silva, A. M., & Silbiger, V. N. (2014). miRNAs as biomarkers of atrial fibrillation. *Biomarkers : Biochemical Indicators of Exposure, Response, and Susceptibility to Chemicals*, *19*(8), 631–636. https://doi.org/10.3109/1354750X.2014.954001

Gong, J., Campos, H., Fiecas, J. M. A., McGarvey, S. T., Goldberg, R., Richardson, C., & Baylin, A. (2013). A case-control study of physical activity patterns and risk of non-fatal myocardial infarction. *BMC Public Health*, *13*(1). https://doi.org/10.1186/1471-2458-13-122

Goodman, S. G., Steg, P. G., Eagle, K. A., Fox, K. A. A., López-Sendón, J., Montalescot, G., Budaj, A., Kennelly, B. M., Gore, J. M., Allegrone, J., Granger, C. B., & Gurfinkel, E. P. (2006). The diagnostic and prognostic impact of the redefinition of acute myocardial infarction: lessons from the Global Registry of Acute Coronary Events (GRACE). *American Heart Journal*, *151*(3), 654–660. https://doi.org/10.1016/J.AHJ.2005.05.014

Görlach, A., Bertram, K., Hudecova, S., & Krizanova, O. (2015). Calcium and ROS: A mutual interplay. *Redox Biology*, *6*, 260. https://doi.org/10.1016/J.REDOX.2015.08.010

Guo, C. J., Pan, Q., Li, D. G., Sun, H., & Liu, B. W. (2009). miR-15b and miR-16 are implicated in activation of the rat hepatic stellate cell: An essential role for apoptosis. *Journal of Hepatology*, *50*(4), 766–778. https://doi.org/10.1016/J.JHEP.2008.11.025

Ha, M., & Kim, V. N. (2014). Regulation of microRNA biogenesis. *Nature Reviews Molecular Cell Biology*, *15*(8), 509–524. https://doi.org/10.1038/NRM3838

Hasanuzzaman, M., Bhuyan, M. H. M. B., Zulfiqar, F., Raza, A., Mohsin, S. M., Al Mahmud, J., Fujita, M., & Fotopoulos, V. (2020). Reactive Oxygen Species and Antioxidant Defense in Plants under Abiotic Stress: Revisiting the Crucial Role of a Universal Defense Regulator. *Antioxidants*, *9*(8), 1–52. https://doi.org/10.3390/ANTIOX9080681

Hayashi, I., Morishita, Y., Imai, K., Nakamura, M., Nakachi, K., & Hayashi, T. (2007). High-throughput spectrophotometric assay of reactive oxygen species in serum. *Mutation Research*, *631*(1), 55–61. https://doi.org/10.1016/J.MRGENTOX.2007.04.006

He, D., Ruan, Z. B., Song, G. X., Chen, G. C., Wang, F., Wang, M. X., Yuan, M. K., & Zhu, L. (2021). MiR-15a-5p regulates myocardial fibrosis in atrial fibrillation by targeting Smad7. *PeerJ*, *9*. https://doi.org/10.7717/PEERJ.12686/SUPP-7

Heart Disease and Stroke Statistics-2021 Update A Report from the American Heart Association. (2021). *Circulation*, E254–E743. https://doi.org/10.1161/CIR.0000000000000950

Horn, A., & Jaiswal, J. K. (2019). Structural and signaling role of lipids in plasma membrane repair. *Current Topics in Membranes*, *84*, 67. https://doi.org/10.1016/BS.CTM.2019.07.001

Hsu, H. L., Huang, C. Y., Chen, P. L., Chen, Y. Y., Hsu, C. P., Chen, I. M., & Shih, C. C. (2019). Efficacy of ascending aortic banding technique concomitant with type I hybrid aortic arch repair in high-risk patients. *Heart and Vessels*, *34*(9), 1524–1532. https://doi.org/10.1007/S00380-019-01384-3

Hullinger, T. G., Montgomery, R. L., Seto, A. G., Dickinson, B. A., Semus, H. M., Lynch, J. M., Dalby, C. M., Robinson, K., Stack, C., Latimer, P. A., Hare, J. M., Olson, E. N., & Van Rooij, E. (2012). Inhibition of miR-15 Protects Against

Cardiac Ischemic Injury. *Circulation Research*, *110*(1), 71. https://doi.org/10.1161/CIRCRESAHA.111.244442

Huma, S., Tariq, R., Amin, F., & Tahir Mahmood, K. (2012). Modifiable and Non-modifiable predisposing Risk Factors of Myocardial Infarction-A Review. *J Pharm Sci Res*, *4*, 1649–1653.

Hurtubise, J., McLellan, K., Durr, K., Onasanya, O., Nwabuko, D., & Ndisang, J. F. (2016). The Different Facets of Dyslipidemia and Hypertension in Atherosclerosis. *Current Atherosclerosis Reports*, *18*(12). https://doi.org/10.1007/S11883-016-0632-Z

Ishtiaq, A., Bakhtiar, A., Silas, E., Saeed, J., Ajmal, S., Mushtaq, I., Ali, T., Wahedi, H. M., Khan, W., Khan, U., Anees, M., Sultan, A., & Murtaza, I. (2020). Pistacia integerrima alleviated Bisphenol A induced toxicity through Ubc13/p53 signalling. *Molecular Biology Reports*, *47*(9), 6545–6559. https://doi.org/10.1007/S11033-020-05706-X

Jensen, D. H., Hedback, N., Specht, L., Høgdall, E., Andersen, E., Therkildsen, M. H., Friis-Hansen, L., Norrild, B., & Von Buchwald, C. (2014). Human papillomavirus in head and neck squamous cell carcinoma of unknown primary is a common event and a strong predictor of survival. *PloS One*, *9*(11). https://doi.org/10.1371/JOURNAL.PONE.0110456

Joshi, P., Islam, S., Pais, P., Reddy, S., Dorairaj, P., Kazmi, K., Pandey, M. R., Haque, S., Mendis, S., Rangarajan, S., & Yusuf, S. (2007). Risk factors for early myocardial infarction in South Asians compared with individuals in other countries. *JAMA*, *297*(3), 286–294. https://doi.org/10.1001/JAMA.297.3.286

Jung, F., Weiland, U., Johns, R. A., Ihling, C., & Dimmeler, S. (2001). Chronic hypoxia induces apoptosis in cardiac myocytes: a possible role for Bcl-2-like proteins. *Biochemical and Biophysical Research Communications*, *286*(2), 419–425. https://doi.org/10.1006/BBRC.2001.5406

Kalogeris, T., Baines, C. P., Krenz, M., & Korthuis, R. J. (2012). Cell Biology of Ischemia/Reperfusion Injury. *International Review of Cell and Molecular Biology*, *298*, 229. https://doi.org/10.1016/B978-0-12-394309-5.00006-7

Kannel, W. B. (2000). Incidence and epidemiology of heart failure. *Heart Failure*

Reviews, *5*(2), 167–173. https://doi.org/10.1023/A:1009884820941

Keaney, J. F., & Vita, J. A. (1995). Atherosclerosis, oxidative stress, and antioxidant protection in endothelium-derived relaxing factor action. *Progress in Cardiovascular Diseases*, *38*(2), 129–154. https://doi.org/10.1016/S0033-0620(05)80003-9

Kearney, P. M., Whelton, M., Reynolds, K., Muntner, P., Whelton, P. K., & He, J. (2005). Global burden of hypertension: analysis of worldwide data. *Lancet (London, England)*, *365*(9455), 217–223. https://doi.org/10.1016/S0140-6736(05)17741-1

Khalil, M. I., Ahmmed, I., Ahmed, R., Tanvir, E. M., Afroz, R., Paul, S., Gan, S. H., & Alam, N. (2015). Amelioration of Isoproterenol-Induced Oxidative Damage in Rat Myocardium by Withania somnifera Leaf Extract. *BioMed Research International*, *2015*. https://doi.org/10.1155/2015/624159

Khaper, N., & Singal, P. K. (2001). Modulation of oxidative stress by a selective inhibition of angiotensin II type 1 receptors in MI rats. *Journal of the American College of Cardiology*, *37*(5), 1461–1466. https://doi.org/10.1016/S0735-1097(01)01126-3

Korshunova, A. Y., Blagonravov, M. L., Neborak, E. V., Syatkin, S. P., Sklifasovskaya, A. P., Semyatov, S. M., & Agostinelli, E. (2021). BCL2-regulated apoptotic process in myocardial ischemia-reperfusion injury (Review). *International Journal of Molecular Medicine*, *47*(1), 23–36. https://doi.org/10.3892/IJMM.2020.4781/HTML

Krijnen, P. A. J., Meischl, C., Hack, C. E., Meijer, C. J. L. M., Visser, C. A., Roos, D., & Niessen, H. W. M. (2003). Increased Nox2 expression in human cardiomyocytes after acute myocardial infarction. *Journal of Clinical Pathology*, *56*(3), 194–199. https://doi.org/10.1136/JCP.56.3.194

Kurian, G. A., Rajagopal, R., Vedantham, S., & Rajesh, M. (2016). The Role of Oxidative Stress in Myocardial Ischemia and Reperfusion Injury and Remodeling: Revisited. *Oxidative Medicine and Cellular Longevity*, *2016*. https://doi.org/10.1155/2016/1656450

Kuwabara, Y., Ono, K., Horie, T., Nishi, H., Nagao, K., Kinoshita, M., Watanabe, S.,

Baba, O., Kojima, Y., Shizuta, S., Imai, M., Tamura, T., Kita, T., & Kimura, T. (2011). Increased microRNA-1 and microRNA-133a levels in serum of patients with cardiovascular disease indicate myocardial damage. *Circulation: Cardiovascular Genetics*, *4*(4), 446–454. https://doi.org/10.1161/CIRCGENETICS.110.958975

Li, H. W., Meng, Y., Xie, Q., Yi, W. J., Lai, X. L., Bian, Q., Wang, J., Wang, J. F., & Yu, G. (2015). miR-98 protects endothelial cells against hypoxia/reoxygenation induced-apoptosis by targeting caspase-3. *Biochemical and Biophysical Research Communications*, *467*(3), 595–601. https://doi.org/10.1016/J.BBRC.2015.09.058

Li, J., Ichikawa, T., Villacorta, L., Janicki, J. S., Brower, G. L., Yamamoto, M., & Cui, T. (2009). Nrf2 protects against maladaptive cardiac responses to hemodynamic stress. *Arteriosclerosis, Thrombosis, and Vascular Biology*, *29*(11), 1843–1850. https://doi.org/10.1161/ATVBAHA.109.189480

Liu, L. F., Liang, Z., Lv, Z. R., Liu, X. H., Bai, J., Chen, J., Chen, C., & Wang, Y. (2012). MicroRNA-15a/b are up-regulated in response to myocardial ischemia/reperfusion injury. *Journal of Geriatric Cardiology : JGC*, *9*(1), 28. https://doi.org/10.3724/SP.J.1263.2012.00028

Lobo, R., Chandrasekhar Sagar, B., & Shenoy, C. (2017). Bio-tea prevents membrane destabilization during Isoproterenol-induced myocardial injury. *Journal of Microscopy and Ultrastructure*, *5*(3), 146–154. https://doi.org/10.1016/J.JMAU.2016.09.001

Long, G., Wang, F., Duan, Q., Chen, F., Yang, S., Gong, W., Wang, Y., Chen, C., & Wang, D. W. (2012). Human circulating microRNA-1 and microRNA-126 as potential novel indicators for acute myocardial infarction. *International Journal of Biological Sciences*, *8*(6), 811–818. https://doi.org/10.7150/IJBS.4439

Ma, K. K., Banas, K., & De Bold, A. J. (2005). Determinants of inducible brain natriuretic peptide promoter activity. *Regulatory Peptides*, *128*(3), 169–176. https://doi.org/10.1016/J.REGPEP.2004.12.025

Mann, D. L. (1996). Stress activated cytokines and the heart. *Cytokine and Growth Factor Reviews*, *7*(4), 341–354. https://doi.org/10.1016/S1359-6101(96)00043-3

Mechanic, O. J., Gavin, M., & Grossman, S. A. (2022). Acute Myocardial Infarction.

StatPearls. https://www.ncbi.nlm.nih.gov/books/NBK459269/

Meldrum, D. R., Dinarello, C. A., Cleveland, J., Cain, B. S., Shames, B. D., Meng, X., Harken, A. H., Zwischenberger, J. B., & Billiar, T. R. (1998). Hydrogen peroxide induces tumor necrosis factor α–mediated cardiac injury by a P38 mitogen-activated protein kinase–dependent mechanism. *Surgery*, *124*(2), 291–297. https://doi.org/10.1016/S0039-6060(98)70133-3

Meng, S. L., Chen, J. Z., Xu, P., Qu, J. H., Fan, L. M., Song, C., & Qiu, L. P. (2014). Hepatic antioxidant enzymes SOD and CAT of nile tilapia (oreochromis niloticus) in response to pesticide methomyl and recovery pattern. *Bulletin of Environmental Contamination and Toxicology*, *92*(4), 388–392. https://doi.org/10.1007/S00128-014-1232-7/TABLES/2

Mitchell, P. S., Parkin, R. K., Kroh, E. M., Fritz, B. R., Wyman, S. K., Pogosova-Agadjanyan, E. L., Peterson, A., Noteboom, J., O'Briant, K. C., Allen, A., Lin, D. W., Urban, N., Drescher, C. W., Knudsen, B. S., Stirewalt, D. L., Gentleman, R., Vessella, R. L., Nelson, P. S., Martin, D. B., & Tewari, M. (2008). Circulating microRNAs as stable blood-based markers for cancer detection. *Proceedings of the National Academy of Sciences of the United States of America*, *105*(30), 10513–10518. https://doi.org/10.1073/PNAS.0804549105

Moliterno, D. J., Willard, J. E., Lange, R. A., Negus, B. H., Boehrer, J. D., Glamann, D. B., Landau, C., Rossen, J. D., Winniford, M. D., & Hillis, L. D. (1994). Coronary-artery vasoconstriction induced by cocaine, cigarette smoking, or both. *The New England Journal of Medicine*, *330*(7), 454–459. https://doi.org/10.1056/NEJM199402173300702

Molkentin, J. D. (2004). Calcineurin-NFAT signaling regulates the cardiac hypertrophic response in coordination with the MAPKs. *Cardiovascular Research*, *63*(3), 467–475. https://doi.org/10.1016/J.CARDIORES.2004.01.021/2/63-3-467-FIG3.GIF

Moris, D., Spartalis, M., Spartalis, E., Karachaliou, G. S., Karaolanis, G. I., Tsourouflis, G., Tsilimigras, D. I., Tzatzaki, E., & Theocharis, S. (2017). The role of reactive oxygen species in the pathophysiology of cardiovascular diseases and the clinical significance of myocardial redox. *Annals of Translational Medicine*, *5*(16). https://doi.org/10.21037/ATM.2017.06.27

Mostofsky, E., MacLure, M., Sherwood, J. B., Tofler, G. H., Muller, J. E., & Mittleman, M. A. (2012). Risk of acute myocardial infarction after the death of a significant person in one's life: the Determinants of Myocardial Infarction Onset Study. *Circulation*, *125*(3), 491–496. https://doi.org/10.1161/CIRCULATIONAHA.111.061770

Muller, J. E., Abela, G. S., Nesto, R. W., & Tofler, G. H. (1994). Triggers, acute risk factors and vulnerable plaques: the lexicon of a new frontier. *Journal of the American College of Cardiology*, *23*(3), 809–813. https://doi.org/10.1016/0735-1097(94)90772-2

Mutlak, M., & Kehat, I. (2015). Extracellular signal-regulated kinases 1/2 as regulators of cardiac hypertrophy. *Frontiers in Pharmacology*, *6*(JUL). https://doi.org/10.3389/FPHAR.2015.00149

Nakamura, A., Kaneko, N., Villemagne, V. L., Kato, T., Doecke, J., Doré, V., Fowler, C., Li, Q. X., Martins, R., Rowe, C., Tomita, T., Matsuzaki, K., Ishii, K., Ishii, K., Arahata, Y., Iwamoto, S., Ito, K., Tanaka, K., Masters, C. L., & Yanagisawa, K. (2018). High performance plasma amyloid-β biomarkers for Alzheimer's disease. *Nature 2018 554:7691*, *554*(7691), 249–254. https://doi.org/10.1038/nature25456

Navarro-Yepes, J., Burns, M., Anandhan, A., Khalimonchuk, O., Del Razo, L. M., Quintanilla-Vega, B., Pappa, A., Panayiotidis, M. I., & Franco, R. (2014). Oxidative stress, redox signaling, and autophagy: Cell death versus survival. *Antioxidants and Redox Signaling*, *21*(1), 66–85. https://doi.org/10.1089/ARS.2014.5837

Nian, M., Lee, P., Khaper, N., & Liu, P. (2004). Inflammatory cytokines and postmyocardial infarction remodeling. *Circulation Research*, *94*(12), 1543–1553. https://doi.org/10.1161/01.RES.0000130526.20854.fa

O'Brien, J., Hayder, H., Zayed, Y., & Peng, C. (2018). Overview of microRNA biogenesis, mechanisms of actions, and circulation. *Frontiers in Endocrinology*, *9*(AUG), 402. https://doi.org/10.3389/FENDO.2018.00402/BIBTEX

Ojha, N., & Dhamoon, A. S. (2021). Myocardial Infarction. *Treasure Island (FL): StatPearls Publishing*. https://www.ncbi.nlm.nih.gov/books/NBK537076/

Okada, C., Yamashita, E., Lee, S. J., Shibata, S., Katahira, J., Nakagawa, A., Yoneda,

Y., & Tsukihara, T. (2009). A high-Resolution structure of the pre-microrna nuclear export machinery. *Science*, *326*(5957), 1275–1279. https://doi.org/10.1126/SCIENCE.1178705/SUPPL_FILE/OKADA.SOM.PDF

Patel, V., Upaganlawar, A., Zalawadia, R., & Balaraman, R. (2010). Cardioprotective effect of melatonin against isoproterenol induced myocardial infarction in rats: A biochemical, electrocardiographic and histoarchitectural evaluation. *European Journal of Pharmacology*, *644*(1–3), 160–168. https://doi.org/10.1016/J.EJPHAR.2010.06.065

Peoples, J. N., Saraf, A., Ghazal, N., Pham, T. T., & Kwong, J. Q. (2019). Mitochondrial dysfunction and oxidative stress in heart disease. *Experimental & Molecular Medicine 2019 51:12*, *51*(12), 1–13. https://doi.org/10.1038/s12276-019-0355-7

Priscilla, D. H., & Prince, P. S. M. (2009). Cardioprotective effect of gallic acid on cardiac troponin-T, cardiac marker enzymes, lipid peroxidation products and antioxidants in experimentally induced myocardial infarction in Wistar rats. *Chemico-Biological Interactions*, *179*(2–3), 118–124. https://doi.org/10.1016/J.CBI.2008.12.012

Rajput, V. D., Harish, Singh, R. K., Verma, K. K., Sharma, L., Quiroz-Figueroa, F. R., Meena, M., Gour, V. S., Minkina, T., Sushkova, S., & Mandzhieva, S. (2021). Recent Developments in Enzymatic Antioxidant Defence Mechanism in Plants with Special Reference to Abiotic Stress. *Biology*, *10*(4). https://doi.org/10.3390/BIOLOGY10040267

Rathore, V., Anabilim Dali, B., & Raja Tip Fakultesi, G. (2018). *Risk Factors for Acute Myocardial Infarction: A Review*. https://doi.org/10.14744/ejmi.2018.76486

Reid, G., Kirschner, M. B., & van Zandwijk, N. (2011). Circulating microRNAs: Association with disease and potential use as biomarkers. *Critical Reviews in Oncology/Hematology*, *80*(2), 193–208. https://doi.org/10.1016/J.CRITREVONC.2010.11.004

Reimer, K. A., Jennings, R. B., & Tatum, A. H. (1983). Pathobiology of acute myocardial ischemia: metabolic, functional and ultrastructural studies. *The American Journal of Cardiology*, *52*(2), 72–81. https://doi.org/10.1016/0002-9149(83)90180-7

Roth, G. A., Mensah, G. A., Johnson, C. O., Addolorato, G., Ammirati, E., Baddour, L. M., Barengo, N. C., Beaton, A., Benjamin, E. J., Benziger, C. P., Bonny, A., Brauer, M., Brodmann, M., Cahill, T. J., Carapetis, J. R., Catapano, A. L., Chugh, S., Cooper, L. T., Coresh, J., … Fuster, V. (2020). Global Burden of Cardiovascular Diseases and Risk Factors, 1990–2019: Update From the GBD 2019 Study. *Journal of the American College of Cardiology*, *76*(25), 2982–3021. https://doi.org/10.1016/J.JACC.2020.11.010

Ruby, J. G., Jan, C. H., & Bartel, D. P. (2007). Intronic microRNA precursors that bypass Drosha processing. *Nature 2007 448:7149*, *448*(7149), 83–86. https://doi.org/10.1038/nature05983

Sakuma, K., & Yamaguchi, A. (2010). The functional role of calcineurin in hypertrophy, regeneration, and disorders of skeletal muscle. *Journal of Biomedicine and Biotechnology*, *2010*. https://doi.org/10.1155/2010/721219

Sala, V., Bergerone, S., Gatti, S., Gallo, S., Ponzetto, A., Ponzetto, C., & Crepaldi, T. (2014). MicroRNAs in myocardial ischemia: Identifying new targets and tools for treating heart disease. New frontiers for miR-medicine. *Cellular and Molecular Life Sciences*, *71*(8), 1439–1452. https://doi.org/10.1007/S00018-013-1504-0/TABLES/1

Saleheen, D., Zaidi, M., Rasheed, A., Ahmad, U., Hakeem, A., Murtaza, M., Kayani, W., Faruqui, A., Kundi, A., Zaman, K. S., Yaqoob, Z., Cheema, L. A., Samad, A., Rasheed, S. Z., Mallick, N. H., Azhar, M., Jooma, R., Gardezi, A. R., Memon, N., … Danesh, J. (2009). The Pakistan Risk of Myocardial Infarction Study: a resource for the study of genetic, lifestyle and other determinants of myocardial infarction in South Asia. *European Journal of Epidemiology*, *24*(6), 329. https://doi.org/10.1007/S10654-009-9334-Y

Schulman, H., & Anderson, M. E. (2010). Ca2+/Calmodulin-dependent Protein Kinase II in Heart Failure. *Drug Discovery Today. Disease Mechanisms*, *7*(2), e117. https://doi.org/10.1016/J.DDMEC.2010.07.005

Schulte, C., & Zeller, T. (2015). microRNA-based diagnostics and therapy in cardiovascular disease—Summing up the facts. *Cardiovascular Diagnosis and Therapy*, *5*(1), 17. https://doi.org/10.3978/J.ISSN.2223-3652.2014.12.03

Severino, P., D'Amato, A., Pucci, M., Infusino, F., Birtolo, L. I., Mariani, M. V.,

Lavalle, C., Maestrini, V., Mancone, M., & Fedele, F. (2020). Ischemic Heart Disease and Heart Failure: Role of Coronary Ion Channels. *International Journal of Molecular Sciences*, *21*(9). https://doi.org/10.3390/IJMS21093167

Sia, Y. T., Parker, T. G., Liu, P., Tsoporis, J. N., Adam, A., & Rouleau, J. L. (2002). Improved post-myocardial infarction survival with probucol in rats: Effects on left ventricular function, morphology, cardiac oxidative stress and cytokine expression. *Journal of the American College of Cardiology*, *39*(1), 148–156. https://doi.org/10.1016/S0735-1097(01)01709-0

Simons, M., & Raposo, G. (2009). Exosomes--vesicular carriers for intercellular communication. *Current Opinion in Cell Biology*, *21*(4), 575–581. https://doi.org/10.1016/J.CEB.2009.03.007

Singh, R. M., Cummings, E., Pantos, C., & Singh, J. (2017). Protein kinase C and cardiac dysfunction: a review. *Heart Failure Reviews*, *22*(6), 843. https://doi.org/10.1007/S10741-017-9634-3

Stansfield, W. E., Ranek, M., Pendse, A., Schisler, J. C., Wang, S., Pulinilkunnil, T., & Willis, M. S. (2014). The Pathophysiology of Cardiac Hypertrophy and Heart Failure. *Cellular and Molecular Pathobiology of Cardiovascular Disease*, 51–78. https://doi.org/10.1016/B978-0-12-405206-2.00004-1

Strynadka, N. C. J., & James, M. N. G. (2003). CRYSTAL STRUCTURES OF THE HELIX-LOOP-HELIX CALCIUM-BINDING PROTEINS. *Https://Doi.Org/10.1146/Annurev.Bi.58.070189.004511*, *58*(1), 951–999. https://doi.org/10.1146/ANNUREV.BI.58.070189.004511

Sucher, R., Gehwolf, P., Kaier, T., Hermann, M., Maglione, M., Oberhuber, R., Ratschiller, T., Kuznetsov, A. V., Bösch, F., Kozlov, A. V., Ashraf, M. I., Schneeberger, S., Brandacher, G., Öllinger, R., Margreiter, R., & Troppmair, J. (2009). Intracellular signaling pathways control mitochondrial events associated with the development of ischemia/ reperfusion-associated damage. *Transplant International : Official Journal of the European Society for Organ Transplantation*, *22*(9), 922–930. https://doi.org/10.1111/J.1432-2277.2009.00883.X

Sun, C., Liu, H., Guo, J., Yu, Y., Yang, D., He, F., & Du, Z. (2017). MicroRNA-98 negatively regulates myocardial infarction-induced apoptosis by down-regulating

Fas and caspase-3. *Scientific Reports 2017 7:1*, *7*(1), 1–11. https://doi.org/10.1038/s41598-017-07578-x

Sun, H., Zhou, F., Wang, Y., Zhang, Y., Chang, A., & Chen, Q. (2006). Effects of beta-adrenoceptors overexpression on cell survival are mediated by Bax/Bcl-2 pathway in rat cardiac myocytes. *Pharmacology*, *78*(2), 98–104. https://doi.org/10.1159/000095785

Thygesen, K., Alpert, J. S., Jaffe, A. S., Chaitman, B. R., Bax, J. J., Morrow, D. A., White, H. D., Corbett, S., Chettibi, M., Hayrapetyan, H., Roithinger, F. X., Aliyev, F., Sujayeva, V., Claeys, M. J., Smajić, E., Kala, P., Iversen, K. K., Hefny, E. El, Marandi, T., … Parkhomenko, A. (2018). Fourth Universal Definition of Myocardial Infarction (2018). *Circulation*, *138*(20), e618–e651. https://doi.org/10.1161/CIR.0000000000000617

Thygesen, K., Mair, J., Giannitsis, E., Mueller, C., Lindahl, B., Blankenberg, S., Huber, K., Plebani, M., Biasucci, L. M., Tubaro, M., Collinson, P., Venge, P., Hasin, Y., Galvani, M., Koenig, W., Hamm, C., Alpert, J. S., Katus, H., & Jaffe, A. S. (2012). How to use high-sensitivity cardiac troponins in acute cardiac care. *European Heart Journal*, *33*(18). https://doi.org/10.1093/EURHEARTJ/EHS154

Tsai, N. W., Chang, Y. T., Huang, C. R., Lin, Y. J., Lin, W. C., Cheng, B. C., Su, C. M., Chiang, Y. F., Chen, S. F., Huang, C. C., Chang, W. N., & Lu, C. H. (2014). Association between oxidative stress and outcome in different subtypes of acute ischemic stroke. *BioMed Research International*, *2014*. https://doi.org/10.1155/2014/256879

Tzifi, F., Economopoulou, C., Gourgiotis, D., Ardavanis, A., Papageorgiou, S., & Scorilas, A. (2012). The role of BCL2 family of apoptosis regulator proteins in acute and chronic leukemias. *Advances in Hematology*, *2012*. https://doi.org/10.1155/2012/524308

Venditti, P., Masullo, P., & Di Meo, S. (2001). Effects of myocardial ischemia and reperfusion on mitochondrial function and susceptibility to oxidative stress. *Cellular and Molecular Life Sciences CMLS 2001 58:10*, *58*(10), 1528–1537. https://doi.org/10.1007/PL00000793

Vickers, K. C., Palmisano, B. T., Shoucri, B. M., Shamburek, R. D., & Remaley, A. T. (2011). MicroRNAs are transported in plasma and delivered to recipient cells by

high-density lipoproteins. *Nature Cell Biology*, *13*(4), 423–435. https://doi.org/10.1038/NCB2210

Wang, J. F., Yi, Z. F., Li, H. W., Wang, F., Bian, Q., Lai, X. L., & Yu, G. (2014). Screening plasma miRNAs as biomarkers for renal ischemia-reperfusion injury in rats. *Medical Science Monitor : International Medical Journal of Experimental and Clinical Research*, *20*, 283. https://doi.org/10.12659/MSM.889937

Wei, M., Brandhorst, S., Shelehchi, M., Mirzaei, H., Cheng, C. W., Budniak, J., Groshen, S., Mack, W. J., Guen, E., Di Biase, S., Cohen, P., Morgan, T. E., Dorff, T., Hong, K., Michalsen, A., Laviano, A., & Longo, V. D. (2017). Fasting-mimicking diet and markers/risk factors for aging, diabetes, cancer, and cardiovascular disease. *Science Translational Medicine*, *9*(377). https://doi.org/10.1126/SCITRANSLMED.AAI8700

Weil, B. R., Suzuki, G., Young, R. F., Iyer, V., & Canty, J. M. (2018). Troponin Release and Reversible Left Ventricular Dysfunction After Transient Pressure Overload. *Journal of the American College of Cardiology*, *71*(25), 2906–2916. https://doi.org/10.1016/J.JACC.2018.04.029

Xia, L., Zhang, D., Du, R., Pan, Y., Zhao, L., Sun, S., Hong, L., Liu, J., & Fan, D. (2008). miR-15b and miR-16 modulate multidrug resistance by targeting BCL2 in human gastric cancer cells. *International Journal of Cancer*, *123*(2), 372–379. https://doi.org/10.1002/IJC.23501

Xiang, Y. K. (2011). Compartmentalization of Beta-Adrenergic Signals in Cardiomyocytes. *Circulation Research*, *109*(2), 231. https://doi.org/10.1161/CIRCRESAHA.110.231340

Xu, M., Millard, R. W., & Ashraf, M. (2012). Role of GATA-4 in differentiation and survival of bone marrow mesenchymal stem cells. *Progress in Molecular Biology and Translational Science*, *111*, 217–241. https://doi.org/10.1016/B978-0-12-398459-3.00010-1

Yanazume, T., Hasegawa, K., Wada, H., Morimoto, T., Abe, M., Kawamura, T., & Sasayama, S. (2002). Rho/ROCK pathway contributes to the activation of extracellular signal-regulated kinase/GATA-4 during myocardial cell hypertrophy. *The Journal of Biological Chemistry*, *277*(10), 8618–8625. https://doi.org/10.1074/JBC.M107924200

Yao, S. (2016). MicroRNA biogenesis and their functions in regulating stem cell potency and differentiation. *Biological Procedures Online*, *18*(1). https://doi.org/10.1186/S12575-016-0037-Y

Yoda, M., Kawamata, T., Paroo, Z., Ye, X., Iwasaki, S., Liu, Q., & Tomari, Y. (2010). ATP-dependent human RISC assembly pathways. *Nature Structural and Molecular Biology*, *17*(1), 17–24. https://doi.org/10.1038/NSMB.1733

Youle, R. J., & Strasser, A. (2008). The BCL-2 protein family: opposing activities that mediate cell death. *Nature Reviews Molecular Cell Biology 2008 9:1*, *9*(1), 47–59. https://doi.org/10.1038/nrm2308

Yusuf, P. S., Hawken, S., Ôunpuu, S., Dans, T., Avezum, A., Lanas, F., McQueen, M., Budaj, A., Pais, P., Varigos, J., & Lisheng, L. (2004). Effect of potentially modifiable risk factors associated with myocardial infarction in 52 countries (the INTERHEART study): case-control study. *Lancet (London, England)*, *364*(9438), 937–952. https://doi.org/10.1016/S0140-6736(04)17018-9

Zhang, H., Kolb, F. A., Jaskiewicz, L., Westhof, E., & Filipowicz, W. (2004). Single processing center models for human Dicer and bacterial RNase III. *Cell*, *118*(1), 57–68. https://doi.org/10.1016/J.CELL.2004.06.017/ATTACHMENT/93ED1003-87C4-4FDA-B915-4C3AA8DB2601/MMC1.PDF

Zhu, J., Su, X., Li, G., Chen, J., Tang, B., & Yang, Y. (2014). The incidence of acute myocardial infarction in relation to overweight and obesity: a meta-analysis. *Archives of Medical Science : AMS*, *10*(5), 855–862. https://doi.org/10.5114/AOMS.2014.46206